# Bacteria-Protein Interactions in Bacterial Adhesion

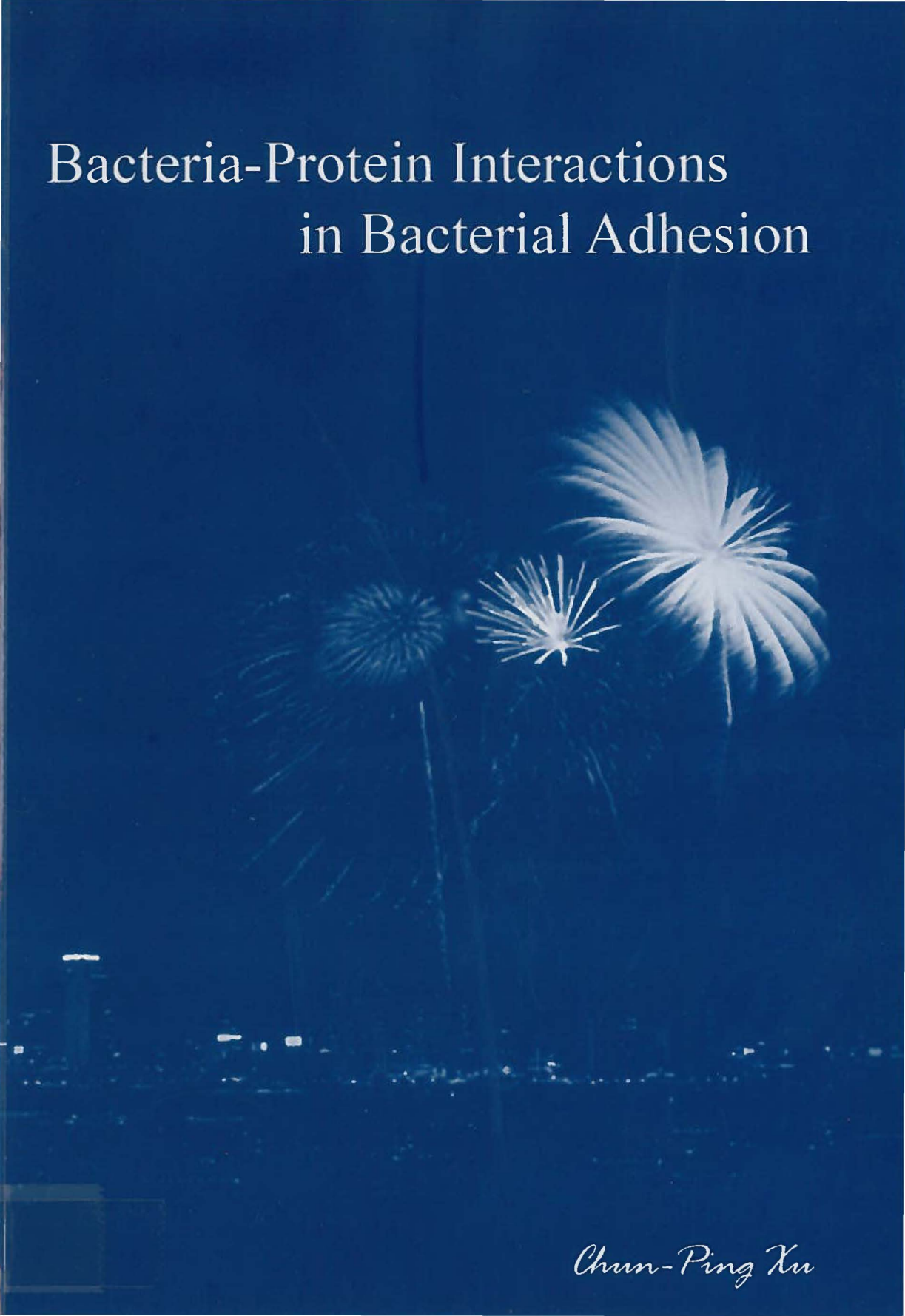

Chun-Ping Xu

# Bacteria-Protein Interactions in Bacterial Adhesion

Cover picture "fireworks (烟花，はなび，꽃불)" by: Li Mei
Cover design: Li-Jun Tan and Qing-Jun Qiu
Printed by Drukkerij van Denderen B.V., Groningen, The Netherlands

ISBN paper version: 978-90-367-3387-8

# Stellingen



1. Antigen I/II at the surface of *Streptococcus mutans* LT11 specifically binds different protein species with different affinities from the large pool of proteins present in whole saliva. *This thesis*

2. The specific contribution to the interaction between *Streptococcus mutans* and salivary proteins is mediated by electrostatic interactions. *This thesis*

3. Convective-diffusional mass transport in a parallel plate flow chamber results in a milder contact than established during AFM or stirring in a microcalorimeter. *This thesis*

4. Bond strengthening in case of specific adhesion of *Staphylococcus aureus* strains to Fn-films occurs on a much faster time scale than in case of non-specific adhesion. *This thesis*

5. Bond strength energies calculated from the retract force-distance curves in AFM are orders of magnitude larger than calculated from desorption rate coefficients, suggesting that the penetrating Fn-coated AFM tip probes multiple receptor sites in the cell surface. *This thesis*

6. The spectacle of fireworks blooming beautifully, then disappearing with a pop can be taken as a symbol of plangent and graceful resignation, or vital ephemerality like cherry blossoms.

7. Life is what happens to you while you are busy making other plans. *John Lennon* (1940–1980).

8. Most research follows formerly published work, but only research based on an absolutely new idea may receive a Nobel Prize.

9. A smoking room in a public place is meant to protect the rights and demands of smokers and non-smokers.

10. The common point in Chinese and Dutch life styles is in the number of bicycles per head of the population.

rijksuniversiteit groningen

# Bacteria-Protein Interactions in Bacterial Adhesion

Proefschrift

ter verkrijging van het doctoraat in de
Medische Wetenschappen
aan de Rijksuniversiteit Groningen
op gezag van de
Rector Magnificus, Dr. F. Zwarts,
in het openbaar te verdedigen op
woensdag 17 september 2008
om 14.45 uur

door

Chun-Ping Xu

geboren op 7 mei 1977
te Jiaozuo, China

| | |
|---|---|
| Promotores: | Prof.dr.ir. W. Norde<br>Prof.dr.ir. H.J. Busscher<br>Prof.dr. H.C. van der Mei |
| Beoordelingscommissie: | Prof.dr. L. Dijkhuizen<br>Prof.dr. J.M. van Dijl<br>Prof.dr. P.G. Rouxhet |

Paranimfen:
Mervyn Chin Yeen Hoong
Peter Li Mei

*献给我的父亲母亲*

*To my parents*

## Contents

# 1

# Introduction

Bacterial adhesion is of significance in widely different aspects of nature and human life, such as the marine environment, soil and plant ecology, food industry, and most importantly, the biomedical field. Once microorganisms are attached to a surface, a multi-step process starts resulting in the formation of a complex adhering microbial community, called a "biofilm". A biofilm can be defined as a micro-ecosystem in which different strains and species of microorganisms efficiently cooperate in order to protect themselves against environmental stresses and to facilitate more efficient nutrient uptake (Gottenbos *et al.,* 1999).

The human body serves as a reservoir for many different biofilms. Some of these biofilms are believed to play a role in the maintenance of health. Autochthonous bacterial biofilms on the epithelia of the human urethra, cervix, and vagina are believed to act as barriers preventing colonization by pathogens (Chan *et al.*, 1985). However, in many instances, bacterial biofilms develop to take advantage of the nutrients supplied by the body, and cause damage. Dental plaque, found in the oral cavity is one such biofilm. Organisms in an oral biofilm feed on food remnants in the mouth, notably sugars and the proteins and carbohydrates of the saliva, yielding the production of acids which leads to the breakdown of the crystalline structure of the tooth surface. Streptococci play a major role in the initiation of dental caries, which is one of most prevalent and costly infectious diseases worldwide. In addition, when medical devices, such as for instance urethral catheters and voice prostheses, are used to restore function in the body, the foreign surfaces often introduce pathogenic organisms to previously restricted areas and serve as foci for infection (Dankert *et al.*, 1986). Staphylococci are major causes of infection related to biofilms formed on indwelling medical devices.

## Biofilm Formation

Although the function and appearance of biofilms in various environments may be different, in the pathogenesis of infection all biofilms are formed according to the following basic sequence of events (Escher and Characklis, 1990). Due to their smaller dimensions and therefore higher transport rates, proteins from biological fluids adsorb

faster than microorganisms adhere and as a consequence, microbial adhesion always occurs to a proteinaceous conditioning film rather than to a bare material surface. Bacterial adhesion to a material surface can be described as a two-phase process including an initial, instantaneous, and reversible physical phase (phase one) and a time-dependent and irreversible molecular and cellular phase (phase two), as was first proposed by Marshall and colleagues (Marshall *et al.*, 1971; Marshall, 1985) and has been accepted by the majority of researchers (Dankert *et al.*, 1986; Gristina, 1988; An and Friedman, 1998). Different steps may be distinguished in both the physical phase as well as the molecular phase as schematically summarized in Fig. 1 and explained below:

***Phase 1***- Physical-chemical interactions between bacterial and material surfaces:

1. Formation of a conditioning film of adsorbed proteins and other organic molecules on the substratum surface prior to bacterial deposition. For example, oral microorganisms are deposited on top of the pellicle, a protein layer on the teeth. Sometimes protein adsorption stimulates bacterial adhesion like in case of "adhesive proteins" such as fibronectin, vitronectin, and laminin.
2. Transport of bacteria towards the substratum surface through diffusion, convection, sedimentation, or by intrinsic bacterial motility.
3. Initial bacterial adhesion, followed by co-adhesion of planktonic bacteria with already adhered ones.

***Phase 2*** - Molecular and cellular interactions between bacterial surfaces:

4. Strong attachment or anchoring of bacteria at the surface through surface appendages and production of extracellular polymeric substances (EPS), composed of poly-saccharides, proteins, humic substances, nucleic acids and lipids.
5. Colony formation by already adhering bacteria and continued secretion of EPS.
6. Localized detachment of isolated or clumps of bacteria caused by occasionally high fluid stress, liquid-air interfaces or other detachment forces operative in the environment of the biofilm.

Of course, the model is simplified and ignores detailed aspects of biofilm formation. However, it is envisaged that the initial events as summarized above, will determine the final structure and microbial composition of a mature biofilm (Reid *et al.*, 1998).

## Bacteria-Biomaterial Interactions According to Theoretical Models

Bacterial adhesion is a complicated process that is affected by many factors, including characteristics of the surfaces of the bacterial cell and the substratum (hydrophobicity, charge, roughness and the possible presence of specific receptors) and environmental factors, such as pH, ionic strength, temperature and the presence of serum proteins or bactericidal substances.

Several theories have been proposed in order to understand bacterial adhesion to various substratum surfaces. They may be classified in physico-chemical models (the classical DLVO (Derjaguin, Landau, Verwey, Overbeek) theory, the extended DLVO theory and the thermodynamic approach), involving properties like electrostatic potential, hydrophobicity and surface free energy (Busscher and Weerkamp, 1987; Fletcher, 1987) and a specific receptor model, involving stereo-chemical molecular interactions between components on the bacterial cell and substratum surface, such as in lectin-like interactions.

### *Physico-chemical models*

Physico-chemical models may be divided in two types, based on an electrokinetic concept and based on a thermodynamic concept. In these models, bacteria are considered as inert particles which do not change during the course of attachment. The electrokinetic concept focuses on the significance of electrostatic potentials and Lifshitz-Van der Waals forces and is summarized in the classical DLVO theory, in which bacterial adhesion is described as a result of attractive Lifshitz-Van der Waals forces and repulsive or attractive electrostatic forces. Accordingly, the total interaction free energy ($G^{TOT}$) between two interacting surfaces can be separated as

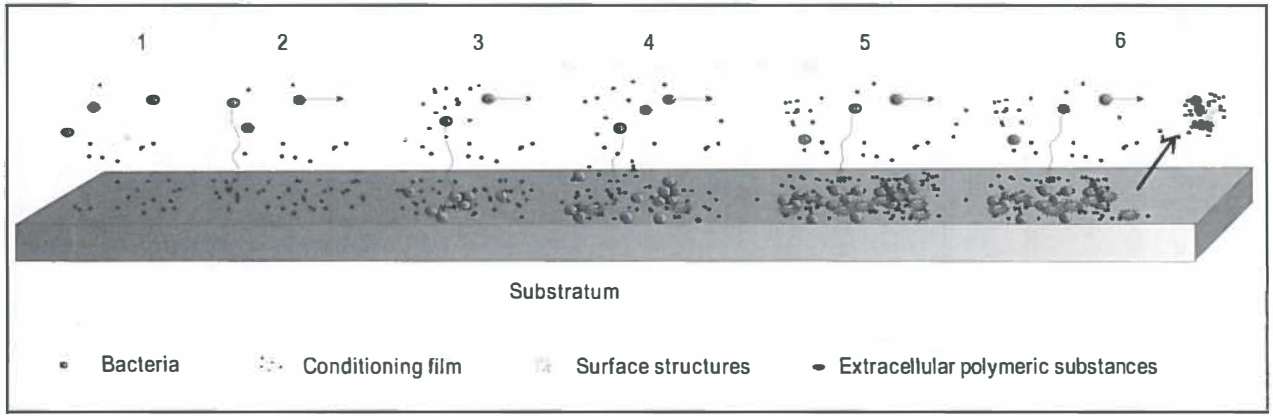


**Figure 1.** Schematic presentation of the sequential steps involved in biofilm formation.

1. Conditioning film
2. Transport
3. Initial adhesion
4. Attachment
5. Growth
6. Detachment

$$G^{TOT}(d) = G^{LW}(d) + G^{EL}(d) \quad (1)$$

in which $G^{LW}$ and $G^{EL}$ denote the Lifshitz-Van der Waals and electrostatic contributions, respectively. The variation with distance ($d$) of these interaction free energies depends on the geometry of the interacting bodies and is summarized in Table 1 for the configuration of a sphere (bacterium) opposed to a semi-infinite flat plate (a substratum surface) and for two interacting bacteria ((co)aggregation) (Bos *et al.*, 1999). The Lifshitz-Van der Waals attraction is not strongly influenced by ionic strength, but both the range and the magnitude of the electrostatic interactions decrease with increasing ionic strength. Note that, dependent on the ionic strength, at a few nm separation between two surfaces, a potential energy barrier for irreversible adhesion in the primary minimum (at close approach of the surface) may exist. However, depending on the ionic strength as well, the bacteria may become reversible captured in a more shallow secondary minimum before encountering this barrier for deposition.

Van Oss *et al.* (1986) introduced the so-called extended DLVO theory by including short-range Lewis acid-base interactions in the classical DLVO approach, therewith accounting for the hydrophobic/hydrophilic interactions. For bacterial cells it was concluded that osmotic interactions are negligibly small, so that the total adhesion energy can be expressed as:

$$G^{TOT}(d) = G^{LW}(d) + G^{EL}(d) + G^{AB}(d) \quad (2)$$

in which $G^{AB}$ relates to the polar acid-base interfacial free energy. Inclusion of acid-base interactions in the classical DLVO approach (Van Oss *et al.*, 1988), implies that "hydrophobic attractive" (Wood and Sharma, 1995) and "hydrophilic repulsive" (Pashley and Israelachvili, 1984; Elimelech, 1990) interactions can be accounted for in a more formal way. $\Delta G^{AB}$ is incorporated in the extended DLVO approach by attributing a decay function to this balance. The decay with distance of the acid-base interaction energy is assumed to describe the distance dependence of the ordering in the boundary layer, while the Lifshitz-Van der Waals and electrostatic interaction

energies are identical for the extended and classical DLVO approach. The variation with distance of the acid-base interaction free energies for the sphere-plate (bacterium-substratum) and sphere-sphere (bacterium-bacterium) configurations is summarized in Table 2 (Bos *et al.*, 1999).

In the thermodynamic concept, the interacting surfaces are assumed to physically contact each other under conditions of thermodynamic equilibrium. The thermodynamic concept is based on interfacial tensions of the substratum, the bacterial surface and the suspending medium. Subsequently, these three interfacial tensions can be used to calculate the interfacial free energy ($\Delta G_{adh}$) between the pairs of surfaces involved in adhesion, at constant pressure and temperature

$$\Delta G_{adh} = \gamma_{sb}-\gamma_{sl}-\gamma_{bl} \qquad (3)$$

in which: $\gamma_{sb}$, $\gamma_{sl}$, and $\gamma_{bl}$ are the substratum-bacterium, substratum-liquid, bacterium-liquid interfacial tensions, respectively.

Adhesion will be favorable if $\Delta G_{adh}$ is negative. Both electrokinetic concept and thermodynamic concept have proven merits for microbial adhesion, when certain collections of strains and species are considered, but have failed so far to yield a generalized description of all aspects of microbial adhesion valid for each and every strain (Van Loosdrecht *et al.*, 1989).

The DVLO theory and the thermodynamic approach of calculating the adhesion energy are clearly relevant in different phases of the adhesion process, i.e. at different separation distances between the organism and the substratum surface. The promising extended DLVO theory uses components from both models, and includes distance dependent hydrophobicity: the hydration effects accounted for by the $\Delta G^{AB}$ component, in addition to the Lifshitz-Van der Waals and electrostatic interactions. In some cases the extended DLVO theory seems to qualitatively predict experimental adhesion results better than the classical DLVO theory and the thermodynamic approach (Hermansson, 1999).

**Table 1**. The Lifshitz-Van der Waals $G^{LW}(d)$ and electrostatic $G^{EL}(d)$ interaction energies for a bacterium with radius a opposed to a substratum surface and for two interacting bacteria with radii $a_1$ and $a_2$ as a function of the separation distance $d$ (adapted from Bos *et al.*, 1999).

| Configuration | Interaction energies (J) | |
|---|---|---|
| | Lifshitz-Van der Waals[a] | Electrostatic[b] |
| **bacterium-substratum** | $-\frac{A}{6}\left[\frac{a}{d}+\frac{a}{d+2a}+ln\left(\frac{d}{d+2a}\right)\right]$ | $\pi\varepsilon a\left(\zeta_1^2+\zeta_2^2\right)\left[\frac{2\zeta_1\zeta_2}{\zeta_1^2+\zeta_2^2}ln\frac{1+exp(-\kappa d)}{1-exp(-\kappa d)}+ln\{1-exp(-2\kappa d)\}\right]$ |
| **bacterium-bacterium** | $\frac{-Aa_1a_2}{6d(a_1+a_2)}$ | $\frac{\pi\varepsilon a_1a_2\left(\zeta_1^2+\zeta_2^2\right)}{(a_1+a_2)}\left[\frac{2\zeta_1\zeta_2}{\zeta_1^2+\zeta_2^2}ln\frac{1+exp(-\kappa d)}{1-exp(-\kappa d)}+ln\{1-exp(-2\kappa d)\}\right]$ |

[a] $A$ denotes the Hamaker constant.

[b] $\varepsilon$ denotes the permittivity of the medium, $\zeta$ the zeta potential and $\kappa^{-1}$ is the double layer thickness. $\kappa^{-1}$ can be calculated from $\kappa=\left[\frac{e^2}{\varepsilon kT}\cdot\sum_i z_i\cdot n_i\right]^{1/2}$ [$m^{-1}$] in which $e$ denotes the electron charge, $k$ the Boltzmann constant, $T$ the absolute temperature, $z_i$ is the valency of the ions present and $n_i$ is the number of ions per unit volume. For a symmetrical 1-1 electrolyte this equation reduces to $\kappa = 0.328 \times 1010\ (z_iM_i)^{1/2}$ [$m^{-1}$], where $M_i$ is molarity [mol $l^{-1}$] of the ions.

**Table 2.** The Lewis acid-base $G^{AB}(d)$ interaction free energies for a bacterium with radius $a$ opposed to a substratum surface and for two interacting bacteria ((co-)aggregation) as a function of the separation distance $d$ (adapted from Bos *et al.*, 1999).

| Configuration | Lewis acid-basea interaction free energies (J) |
|---|---|
| **bacterium-substratum** | $2\pi a\lambda\Delta G^{AB}\exp[(d_0-d)/\lambda]$ |
| **bacterium-bacterium** | $\pi a\lambda\Delta G^{AB}\exp[(d_0-d)/\lambda]$ |

[a] $d_0$ is the distance of closest approach between two surfaces (1.57 Å; Van Oss,1990), while $\lambda$ denotes the correlation length of the molecules of the liquid medium, and reportedly equals 0.6 nm for hydrophilic repulsion. For situations in which hydrophobic attraction occurs, $\lambda$ may become as high as 13 nm (Van Oss, 1994).

***Specific receptor model***

Proteinaceous structures on bacterial cell surfaces with a known role in adhesion are called "adhesins". Adhesins are often lectins, which can bind to saccharides or proteinaceous receptors. Most of the bindings between bacteria and proteins are specific ligand-receptor like interactions. Bacterial adhesins appear in close association with surface appendages and on a single cell surface several different appendages with various specific functions may be present. The specific receptor model is mostly used for interactions between bacteria and protein-coated surfaces.

Many proteins have been studied for their effects on bacterial adhesion to substratum surfaces (Fletcher 1976; Kuusela *et al.*, 1985; Pratt–Terpstra *et al.*, 1987; Muller *et al.*, 1991; McDowell *et al.*, 1995), including albumin, fibronectin, fibrinogen, laminin, denatured collagen, and others. Specific proteins promote or inhibit bacterial adhesion, not only due to their adsorption to a substratum surface, but also because of their adsorption to bacterial surfaces. Adhesion of bacteria to specific, adsorbed proteins is believed to be important in the pathogenesis of prosthetic infections (Tojo *et al.*, 1988; Timmerman *et al.*, 1991). For instance, fibronectin binding proteins (FnBPA and FnBPB) and antigen I/II can be found on staphylococcal and streptococcal cell surfaces, respectively and are involved in specific interactions with fibronectin and salivary proteins (Hajishengallis *et al.*, 1994; Kuusela *et al.*, 1985).

It is important to realize that all types of interaction originate from the same fundamental forces (Van Oss, 1994), including the ever present Lifshitz-Van der

Waals forces, electrostatic forces, hydrogen bonding, hydrophobic bonding, and Brownian motion forces. Moreover, whereas specific interactions are highly directional, spatially confined and consequently operative over short distances, say smaller than 1 nm, the so-called non-specific association in microbial adhesion arises from interaction forces between all molecules in the entire cell and substratum and are consequently of a more long-range character. Therefore, in order to adequately describe microbial adhesive interactions, either between two bacterial species or between a bacterium and substratum surface, both the long-range, non-specific interaction forces and the short-range, specific interactions must be taken into consideration (Busscher and Weerkamp, 1987; Van Oss, 1990; Busscher *et al.*, 1992), as schematically indicated in Fig. 2. A specific bond is the result of short-range stereochemical molecular favorable interaction between highly localized groups on the bacterium and substratum. Non-specific forces, arising from Lifshitz-Van der Waals, electrostatic forces, hydrogen bonding, and hydrophobic bonding may be able to cause adhesion, i.e. to keep adhering cells on a substratum surface, but, unlike specific short-range stereochemical bonds, they often allow for sliding, an aspect that can be of major medical and ecological importance. Furthermore it has been argued that specific bonds are stronger than non-specific bonding, and that non-specific binding occurs immediately when the bacterium comes in the vicinity of a surface. However, specific bonding may be more time-consuming due to possible necessary rearrangement of stereochemical, molecular groups to interact, or even expression of new macromolecules by the organism in response to a surface (Jensen, 1992; McCarter, 1992).

## Aim of this Thesis

The aim of this thesis is to investigate the physical-chemical mechanisms of bacterial adhesion to adsorbed protein films, using innovative techniques including atomic force microscopy and microcalorimetry.

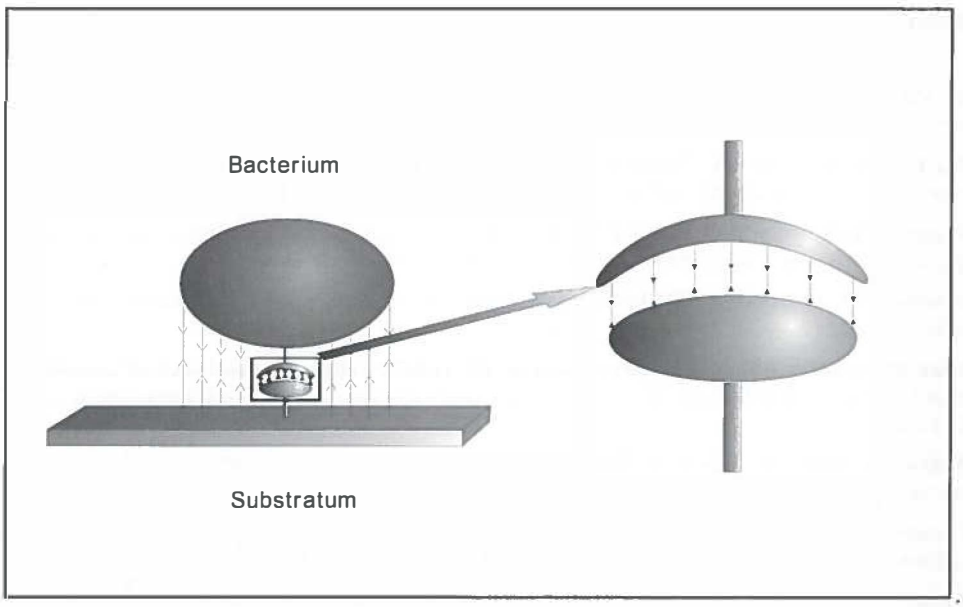


**Figure 2.** Both non-specific and specific interactions originate from the same fundamental physico-chemical forces.
A: Non-specific forces (Lifshitz-Van der Waals and electrostatic forces, hydrogen bonding and hydrophobic bonding) originate from the entire bacterium and for that reason may not be neglected as compared to the effect of specific adhesins.
B: A specific bond between stereo-chemical molecular groups on the cell and substratum surfaces consists of a combination of attractive Lifshitz-Van der Waals and electrostatic forces, hydrogen bonding and hydrophobic bonding, originating from highly localized chemical groups, which together form a stereo-chemical combination.

## References

**An YH, Friedman RJ (1998).** Concise review of mechanisms of bacterial adhesion to biomaterial surfaces. *J. Biomed. Mater. Res. Part B: Appl Biomater.* 43:338–348.

**Bos R, Van der Mei HC, Busscher HJ (1999).** Physico-chemistry of initial microbial adhesive interactions – its mechanisms and methods for study. *FEMS Microbiol. Rev.* 23: 179–230.

**Busscher HJ, Cowan MM, Van der Mei HC (1992).** On the relative importance of specific and non-specific approaches to oral microbial adhesion. *FEMS Microbial Rev.* 88:199–210.

**Busscher HJ, Weerkamp AH (1987).** Specfic and non-specific interactions in bacteria adhesion to solid substrata. *FEMS Microbiol. Rev.* 46:165–173.

**Chan RCY, Irvin RT, Bruce AW, Costerton JW (1985).** Competitive exclusion of uropathogens from human uroepithelial cells by lactobacillus whole cells and cell wall fragments. *Infect. Immun.* 47:84–89.

**Dankert J, Hogt AH, Feijen J (1986).** Biomedical polymers: bacterial adhesion, colonization and infection. *CRC Crit. Rev. Biocompatibility* 2:219–301.

**Elimelech M (1990).** Indirect evidence for hydratation forces in the deposition of polystyrene latex colloids on glass surfaces. *J. Chem. Soc. Faraday Trans.* 86:1623–1624.

**Escher A, Characklis WG (1990).** Modeling the initial events in biofilm accumulation. In Biofilms. pp. 445-486. Edited by W.G. Characklis & K.C. Marshall, John Wiley & Sons, New York, US.

**Fletcher M (1976).** The effects of proteins on bacterial attachment to polystyrene. *J. Gen. Microbiol.* 94:400-404.

**Fletcher M (1987).** How do bacteria attach to solid surfaces. *Microbiol. Sci.* 4:133-136.

**Gottenbos B, Van der Mei HC, Busscher HJ (1999).** Models for studying initial adhesion and surface growth in biofilm formation on surfaces. *Methods Enzymol.* 310:523–534.

**Gristina AG (1988).** Biomaterial-centered infection: microbial adhesion versus tissue integration. *Science* 237:1588–1595.

**Hajishengallis G, Koga T, Russell MW (1994).** Affinity and specificity of the interactions between *Streptococcus mutans* antigen I/II and salivary components. *J. Dent. Res.* 73:1493–1502.

**Hermansson M (1999).** The DLVO theory in microbial adhesion. *Coll. Surfaces B: Biointerfaces* 14:105–119.

**Jensen RA (1992).** Marine bioadhesive: Role of chemosensory recognition in marine invertebrates. *Biofouling*, 5:177–193.

**Kuusela P, Vartio T, Vuento M, Myhre EB (1985).** Attachment of staphylococci and streptococci on fibronectin, fibronectin fragments, and fibrinogen bound to a solid phase. *Infect. Immunol.* 50:77–85.

**Marshall KC (1985).** Mechanisms of bacterial adhesion at solid-water interfaces. In Bacterial Adhesion, pp. 133–161. Edited by D.C, Savage, M. Fletcher, Plenum Press, New York, US.

**Marshall KC, Stout R, Mitchell R (1971).** Mechanism of initial events in the sorption of marine bacteria to surfaces. *J. Gen. Microbiol.* 68:337–348.

**McCarter LL, Showalter RE, Sliverman MR (1992).** Genetic analysis of surface sensing in Vibrio parahaemolyticus. *Biofouling* 5:163–175.

**McDowell SG, An YH, Draughn RA, Friedman RJ (1995).** Application of a fluorescent redox dye for enumeration of metabolically active bacteria on titanium surfaces. *Lett. Appl. Microbiol.* 21:1–4.

**Muller E, Takeda S, Goldmann D, Pier GB (1991).** Blood proteins do not promote adherence of coagulase-negative staphylococci to biomaterials. *Infect. Immunol.* 59:3323–3326.

**Pashley RM, Israelachvili JN (1984).** DLVO and hydration forces between mica surfaces in $Mg^{2+}$, $Ca^{2+}$, $Sr^{2+}$ and $Ba^{2+}$ chloride solutions. *J. Coll. Interf. Sci.* 97:446–455.

**Pratt–Terpstra I, Weerkamp AH, Busscher HJ (1987).** Adhesion of oral streptococci from a flowing suspension to uncoated and albumin-coated surfaces. *J. Gen. Microbiol.* 133:3199–3260.

**Reid G, Van der Mei HC, Busscher HJ (1998).** Microbial biofilms and urinary tract infections. In Urinary Tract Infections, pp. 111–118. Edited by W. Brumfitt, T, Hamilton-Miller, and R.R. Bailey, Chapman & Hall, UK.

**Timmerman CP, Pleer A, Besnier JM, de Graaf L, Cremers F, Verhoef J (1991).** Characterization of a proteinaceous adhesin of *Staphylococcus epidermidis* which mediates attachment to polystyrene. *Infect. Immunol.* 59:4187–4192.

**Tojo M, Yamashita N, Goldmann DA, Pier GB (1988).** Isolation and characterization of a capsular polysaccharide adhesin from *Staphylococcus epidermidis*. *J. Infect. Dis.* 157:713–722.

**Van Loosdrecht MCM, Lyklema J, Norde W, Zehnder JB (1989).** Bacterial adhesion: A physicochermical approach. *Microb. Ecol.* 17:1–15.

**Van Oss CJ, Good RJ, Chaudhury MK (1986).** The role of Van der Waals forces and hydrogen bonds in "Hydrophobic interactions" between biopolymers and low energy surfaces. *J. Coll. Interf. Sci.* 111:378–390.

**Van Oss CJ, Good RJ, Chaudhury MK (1988).** Additive and nonadditive surface tension components and the interpretation of contact angles. *Langmuir* 4:884–891.

**Van Oss, CJ (1990).** A specific and specific intermolecular interactions in aqueous media. *J. Molecular Recognition* 3:128–136.

**Van Oss CJ (1994).** Polar or Lewis acid-base interactions. In Interfacial forces in aqueous media, pp. 18–46. Edit by C.J. Van Oss, Marcel Dekker, New York, US.

**Wood J, Sharma R (1995).** How long is the long-range hydrophobic attraction? *Langmuir* 11:4797–4802.

# 2

# Main techniques used in this study

In this chapter, the main techniques used in this thesis to evaluate the interaction of bacteria with protein-coated substrata, are described in detail. The techniques employed are either aimed at measuring the probability of adhesion, the force or the enthalpy of adhesion at the level of a single bacterial cell. It should be emphasized, however, that these, *in vitro* measurements may deviate from the *in vivo* situation where the whole system is much more complex and dynamic. *In vivo*, the substratum is usually under a dynamic mechanical stress, the surface may change composition with time and biological fluid flow may interact with the surface. Moreover, an incoming bacterium may just attach to the surface (reversibly), adhere firmly (irreversibly) or release a number of substances and/or present a number of adhesive receptors whose specificity, activity and numbers may be a function of time. Further investigations are needed to advance our understanding of the mechanisms of bacterial adhesion and prosthetic infection and the techniques described below are considered to be innovative and most appropriate for this purpose.

## Parallel Plate Flow Chamber

Bacterial adhesion to surfaces can, amongst other methods, be measured in a parallel plate flow chamber (PPFC). The parallel plate flow configuration is very common as it is simple to construct and the flow within the chamber can be mathematically analyzed rather easily. In the most commonly used experimental set-up, a pump provides a steady-state flow. The fluid enters a rectangular chamber from one side and leaves from the opposite side (Bruinsma *et al.*, 2001; Bakker *et al.*, 2003).

A typical schematic of a parallel plate flow chamber system is shown in Fig 1. The chamber consists of a stainless steel bottom and top part which encloses two plates separated from each other through a teflon spacer. The upper plate is usually made of glass, while the bottom plate is the surface under study. The bottom plate of the parallel plate flow chamber can be observed with a CCD-MXR camera mounted on a phase-contrast microscope. The camera can be coupled to an image analyzer, installed in a computer. With this set-up, direct observation of the deposition process in situ is possible without any additional shear forces acting on the deposited bacteria.

Thus the spatial arrangement of deposited bacteria with respect to each other is fully preserved. A pulse-free flow can be created by hydrostatic pressure and recirculation of the suspension by a roller pump. By means of a valve system it is possible to connect flasks which contain e.g. buffer, protein solution or bacterial suspension to the flow chamber without passing an air-liquid interface over the adsorbed conditioning film and/or adhering organisms.

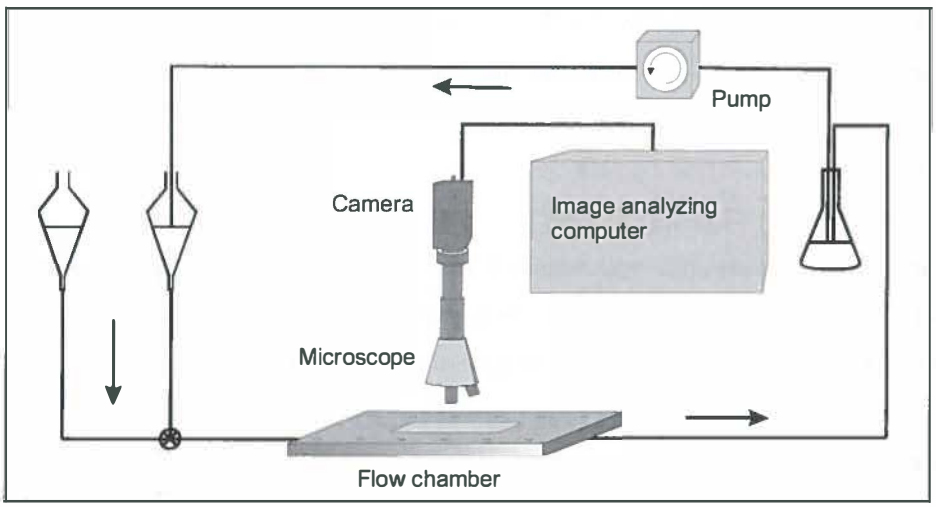


**Figure 1**. Schematic diagram of the parallel-plate flow chamber (PPLC). The arrow indicates the direction of the fluid flow.

The hydrodynamic force per unit of surface area exposed to a flow is defined as the shear stress ($\tau_w$), which is obtained by multiplying the shear rate ($\sigma$) by the absolute viscosity ($\eta$) of the fluid involved (McCabe, 1976):

$$\tau_w = \sigma\eta \qquad (1)$$

For most aqueous fluids, including buffers, urine, seawater and dilute suspensions of bacteria, the absolute viscosity is around $1 \times 10^{-3}$ Pa s at room temperature.

When laminar flow is well established, the theoretical shear rate in a PPFC at the bottom plate is given by the following formula (Elimelech, 1994):

$$\sigma = \frac{3Q_{pp}}{2(h_0/2)^2 w_0} \quad (2)$$

where $Q_{pp}$ is the volumetric flow rate, $w_0$ is the width of the flow chamber, $h_0$ is the distance between the parallel plates.

The shear force ($F$) exerted by the flow on an adhering organism is determined by multiplying the hydrodynamic force per unit of surface area by surface area (S):

$$F = \tau_w S \quad (3)$$

In our study, the flow rate was adjusted by hydrostatic pressure to 1.4 ml $min^{-1}$ yielding a shear rate of 15 $s^{-1}$ which, for a bacterial cell of 1 µm diameter (S = ½ bacterial surface area) implies a shear force of about $2.5 \times 10^{-5}$ nN.

## Atomic Force Microscopy

The Atomic Force Microscope (AFM) has become a powerful tool in biology and microbiology (Zlatanova *et al.*, 2000; Bolshakova *et al.*, 2001; Dufrene, 2001; Dufrene, 2002). Apart from the fact that AFM has proven useful in imaging the morphology of individual microbial cells and bacterial biofilms on solid surfaces, both in dried and hydrated states (Robichon *et al.*, 1999), it is being used increasingly for mapping interaction forces at microbial surfaces (Bowen *et al.*, 1998; Willing *et al.*, 2000; Beech *et al.*, 2002; Boyd *et al.*, 2002; Alfonso and Goldmann, 2003; Dufrene, 2003), such as Lifshitz-Van der Waals and electrostatic forces, solvation forces and steric-bridging forces. Moreover, local mechanical properties of bacterial surfaces have been probed (Fig. 2A).

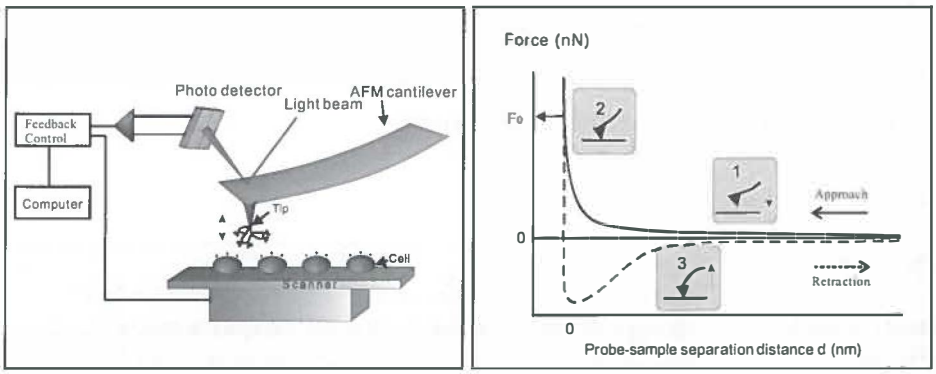


A B

**Figure 2**. Atomic force microscope. A: Schematic diagram. B: Force-separation curves. 1. No interaction forces were detected when the probe and the sample surface are far apart. 2. The repulsive forces are detected till the probe touches the sample surface. 3. The adhesive forces are recoded as the probe is retracted from the sample surface.

In principle, the AFM resembles a record player and a stylus profilometer. The ability of an AFM to achieve near atomic scale resolution depends on the three essential components as shown in Table 1 (Braga and Ricci, 1998).

Force measurements are made by recording the deflection of the cantilever while the cantilever is moved up and down, resulting in a "force-distance curve". These curves are converted to "force separation curves" (Fig. 2B) in which the force experienced by the probe is plotted as a function of the probe-sample separation distance. Approach curves can be fitted to a simple exponential function, where the interaction force $F$ is described as

$$F = F_0 \exp(-d/\Lambda) \quad (4)$$

in which $F_0$ is the repulsive force at zero separation between the interacting surfaces, $d$ the separation distance and $\Lambda$ the decay length of the interaction force $F$.

A force-distance curve records the variations of interaction forces as a bacterium or sample surface approaches the AFM tip, makes contact and then retracts from the tip. Such a force-distance curve provides valuable information on the tip-

bacteria interaction forces over the various sections of a bacterial cell surface. Adhesion maps can be produced from the retracting curves by taking the strongest adhesion force detected during retraction at each position and by plotting that value against the *x*-*y* position of each force-distance curve.

**Table 1**. The main components of AFM.

| Main components | Function |
|---|---|
| **Cantilever with sharp tip** | The tip is attached to the end of a cantilever with a low spring constant. The forces that are exerted between the tip and sample are measured by the extent of bending (or deflection) of the cantilever. |
| **Scanner** | A piezo-tube scanner controls the movement of the tip or sample in the *x*, *y* and *z*-directions. Typically, the maximum ranges are 80 × 80 μm in the *x*-*y* plane and 5 μm for the *z* – direction. |
| **Feedback control** | By calculating the difference signal in the photodiode quadrants, the interaction force between the tip and the sample can then be determined by Hooke's Law. |

## Microcalorimetry

Many biological processes, e.g. the assembly of viruses, protein folding, and biopolymer aggregation and adsorption, are characterized by a strong enthalpy-entropy compensation (Haynes and Norde,1995), that is, they occur spontaneously by virtue of an entropy increase that compensates for an unfavorable enthalpy effect, or vice versa. At constant temperature and pressure, which is usually the case in biological systems, all physico-chemical interactions, including adsorption, adhesion, coaggregation and co-adhesion, are determined by changes in the Gibbs energy ($G$) of a system. $\Delta G$ is composed of a change in enthalpy (H) and in entropy (S), according to

$$\Delta G = \Delta H - T\Delta S \tag{5}$$

where T is the temperature in Kelvin.

For a process to occur spontaneously, the change in Gibbs energy ($\Delta G$) is negative. The enthalpy tends to reach a minimum value reflecting the energetically most stable state, whereas the entropy strives for a maximum corresponding to the highest degree of randomness. As $\Delta G = \Delta H - T\Delta S$, this condition could be realized by either:

- a negative value for $\Delta H$ and a positive value for $T\Delta S$
- a negative value for $\Delta H$ and a less negative value for $T\Delta S$
- a positive value for $\Delta H$ and a more positive value for $T\Delta S$

The Gibbs energy ($\Delta G$) may be obtained from adsorption isotherms, given the condition that they are reversible (i.e., reflect thermodynamic equilibrium). However, this condition is usually not satisfied for protein adsorption and bacterial adhesion.

The enthalpy of a system is directly related to its heat content. More precisely, at constant pressure, and if no work other than that related to volume change is involved, changes in the enthalpy can be determined as the heat exchange between a system and its environment.

The entropy is a measure for the amount of energy in a system which is no longer available for doing work. It is related to the disorder or randomness in a system i.e. the more randomness, the higher the entropy. A positive entropy change is favorable. Direct determination of the entropy, however, is virtually impossible as it would require counting all conformationally and configurationally possibilities before and after a process.

In this study, dealing with irreversible protein adsorption, $\Delta S$ of the process is unknown. Thus, if a process is exothermic, $\Delta H < 0$, $T\Delta S$ may either be $> 0$ (favoring the process as well) or $< 0$ (opposing the process), as long as $\Delta G$ remains $< 0$. If it is endothermic, $\Delta H \geq 0$, the process must be entropy driven, i.e., $T\Delta S > 0$.

The enthalpy of interaction between bacterial cell surfaces and proteins can be directly determined using isothermal titration calorimetry (ITC) (Fig. 3A). Calorimetry allows the determination of heat exchanges between a system and its environment. ITC is a high-accuracy titration method for measuring the enthalpic part of binding affinities. In our experiments, four ampoules, connected with separate titration systems

at 25°C, were used inside the microcalorimeter, allowing separate quantification of the protein binding as occurring in the calorimeter. Each experiment consisted of consecutive injections of a ligand (protein) into the sample ampoule containing a solution of receptors (bacterial surface). When the two components bind, heat is either generated or absorbed. The use of a twin-type microcalorimeter allows the measurement of the heat (Q) flowing from the reaction ampoule as compared with a reference ampoule without titration. Signal collection was done using the dedicated Digitam software (Thermometric, Sweden) (Fig. 3B). By convention, the enthalpy change resulting from an exothermic process is negative and from an endothermic process positive.

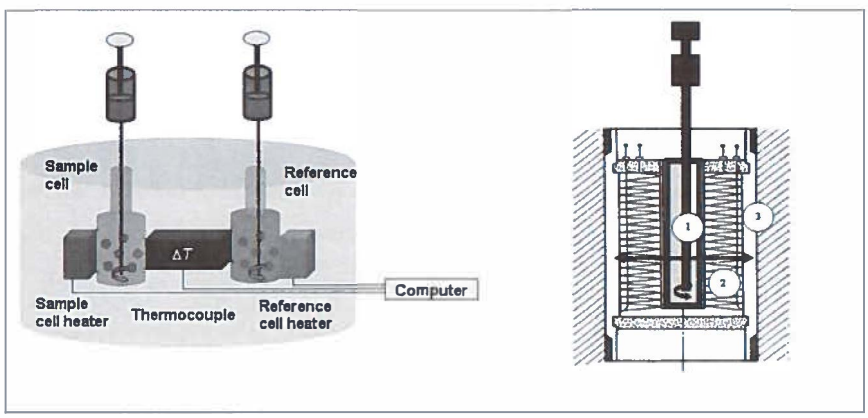


**Figure 3.** A: Schematic diagram of an isothermal titration calorimetry (ITC). B: Schematic view of the measuring unit during ITC experiments. The sample ampoule filled with a macromolecule solution (1) is lowered into the measuring unit and injections of the ligand is proceeded through a cannula. Upon binding a heat flux is generated (black arrow) and channeled through a pair of extremely sensitive thermopile Peltier elements (2) to the heat sink (3). The Peltier elements convert heat into a voltage signal that is proportional to the heat flow.

## References

**Alfonso JL, Goldmann WH (2003).** Feeling the forces: atomic force microscopy in cell biology. *Life Sci.* 72: 2553–2560.

**Bakker DP, Huijs FM, DeVries J, Klijnstra JW, Busscher JH, Van der Mei HC (2003).** Bacterial deposition to fluoridated and non-fluoridated polyurethane coatings with different elastic modulus and surface tension in a parallel plate and a stagnation point flow chamber. *Col. Surf. B: Biointerf* 32: 179–190.

**Beech IB, Smith JR, Steele AA, Penegar I, Campbell SA (2002).** The use of atomic force microscopy for studying interactions of bacterial biofilms with surfaces. *Col. Surf. B: Biointerf.* 23: 231–247.

**Bolshakova AV, Kiselyova OI, Filonov AS, Frolova OY, Lyubchenko YL, Yaminsky IV (2001).** Comperative studies of bacteria with an atomic force microscopy operating in different modes. *Ultramicrosc.* 86: 121–128.

**Boyd RD, Verran J, Jones MV, Bhakoo M (2002).** Use of Atomic Force Microscope to determine the effect of substratum surface topography on bacterial adhesion. *Langmuir* 18: 2343–2346.

**Bowen R, Hilal N, Lovitt RW, Wright CJ (1998).** Direct measurements of a force of adhesion of a single biological cell using an atomic force microscope. *Col. Surf. A: Physicochem. Eng. Asp.* 136: 231–234.

**Braga PC, Ricci D (1998).** Atomic Force Microscopy: Application to Investigation of *Escherichia coli* Morphology before and after Exposure to Cefodizime. *J Antimicrob Chemother* 42: 18–22

**Bruinsma GM, Van der Mei HC, Busscher HJ (2001).** Bacterial adhesion to surface hydrophilic and hydrophobic contact lenses. *Biomaterials* 22: 3217–3224.

**Dufrene YF (2001).** Application of Atomic Force Microscopy to microbial surfaces: from reconstituted cell surface layers to living cells. *Micron.* 32: 153–165.

**Dufrene YF (2002).** Atomic Force Microscopy: a powerful tool in Microbiology. *J. Bacteriol.* 184: 5205–5213.

**Dufrene YF (2003).** Recent progress in the application of atomic force microscopy imaging and force spectroscopy to microbiology. *Cur. Opin. In Microbiol.* 6: 317–323.

**Elimelech, M (1994).** Particle deposition on ideal collectors from dilute flowing suspensions: mathematical formulation, numerical solution, and simulations. *Sep. Technol.* 4:186–212.

**Haynes, C.A. Norde W (1995).** Structures and stabilities of adsorbed proteins, *J. Colloid Interface Sci.* 169, pp. 313–328.

**McCabe, WL, Smith JC (1976).** Fluid mechanics, pp. 84–112. In Unit Operations of Chemical Engineering. Edited by S. D. Kirkpatrick. McGraw-Hill, New York, US.

**Robichon D, Girard JC, Cenatiempo Y, Cavallier JF (1999).** Atomic force microscopy imaging of dried or living bacteria. *C R Acad Sci Paris, Life Sci* 322: 687–693.

**Willing GA, Ibrahim TH, Etzler FM, Neuman RD (2000).** New approach to the study of particle-surface adhesion using atomic force microscopy. *J. Col. Interf. Sci.* 226: 185–188.

**Zlatanova J, Lindsay SM, Leuda SH (2000).** Single molecule force spectroscopy in biology using the atomic force microscopy. *Progr. Bioph. Molec. Biol.* 74: 37–61.

# 3

# Calorimetric comparison of the interactions between salivary proteins and *Streptococcus mutans* with and without antigen I/II

Chun-Ping Xu, Betsy van de Belt-Gritter, Henk J. Busscher, Henny C. van der Mei, Willem Norde

Reprinted from *Colloids and Surfaces B: Biointerfaces* (2007) 54:193–199, with the permission from Elsevier

## Introduction

*Streptococcus mutans* is regarded as a commensal organism in the human oral cavity, but is frequently associated with dental caries. Therefore, considerable attention has been paid to factors that influence the distribution of *S. mutans* in the oral cavity and particularly to the mechanism whereby this organism adheres to and colonizes oral hard and soft tissues (Douglas and Russell, 1984). Oral surfaces *in vivo* are covered with an integument called the acquired pellicle, which is largely composed of a layer of adsorbed salivary proteins (Mayhall, 1970; Ørstavik and Kraus, 1973). The initial adhesion of bacteria to oral surfaces always involves an interaction between bacterial surface components and constituents of the acquired pellicle (Ørstavik, 1978).

The antigen I/II family of polypeptides is expressed at the cell surface of many oral streptococci (Jenkinson and Demuth, 1997) and plays an important role in their adhesion to surfaces. Antigens I/II are multifunctional adhesins that exert diverse binding activities, i.e., with salivary glycoproteins Hajishengallis *et al.*, 1994), host cell receptors (Soell *et al.*, 1994; Vernier *et al.*, 1996), and soluble extracellular matrix glycoprotein (Sciotti *et al.*, 1997; Petersen *et al.*, 2001). Antigen I/II surface proteins of *S. mutans* play a determinant role in its adhesion to salivary pellicles, and strains lacking antigen I/II hardly adhere to pellicles.

At constant temperature and pressure, which is usually the case in biological systems, all physico-chemical interactions, including adsorption, adhesion, coaggregation and co-adhesion, are determined by changes in the Gibbs energy ($G$) of a system. For a spontaneous process, the change in Gibbs energy ($\Delta G$) is negative. $\Delta G$ is composed of a change in enthalpy (H) and in entropy (S), according to

$$\Delta G = \Delta H - T\Delta S \qquad (1)$$

where T is the temperature in Kelvin. The enthalpy tends to reach a minimum value reflecting the energetically most stable state, whereas the entropy strives for a maximum corresponding to the highest degree of randomness. The enthalpy of a system is directly related to its heat content. More precisely, at constant pressure, and

if no work other than that related to volume change is involved, changes in the enthalpy can be determined as the heat exchange between a system and its environment. Direct determination of the entropy, however, is virtually impossible as it would require counting all conformational and configurationally possibilities before and after a process. Many biological processes, e.g. the assembly of viruses, protein folding, and biopolymer aggregation and adsorption, are characterized by a strong enthalpy-entropy compensation (Haynes and Norde, 1995), that is, they occur spontaneously by virtue of an entropy increase that compensates for an unfavorable enthalpy effect, or vice versa.

The enthalpy of interaction between bacterial cell surfaces and salivary proteins can be directly determined using isothermal titration calorimetry (ITC). Isothermal microcalorimetry is one of the most direct methods to measure the enthalpy change of formation of a complex at constant temperature, but has hitherto been used only scarcely in oral microbiology. Sand and Von Rege (1999) used a perfusion microcalorimeter to evaluate the adhesion of *Bacillus subtilis* to a gold surface and found that 85% of the total heat evolved originated from adhesion, whereas only 15% resulted from substrate oxidation. The microbial activity of biofilms on a substratum surface and the effects of biocides on microbial activity have also been monitored using microcalorimetry (Zhao *et al.*, 2000; Yu *et al.*, 2000). Furthermore, microcalorimetry was employed to determine the enthalpy of coaggregation between two oral bacterial pairs (Postollec *et al.*, 2003). Moreover, microcalorimetry was proven to be a useful instrument in the screening of potential antibacterial agents against *S. mutans* by detecting stoichiometric and energetic information on the metabolism of a population of microorganisms (Morgan *et al.*, 2001).

The aim of this study is to elucidate some aspects of the mechanism of adsorption of salivary proteins onto *S. mutans* cell surfaces, in particular with respect to the driving force for adsorption and the influence of pH. We compared the interactions between salivary proteins and *S. mutans* strains with and without antigen I/II. Adsorption of salivary proteins to *S. mutans* cell surfaces with (*S. mutans* LT11) and without (*S. mutans* IB03987) antigen I/II was determined spectrophotometrically

and corresponding adsorption enthalpies were measured using an isothermal titration microcalorimeter.

## Materials and Methods

### *Bacteria and culture conditions*

Two strains of *S. mutans* (LT11 with antigen I/II and the isogenic mutant IB03987 without antigen I/II), were used in this study. The bacterial cells were maintained at -80°C in brain-heart infusion (BHI; OXOID, Basingstoke, UK) broth containing 7% dimethylsulfoxide (DMSO; MERCK, Germany). For culturing, *S. mutans* LT11 was plated onto BHI agar plates, while *S. mutans* IB03987 was plated onto BHI agar supplemented with 5 μg $ml^{-1}$ kanamycine monosulfate (Sigma-Aldrich, Steinheim, Germany) and incubated in 5% $CO_2$ overnight at 37°C. Subsequently, bacterial colonies were precultured in 10 ml BHI batch culture overnight. This preculture was used to inoculate a main culture of 200 ml BHI broth, which was allowed to grow overnight. Bacteria were harvested by centrifugation at 6500*g* for 5 min at 10°C and washed twice with demineralized water. Bacterial chains and aggregates were broken by mild sonication on ice for 3 × 10 s at 30 W (Vibra Cell model 375, Sonics and Materials Inc., Danbury, Connecticut, USA). Sonication was carried out intermittently while cooling in an ice/water bath. This procedure was found not to cause cell lysis in any strain. Finally, bacteria were resuspended in adhesion buffer (2 mM potassium phosphate, 50 mM potassium chloride and 1 mM calcium chloride, pH 6.8 or 5.8 as adjusted by the addition of HCl) to a concentration of $5 \times 10^9$, $5 \times 10^8$, or $5 \times 10^7$ per ml, as determined in a Bürker-Türk counting chamber. Bacteria were used immediately after harvesting.

### *Saliva collection and preparation*

Human whole saliva from 20 healthy volunteers of both sexes was collected after stimulation by chewing Parafilm, into ice-chilled beakers. After the saliva was pooled and centrifuged twice at 10,000*g* for 5 min at 10°C, 0.2 M phenyl-methylsulfonylfluoride was added to a final concentration of 1 mM to inhibit protease

activity and, hence, to reduce protein breakdown. Afterwards, the solution was centrifuged again at 10,000*g* for 5 min, dialyzed overnight at 4°C against demineralized water, and freeze dried for storage. All volunteers gave their informed consent to saliva donation, in agreement with the ethics committee at the University Medical Center Groningen.

For experiments, the lyophilized saliva was dissolved in adhesion buffer (pH 6.8 or 5.8) at a concentration of 6 mg $ml^{-1}$. This solution was centrifuged at 10,000*g* for 5 min at 10°C and the supernatant was used. The protein content in the supernatant was 1.4 mg $ml^{-1}$, according to the Bio-Rad protein assay (Bio-Rad Laboratories, USA), with bovine serum albumin as standard. This protein concentration corresponds with the protein concentration in human whole saliva.

***Isothermal titration calorimetry***

The adsorption enthalpy of salivary proteins to the bacterial cell surfaces was measured in a twin-type, isothermal microcalorimeter TAM 2277 (Thermometric, Sweden). The calorimeter was positioned in a temperature-controlled environment (20 ± 0.1 °C), allowing a baseline stability of ± 0.1 μW over 24 h (Nordmark *et al.*, 1984). The instrument had an electrical calibration with a precision better than ±1 % and the accuracy was regularly determined by measuring the dilution enthalpy of concentrated sucrose solutions (Wu *et al.*, 1996). Experiments were performed isothermally at 25°C in stainless steel ampoules of 4 ml. Four ampoules, connected with separate titration systems at 25°C, were used inside the microcalorimeter, allowing separate quantification of protein adsorption as occurring in the calorimeter after each injection. The use of a twin-type microcalorimeter allows the measurement of the heat (Q) flowing from the reaction ampoule as compared with a reference ampoule. The output signal was collected as power, *P*, versus time, *t*, and was integrated and quantified to evaluate the isobaric heat exchange (i.e., the enthalpy change) during adsorption, using the dedicated Digitam 4.1 software (Thermometric, Sweden). Notably, the measured heat effect should be corrected by the heat of dilution of the proteins to obtain the net adsorption enthalpy (ΔH) (Briggner and Wadsö, 1991).

Typically, all four reaction ampoules were filled with 1.5 ml of bacterial suspension (5 × $10^7$, 5 × $10^8$, or 5 × $10^9$ cells $ml^{-1}$) in adhesion buffer solutions under constant stirring (90 rpm) with a specially designed two-blades stirrer, while the reference ampoules were filled with 1.5 ml adhesion buffer. The ampoules were lowered gradually in the microcalorimeter and left in the measuring position to reach thermal equilibration before data collection started. After equilibration, a stable baseline was obtained and the salivary proteins, dissolved in a buffer identical to the one of the bacterial suspension, were titrated into the reaction ampoules. Titration was done at a controlled rate of 2 $\mu l\ s^{-1}$ via a stainless steel cannula connected to a syringe. In order to study possible saturation of adsorption sites, salivary proteins were added in four consecutive injections of 60 µl into the ampoule with intervals of 40 min. All calorimetric experiments were done in five-fold.

***Determination of the amount of protein adsorbed***

Protein adsorption to the bacterial cell surfaces was determined in an ampoule outside the microcalorimeter, under identical conditions to those applied in the calorimeter. After each injection of salivary proteins solution, the bacterial suspensions were allowed 40 min incubation time, and then centrifuged at 10,000*g* for 5 min. The concentration of salivary proteins in the suspension, i.e. the amount of proteins that was not adsorbed, was determined by spectrophotometry at 280 nm. Subsequently, the amount of adsorbed salivary proteins was derived from a mass balance, i.e., by subtracting the amount of salivary proteins in the supernatant from the amount of proteins originally injected into the bacterial suspension. As a blank, a bacterial suspension was centrifuged without salivary proteins added.

## Results

***Calorimetry***

Adsorption enthalpies of the salivary proteins to the *S. mutans* cell surfaces, after correction for the heat of diluting the proteins in the bacterial suspensions (see Table 1), are presented in Fig. 1. The cumulative adsorption enthalpies after four consecutive injections are shown in Table 2, as expressed per bacterium and per $m^2$ bacterial cell

**Table 1.** Heat effects (μJ) upon injections of 60 μl salivary protein solution (1.4 mg $ml^{-1}$) into 1.5 ml adhesion buffer solution. ± denotes the SD over five separate experiments.

| Injection number | pH6.8 | pH5.8 |
|---|---|---|
| 1st | -908 ± 51 | -930 ± 59 |
| 2nd | -406 ± 14 | -563 ± 85 |
| 3rd | -344 ± 17 | -434 ± 86 |
| 4th | -233 ± 80 | -254 ± 92 |

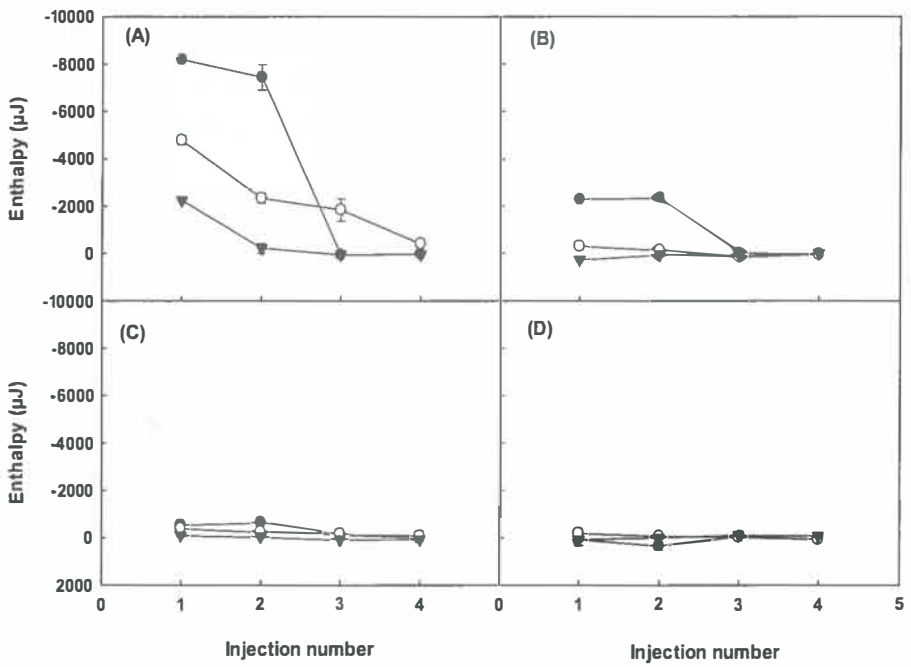


**Figure 1.** Adsorption enthalpies (μJ), after correction for dilution effects, of salivary proteins to *S. mutans* cell surfaces upon consecutive injections of 60 μl salivary protein solution (1.4 mg $ml^{-1}$) into 1.5 ml bacterial suspension of
(A) *S. mutans* LT11 at pH 6.8
(B) *S. mutans* LT11 at pH 5.8
(C) *S. mutans* IB03987 at pH 6.8
(D) *S. mutans* IB03987 at pH 5.8
(●) $5 \times 10^9$ bacteria per ml, (○) $5 \times 10^8$ bacteria per ml, (▼) $5 \times 10^7$ bacteria per ml.
Error bars indicate standard deviation based on five independent measurements.

surface. Metabolic activity of the bacteria will cause negligible heat effects, as all experiments were done in buffer, in the absence of nutrients. Salivary protein adsorption to the bacterial cell surfaces is an exothermic process in all cases, i.e. enthalpy is released upon adsorption. Adsorption of salivary proteins to *S. mutans* LT11 with antigen I/II is enthalpically much more favorable than to *S. mutans* IB03987, regardless of bacterial concentration. However, for *S. mutans* LT11 a hundred-fold increase in bacterial concentration only yielded a four- to five-fold increase in adsorption enthalpy at pH 6.8 and pH 5.8, respectively (see Fig. 1). Consecutive injections of saliva into *S. mutans* LT11 suspensions resulted in a significant decrease in adsorption enthalpy, suggesting fast saturation of binding sites at the bacterial surface by salivary proteins, whereas the smaller adsorption enthalpies for *S. mutans* IB03987 are almost independent of the number of injections. Furthermore, it is of interest to note that the adsorption enthalpy of salivary proteins to *S. mutans* LT11 is considerably smaller at pH 5.8 than at pH 6.8.

***Adsorption of salivary proteins***

Fig. 2 shows the amount of proteins adsorbed to the bacteria present in 1.5 ml suspension for each injection. The data indicate that upon the first injection, the bacterial surface is almost saturated with proteins, and furthermore, that the LT11 strain adsorbs more proteins than the IB03987 strain. The cumulative adsorption of protein after four consecutive injections expressed per bacterium and per $m^2$ bacterial cell surface is summarized in Table 3. The data for *S. mutans* LT11 show considerable protein adsorption at pH 6.8, which decreases only slightly at pH 5.8. To facilitate physical interpretation, the curves of Fig. 2 are converted into adsorption isotherms, displayed in Fig. 3, where the amount of protein adsorbed, $\Gamma$ , expressed in mass per unit of surface (mg $m^{-2}$) is plotted against the protein concentration in solution, $c_p$ (mg $ml^{-1}$), after adsorption. The isotherms show different patterns for *S. mutans* LT11 and *S. mutans* IB03987:

**Table 2.** Cumulative adsorption enthalpies per bacterium ($10^{-9}\mu J$) and per $m^2$ bacterial cell surface (mJ) after four consecutive injections of 60 µl salivary protein solution (1.4 mg $ml^{-1}$) into 1.5 ml bacterial suspensions of different bacterial concentrations. ± denotes the SD over five separate experiments.

| Concentration (per ml) | Cumulative adsorption enthalpies per bacterium ($10^{-9}\mu J$) | | | | Cumulative adsorption enthalpies per $m^2$ (mJ) | | | |
|---|---|---|---|---|---|---|---|---|
| | *S. mutans* LT11 | | *S. mutans* IB03987 | | *S. mutans* LT11 | | *S. mutans* IB03987 | |
| | pH6.8 | pH5.8 | pH6.8 | pH5.8 | pH6.8 | pH5.8 | pH6.8 | pH5.8 |
| $5 \times 10^9$ | -2073 ± 97 | -614 ± 41 | -165 ± 48 | -60 ± 75 | -660 ± 31 | -196 ± 13 | -53 ± 15 | -19 ± 24 |
| $5 \times 10^8$ | -12500±1268 | -293 ± 101 | -1061 ± 283 | 237 ± 142 | -3981 ± 404 | -93 ± 32 | -338± 90 | -75 ± 45 |
| $5 \times 10^7$ | -31707± 976 | 5867 ± 844 | -1107 ± 638 | 7853 ± 1011 | -10098 ± 311 | 1872± 269 | 353± 203 | 2501 ± 322 |

* for calculation of the adsorption enthalpies per $m^2$, it was assumed that the bacterial cell radius was 0.5 µm.

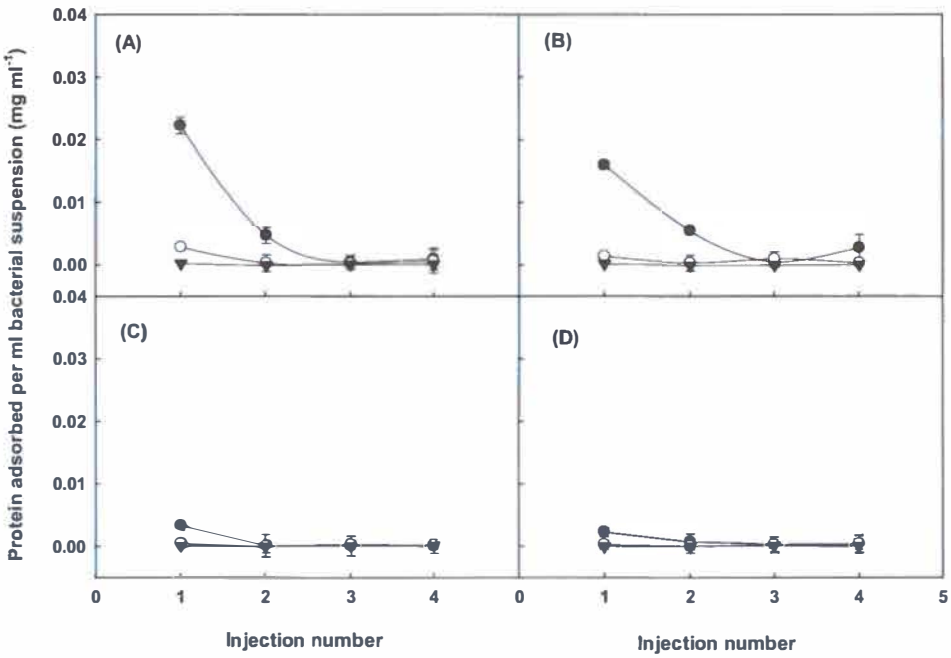


**Figure 2.** Amounts of adsorbed salivary proteins (mg $ml^{-1}$) upon consecutive injections of 60 µl salivary protein solution (1.4 mg $ml^{-1}$) into 1.5 ml bacterial suspension of
(A) *S. mutans* LT11 at pH 6.8
(B) *S. mutans* LT11 at pH 5.8
(C) *S. mutans* IB03987 at pH 6.8
(D) *S. mutans* IB03987 at pH 5.8
(●) $5 \times 10^9$ bacteria per ml, (○) $5 \times 10^8$ bacteria per ml, (▼) $5 \times 10^7$ bacteria per ml.
Error bars indicate standard deviation based on five independent measurements.

a. the (semi-)plateau value of the isotherm is about twice as high for *S. mutans* LT11 than for IB03987;
b. the (semi-)plateau for *S. mutans* LT11 at pH 5.8 is slightly smaller than at pH 6.8, whereas for *S. mutans* IB03987 there is no significant difference between the plateaus of the isotherms at both pH-values;
c. the (semi-)plateau is reached at a lower protein concentration for *S. mutans* LT11 than for IB03987.

**Table 3.** The cumulative amounts of adsorbed proteins per bacterium ($10^{-12}$ mg) and per $m^2$ bacterial cell surface (mg $m^{-2}$) after four consecutive injections of 60 µl salivary protein solution (1.4 mg $ml^{-1}$) into 1.5 ml bacterial suspension of different bacterial concentrations. ± denotes the SD over five separate experiments.

| Concentration (per ml) | Cumulative adsorption per bacterium ($10^{-12}$mg) | | | | Cumulative adsorption per $m^2$ (mg $m^{-2}$) | | | |
|---|---|---|---|---|---|---|---|---|
| | *S. mutans* LT11 | | *S. mutans* IB03987 | | *S. mutans* LT11 | | *S. mutans* IB03987 | |
| | pH6.8 | pH5.8 | pH6.8 | pH5.8 | pH6.8 | pH5.8 | pH6.8 | pH5.8 |
| $5 \times 10^9$ | 3.8 ± 0.7 | 3.3 ± 0.5 | 0.5± 0.2 | 0.5 ± 0.2 | 1.2 ± 0.2 | 1.1± 0.2 | 0.2 ± 0.1 | 0.2 ± 0.1 |
| $5 \times 10^8$ | 5.4 ± 1.2 | 4.2± 1.0 | 1.1 ± 0.9 | 1.1 ± 1.4 | 1.7 ± 0.4 | 1.3 ± 0.3 | 0.4± 0.3 | 0.4 ± 0.4 |
| $5 \times 10^7$ | 6.6 ± 1.9 | 5.0 ± 1.6 | 3.4± 2.6 | 1.8 ± 4.6 | 2.1± 0.6 | 1.6 ± 0.5 | 1.1± 0.8 | 0.6 ± 1.5 |

* for calculation of the adsorbed amounts per $m^2$, it was assumed that the bacterial cell radius was 0.5 µm.

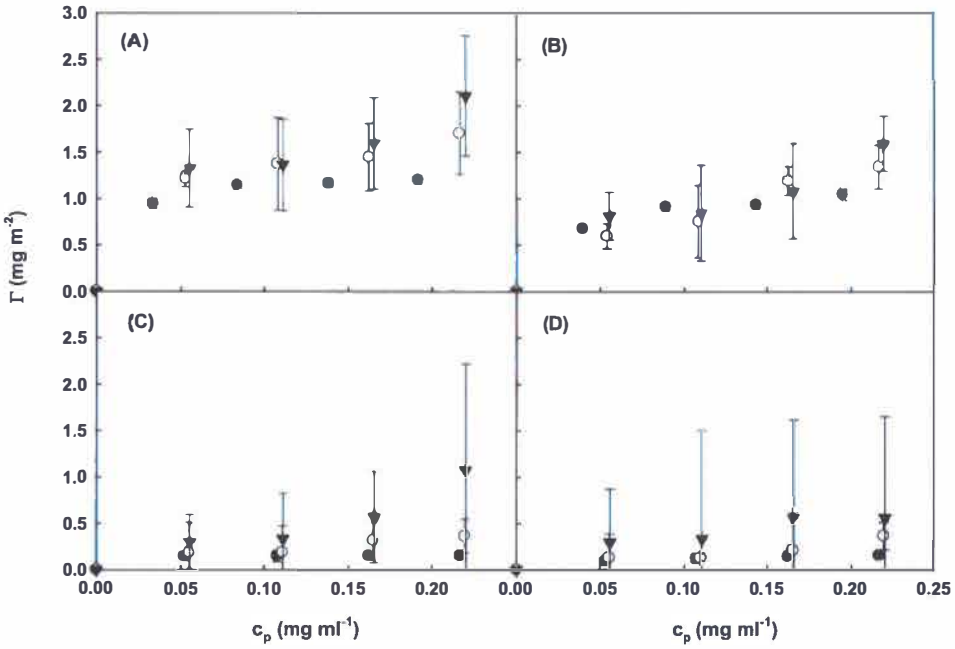


**Figure 3.** Adsorption isotherms of the amount of adsorbed proteins per unit area bacterial cell surface (mg $m^{-2}$) as a function of the concentration of free protein in solution (mg $ml^{-1}$) after consecutive injections of salivary protein solutions (1.4 mg $ml^{-1}$) into 1.5 ml bacterial suspension of
(A) *S. mutans* LT11 at pH 6.8
(B) *S. mutans* LT11 at pH 5.8
(C) *S. mutans* IB03987 at pH 6.8
(D) *S. mutans* IB03987 at pH 5.8
(●) $5 \times 10^9$ bacteria per ml, (○) $5 \times 10^8$ bacteria per ml, (▼) $5 \times 10^7$ bacteria per ml.
Error bars indicate standard deviation based on five independent measurements.

## Discussion

Bacterial adhesion and aggregation in the oral cavity are mediated by salivary components, especially proteins (Kashket and Donaldson, 1972). In adhesion and aggregation involving biological surfaces, two types of interactions may be distinguished: (a) non-specific binding based on e.g. electrostatic and Lifshitz-Van der Waals interactions, and hydrophobic effects and (b) specific binding based on strong,

short-range interactions, such as ligand-receptor binding (Gibbons and Querishi, 1979). Petersen *et al.* (2002) investigated the role of the *S. mutans* antigen I/II proteins in adhesion and modulation of cell surface characteristics and showed that the antigen I/II of *S. mutans* is involved in adhesion of the bacterial cells to a salivary conditioning film.

In this study, we investigated the mechanism of interaction between salivary proteins and two *S. mutans* strains, one with antigen I/II and another one without antigen I/II on its cell surface, in more detail. The observation in Fig. 1 that the interaction of salivary proteins with *S. mutans* LT11 is enthalpically much more favorable than with *S. mutans* IB03987 is in line with the known active involvement of antigen I/II in the binding process. Clearly, some of the salivary proteins bind specifically and with high enthalpy to antigen I/II. The trends in the curves of Figs. 1A and 1B reveal that these specific binding surfaces are saturated after the second or third addition of salivary proteins. It is remarkable that a 100-fold increase in bacterial concentration leads to only a four-fold (*S. mutans* LT11, pH 6.8) or five-fold (*S. mutans* LT11, pH 5.8) increase in interaction enthalpy. This might be caused by depletion of the saliva from specific binding proteins before all available antigen I/II binding sites are saturated. Furthermore, the smaller enthalpy effects at pH 5.8 as compared to those at pH 6.8 indicate a prominent role of electrostatic interaction. Because specific interactions are usually of the short-range type, the electrostatic attraction probably involves ion pairing. More detailed interpretation is not justified as long as the charged groups on the antigen I/II, and the proteins that participate in the binding process are not identified.

The adsorption data are in agreement with the calorimetric results. The adsorption isotherms in Fig. 3 clearly show that the *S. mutans* LT11 strain possessing antigen I/II binding sites at its surface binds higher amounts of proteins and with higher affinity than the IB03987 strain does. Similar to the calorimetric data, the adsorption isotherms indicate that protein binding at LT11 at pH 6.8 is more favorable than at pH 5.8. Tamura *et al.* (1999) also found that the amount of salivary proteins adsorbed at cells of *Streptococcus mitis* ATCC 903 is at a maximum at pH 7.0, and falls off as pH decreased. As a change in pH varies the charge on the proteins as well

as on the bacterial surfaces, Tamura's and our results indicate that adsorption is strongly influenced by electrostatic interactions. In model studies, the protein surface concentration that is compatible with the formation of a full monolayer is in the range of a few mg $m^{-2}$, the exact value depending on the size and shape of the protein molecule involved (Haynes and Norde, 1994). Hence, the adsorbed amounts of salivary proteins at the bacterial surfaces do not seem to exceed monolayer coverage or, in case of adsorption at the cells of *S. mutans* 1B03987, reflect sub-monolayer coverage. Thus, both our calorimetric data and adsorption isotherms strongly confirm the mediating role of antigen I/II in the binding of salivary proteins to the surfaces of *S. mutans* cells.

Of course, the negative value of $\Delta H$ per bacterium is expected to increase with increasing protein coverage (i.e., with increasing saturation of the energetically favorable binding sites). This is indeed shown for the antigen I/II possessing *S. mutans* LT11 strain at pH 6.8. For *S. mutans* 1B03987, without antigen I/II, protein adsorption is essentially a-thermal, i.e., $\Delta H \approx 0$. It implies that the driving force for the non-specific adsorption of salivary proteins at the surface of *S. mutans* 1B03987 is entropy increase ($\Delta S > 0$). Entropy-driven adsorption has quite generally been reported for proteins at non-specifically binding sorbent surfaces (Haynes and Norde, 1994).

A characteristic feature for the *S. mutans* LT11 strain is the surface coverage by the proteins where $\Delta H$ becomes invariant above that coverage. It marks the transition range between specifically and non-specially adsorbing proteins. Fig. 4A shows that at about $5 \times 10^{-12}$ mg proteins per bacterium, the specifically binding antigen I/II sites are fully saturated. Another interesting observation is that $\Delta H$ per bacterium is larger (more negative) for lower bacterial concentrations in the suspensions. This could be well explained by depletion of the energetically most favorably binding protein species from the saliva sample. Among the 35 different proteins present in human saliva Vitorino *et al.*, 2004), Douglas and Russell (1984) recognized six different proteins capable of binding to the surface of *S. mutans*. Most probably, these proteins bind with different energy effects. In case of the lowest bacterial concentration (i.e., $5 \times 10^{7}$ cell $ml^{-1}$), the total number of available antigen I/II binding sites is so limited that they become saturated with the energetically most favorably binding protein. The highest

bacterial concentration ($5 \times 10^9$ cell $ml^{-1}$) offers 100 times more binding sites to the same amount of saliva sample. Then, a much smaller fraction of the antigen I/II binding sites of the LT11 strain may become saturated with the strongest binding protein species, another fraction with the second strongest binding protein, in that order. The result is a lower enthalpy effect per bacterium (under conditions of full saturation of the binding sites) for the higher bacterial concentration, as is observed in Fig. 4A.

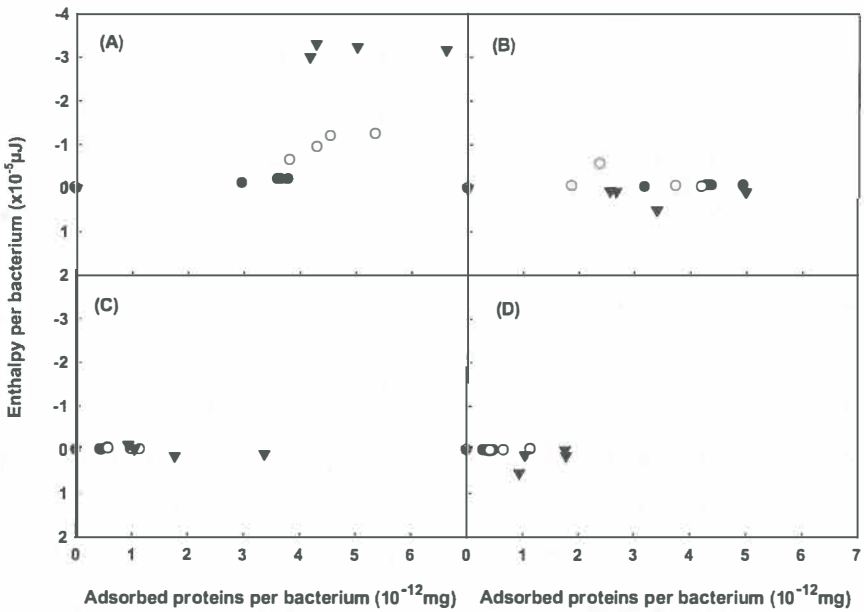


**Figure 4.** Adsorption enthalpies per bacterium (µJ) as a function of the amount of adsorbed proteins per bacterium (mg) after consecutive injections of salivary protein solutions (1.4 mg $ml^{-1}$) into 1.5 ml bacterial suspension of
(A) *S. mutans* LT11 at pH 6.8
(B) *S. mutans* LT11 at pH 5.8
(C) *S. mutans* IB03987 at pH 6.8
(D) *S. mutans* IB03987 at pH 5.8
(●) $5 \times 10^9$ bacteria per ml, (○) $5 \times 10^8$ bacteria per ml, (▼) $5 \times 10^7$ bacteria per ml.

Finally, the binding enthalpy for *S. mutans* LT11 in the suspension containing 5 × $10^7$ cells and at pH 6.8 (i.e., conditions at which all antigen binding sites are assumed to be occupied by specifically binding proteins) may be compared with literature data on non-specific and specific binding. First, in case of physical, non-specific adsorption of proteins at various surfaces the enthalpy effects reported do not exceed a few mJ per $m^2$ (Haynes and Norde, 1994). The adsorption enthalpy of -$10^4$ mJ $m^{-2}$ for salivary protein(s) binding at the surface of LT11 is by orders of magnitude more favorable in enthalpy and, hence, supports a specific, high-affinity binding mechanism. Moreover, assuming ~$10^5$ antigen I/II binding sites on the *S. mutans* LT11 cell (Busscher *et al.*, 2007), a measured enthalpy effect of –32 × $10^{-12}$ μJ per binding site can be calculated, which exceeds the values reported for specific interactions in biological s systems (Moy *et al.*, 1994) by far and supports a specific, extremely high-affinity binding mechanism.

## Conclusion

This study shows that (micro-)calorimetry in combination with binding isotherms, is a powerful technique to investigate such a complicated process as the adsorption of proteins from a complex mixture (e.g. saliva) on the surfaces of bacterial cells. It was thus assessed that antigen I/II at the surface of *S. mutans* LT11 specifically binds different protein species with different affinities from the large pool of proteins present in whole saliva. This antigen I/II protein binding is strongly influenced by electrostatic interactions, as the binding is much more favorable at pH 6.8 than pH 5.8. After saturation of the antigen I/II binding sites, the surface of the *S. mutans* LT11 cells is able to adsorb more protein a-thermally (i.e., with zero enthalpy effect) in a non-specific manner, similar to the non-specific adsorption at the antigen I/II-lacking surfaces of *S. mutans* IB03987.

## References

**Briggner LE, Wadsö I (1991).** Test and calibration processes for microcalorimeters, with special reference to heat conduction instruments used with aqueous systems. *J. Biochem. Biophys. Methods* 22:101–118.

**Busscher HJ, Van de Belt–Gritter B, Dijkstra RJB, Norde W, Van der Mei HC (2007).** Intermolecular Forces and Enthalpies in the Adhesion of *Streptococcus mutans* and an Antigen I/II-Deficient Mutant to Laminin Films. *J. Bacteriol.* 189:2988–2995.

**Douglas CWI, Russell RRB (1984).** The adsorption of human salivary components to strains of the bacterium *Streptococcus mutans*. *Archs. Oral. Biol.* 29:751–757.

**Gibbons RJ, Qureshi JV (1979).** Inhibition of adsorption of *Streptococcus mutans* strains to saliva-treated hydroxyapatite by galactose and certain amines. *Infect. Immun.* 26:1214–1217.

**Hajishengallis G, Koga T, Russell MW (1994).** Affinity and specificity of the interactions between *Streptococcus mutans* antigen I/II and salivary components. *J. Dent. Res.* 73: 1493–1502.

**Haynes CA, Norde W (1994).** Globular proteins at solid/liquid interfaces. *Colloid Surface B* 2 :517–566.

**Haynes CA, Norde W (1995).** Structures and stabilities of adsorbed proteins. *J. Colloid Interface Sci.* 169:313–328.

**Jenkinson HF, Demuth DR (1997).** Structure, function and immunogenicity of streptococcal antigen I/II polypeptides. *Mol. Microbiol.* 23:183–190.

**Kashket S, Donaldson CG (1972).** Saliva-induced aggregation of oral streptococci. *J. Bacteriol.* 112:1127–1133.

**Mayhall CW (1970).** Concerning the composition and source of the acquired enamel pellicle of human teeth. *Archs. Oral. Biol.* 15:1327–1341.

**Morgan TD, Beezer AE, Mitchell JC, Bunch AW (2001).** A microcalorimetric comparison of the anti-*Streptococcus mutans* efficacy of plant extracts and antimicrobial agents in oral hygiene formulations. *J. Applied Microbiol.* 90:53–58.

**Moy VT, Florin EL, Gaub HE (1994).** Intermolecular forces and energies between ligands and receptors. *Science* 266:257–259.

**Nordmark MG, Laynez J, Schön A, Suurkuusk J, Wadsö I (1984).** Design and testing of a new microcalorimetric vessel for use with living cellular systems and in titration experiments. *J. Biochem. Biophys. Methods* 10:187–202.

**Petersen FC, Assev S, Van der Mei HC, Busscher HJ, Scheie AA (2002).** Functional variation of the antigen I/II surface protein in *Streptococcus mutans* and *Streptococcus intermedius*. *Infect. Immun.* 70:249–256.

**Petersen FC, Pasco S, Ogier J, Klein JP, Assev S, Scheie AA (2001).** Expression and functional properties of the *Streptococcus intermedius* surface protein antigen I/II. *Infect. Immun.* 69:4647–4653.

**Postollec F, Norde W, Van der Mei HC, Busscher HJ (2003).** Enthalpy of interaction between coaggregating and non-coaggregating oral bacterial pairs-a microcalorimetric study. *J. Microbiol. Methods* 55:241–247.

**Ørstavik D, Kraus FW (1973).** The acquired pellicle: immunofluorescent demonstration of specific proteins. *J. Oral. Path.* 2:60–76.

**Ørstavik D (1978).** The in-vitro attachment of an oral Streptococcus sp. to the acquired tooth enamel pellicle. *Archs. Oral. Biol.* 23:167–174.

**Sand W, Von Rege H (1999).** Evaluation and quantification of bacterial attachment, microbial activity, and biocide efficacy by microcalorimetry. *Methods Enzymol.* 210:361–374.

**Sciotti MA, Yamodo I, Klein JP, Ogier J (1997).** The N-terminal half part of the oral streptococcal antigen I/IIf contains two distinct binding domains. *FEMS Microbiol. Lett.* 153:439–445.

**Soell M, Holveck F, Scholler M, Wachsmann D, Klein JP (1994).** Binding of *Streptococcus mutans* SR protein to human monocytes: Production of tumor necrosis factor, interleukin 1, and interleukin 6. *Infect. Immun.* 62:1805–1812.

**Tamura M, Hirano Y, Hayashi K (1999).** The phenomenon of salivary protein adsorption onto *Streptococcus mitis* ATCC 903 cells. *J. Oral. Sci.* 41:169–172.

**Vernier A, Diab M, Soell M, Haan-Archipoff G, Beretz A, Wachsmann D, Klein JP (1996).** Cytokine production by human epithelial and endothelial cells following exposure to oral viridans streptococci involves lectin interactions between bacteria and cell surface receptors. *Infect. Immun.* 64:3016–3022.

**Vitorino R, Lobo MJC, Ferrer-Correira AJ, Dubin JR, Tomer KB, Domingues PM, Amado FML (2004).** Identification of human whole saliva protein components using proteomics. *Proteomics* 4:1109–1115.

**Wu CF, Chen WY, Lee JF (1996).** Microcalorimetric Studies of the Interactions of Imidazole with Immobilized Cu(II): Effects of pH Value and Salt Concentration. *J. Colloid Interface Sci.* 183:236–242.

**Yu L, Hu YG, Lon RS, Zhang HL, Nan ZD, Li FH (2000).** The effects of environmental conditions on the growth of petroleum microbes by microcalorimetry. *Thermochim. Acta* 359:95–101.

**Zhao R, Liu Y, Xie Z, Shen P, Qu S (2000).** A microcalorimetric method for studying the biological effects of $La^{3+}$ on Escherichia coli. *J. Biochem. Biophys. Methods* 46:1–9.

# 4

# Interaction forces between salivary proteins and *Streptococcus mutans* with and without antigen I/II

Chun-Ping Xu, Betsy van de Belt-Gritter, René J. B. Dijkstra, Willem Norde, Henny C. van der Mei, Henk J. Busscher

Reprinted from *Langmuir* (2007) 23:9423-9428, with the permission from American Chemical Society

## Introduction

*Streptococcus mutans*, a common inhabitant of the human oral cavity, plays a major role in the initiation of dental caries, which is one of most prevalent and costly infectious diseases worldwide. The mechanisms by which oral streptococci disseminate and contribute to oral diseases involve initial adhesion events to salivary protein-coated oral surfaces. Adhesion of *S. mutans* to salivary protein films has been shown to be mediated by different mechanisms (Troffer-Charlier *et al.*, 2002). Long-range, non-specific interaction forces like Lifshitz-Van der Waals and/or electrostatic interactions are responsible for the approach of an organism to a substratum surface. Once in the close vicinity, specific interactions between the pathogen and components of the salivary coating become operative, as mediated amongst others by the streptococcal antigen I/II protein.

The antigen I/II family of polypeptides is expressed at the cell surface of many oral streptococci and plays an important role in their adhesion to surfaces (Jenkinson and Demuth, 1997). Antigens I/II are multifunctional adhesins that exert diverse binding activities, i.e., with salivary glycoproteins, host cell receptors, and soluble extracellular matrix glycoproteins. Antigen I/II surface proteins in *S. mutans* play a determining role in its adhesion to salivary coatings or pellicles, and strains lacking antigen I/II hardly adhere to pellicles (Hajishengallis *et al.*, 1994; Sciotti *et al.*, 1997; Soell *et al.*, 1994; Petersen *et al.*, 2001; Vernier *et al.*, 1996).

Atomic force microscopy (AFM) is a surface imaging technique, which operates by sensing the force between a very sharp probe attached to a flexible cantilever and a sample surface (Binnig *et al.*, 1986). Recently, AFM has emerged as a powerful tool to directly measure the interaction forces associated with biological systems in an aqueous environment (Dufrêne, 2003). AFM force measurements have been further applied to microbial systems, measuring the interaction between bacteria and a substratum surface (Bowen *et al.*, 2002). After proper immobilization of a bacterium, either to the cantilever tip of the AFM or to an appropriately prepared substratum surface, or both, the two interacting surfaces can be brought together. The force-distance curve measured upon approach usually shows a repulsive barrier that

has to be overcome prior to adhesion, while upon retraction adhesion forces are revealed (Van der Mei *et al.*, 2000). When adhering to biomaterial surfaces, cells of *Enterococcus faecalis* strains expressing Aggregation substance (Agg) showed mutual attraction forces of about -2.5 nN, which is almost two-fold higher than the interaction between cells lacking Agg. The strong interaction forces between the strains with Agg reduced after adsorption of antibodies against Agg, demonstrating the influence of specific antibodies on forces between *E. faecalis* cells (Waar *et al.*, 2005). Moreover, AFM indicated that a pair of co-aggregating actinomyces and streptococci interacted through three- to four-fold higher forces than a pair lacking the ability to co-aggregate and that interact through an adhesion force of only 1 nN (Postollec *et al.*, 2006).

Insight in the forces acting between salivary proteins and streptococcal cell surfaces and the role of antigen I/II in mediating the interaction has not yet been obtained. In this study, we aim at investigating the interaction forces between salivary proteins and *S. mutans* strains with (LT11) and without (IB03987) antigen I/II using AFM. The AFM tip was coated with salivary proteins and bacteria were trapped in a membrane filter. Results are compared with adhesion of the strains to a salivary coating on glass in a parallel plate flow chamber. All experiments are done at pH 5.8 and 6.8 in order to reveal a possible influence of electrostatic interactions.

## Materials and Methods

### *Bacterial Strains and Culture conditions*

Two strains of *S. mutans* (LT11 with antigen I/II and an isogenic mutant IB03987 without antigen I/II), were used in this study. The bacteria were maintained at -80°C in brain-heart infusion (BHI; OXOID, Basingstoke, UK) broth containing 7% dimethylsulfoxide (MERCK, Germany). For culturing, *S. mutans* LT11 was plated onto BHI agar plates, while *S. mutans* IB03987 was plated onto BHI agar supplemented with 5 μg $ml^{-1}$ kanamycine monosulfate (Sigma-Aldrich, Sterinheim, Germany) and incubated in 5% $CO_2$ overnight at 37°C. Subsequently, bacterial colonies were precultured in 10 ml batch culture for 24 h. This preculture was used to inoculate a main culture of 200 ml broth, which was allowed to grow overnight.

Bacteria were harvested by centrifugation at 5000 × g for 5 min at 10°C and washed twice with demineralized water. Bacterial chains and aggregates were broken by mild sonication on ice for 3 × 10 s at 30 W (Vibra Cell model 375, Sonics and Materials Inc., Danbury, Connecticut, USA). Sonication was carried out intermittently while cooling in an ice/water bath. This procedure was found not to cause cell lysis in any strain. Finally, bacteria were resuspended in adhesion buffer (2 mM potassium phosphate, 50 mM potassium chloride and 1 mM calcium chloride, pH 6.8 or 5.8 as adjusted by the addition of HCl) to a concentration of $1 \times 10^5$ cells per ml for AFM experiments or $3 \times 10^8$ cells per ml for flow chamber experiments, as determined in a Bürker-Türk counting chamber. Bacteria were used immediately after harvesting.

***Saliva Collection and Preparation***

Human whole saliva from 20 healthy volunteers of both sexes was collected after stimulation by chewing Parafilm, into ice-chilled beakers. After the saliva was pooled and centrifuged twice at 10,000 × *g* for 5 min at 10°C, 0.2 M phenylmethylsulfonylfluoride, was added to a final concentration of 1 mM to inhibit protease activity and, hence, to reduce protein breakdown. Afterwards, the solution was centrifuged again at 10,000 × *g* for 5 min, dialyzed overnight at 4 °C against demineralized water, and freeze dried for storage. All volunteers gave their informed consent to saliva donation, in agreement with the rules set out by the Ethics Committee at the University Medical Center Groningen.

For experiments, the lyophilized saliva was dissolved in adhesion buffer (pH 6.8 or 5.8) at a concentration of 6 mg $ml^{-1}$ for AFM experiments or 1.5 mg $ml^{-1}$ for flow chamber experiments. This solution was centrifuged at 10,000 × *g* for 5 min at 10°C and the supernatant was used.

***Atomic force microscopy***

For AFM, bacteria were immobilized in an isopore polycarbonate membrane (Kasas and Ikai, 1995), while AFM tips (DNP from Veeco, Woodbury, USA) were coated with a salivary film by immersion in reconstituted saliva (6 mg $ml^{-1}$ in adhesion buffer, pH 5.8 or 6.8) for 30 min with the aid of a micromanipulator. All membranes with

immobilized bacteria and saliva-coated AFM tips were immediately used for measurements.

AFM measurements were done at room temperature in adhesion buffer using a Dimension 3100 system (Nanoscope III Digital Instrument, Woodbury, USA). An array of 32 × 32 force-distances at scan rates of about 2 Hz were collected over the entire field of view when a bacterium was imaged (image size ± 2 × 2 μm). The slopes of the retraction force curves in the region where probe and sample are in contact were used to convert the voltage into cantilever deflection. The conversion of deflection into force was carried out as has been previously described by others using a nominal spring constant for the saliva-coated tips of 0.06 N $m^{-1}$, as determined by the Cleveland method (Cleveland *et al.*, 1993; Dufrêne, 2003). Typically, a 20% standard deviation is found when calibrating 10 cantilevers. Force-distance curves taken over the top of each bacterium studied, were analyzed in order to determine various characteristic parameters. Approach curves were fitted to a simple exponential function, where the interaction force $F$ is described as

$$F = F_0 \exp(-d/\Lambda) \quad (1)$$

in which $F_0$ is the repulsive force at zero separation between the interacting surfaces, $d$ the separation distance and $\Lambda$ the decay length of the interaction force $F$.

Adhesion maps were produced from the retracting curves by taking the strongest adhesion force detected during retraction at each position as the value for adhesion and by plotting that value against x-y position of each force-distance curves. Note that the salivary proteins were irreversibly attached to the AFM tips. Tips without an adsorbed salivary film typically demonstrated adhesion forces on clean glass of -0.2 nN, while in the presence of a salivary coating these forces amounted -1.0 nN. Saliva coated tips prior to and after 32 × 32 scanning of a bacterial cell surface, demonstrated exactly the same forces on clean glass, from which we conclude that if any material comes off the tip, this is not influential on the maximal adhesion forces measured. From the adhesion maps, a selected area of ~ 800 × 800 $nm^2$ over the top of each bacterium was selected to generate distribution histograms. From these histograms

mean, median, mode and range values were calculated for the repulsive force at contact upon approach and its decay length as well as the adhesion force upon retract. A total of five different bacterial cells from separate cultures were examined for each particular case.

***Bacterial adhesion to a salivary film in a parallel plate flow chamber***

The flow chamber (internal dimensions: length × width × height, 175 × 17 × 0.75 mm) and image analysis system have been described in detail previously (Busscher and Van der Mei, 2006). Briefly, glass slides (76 × 26 mm) were sonicated for 3 min in a surfactant solution (2% RBS 35 detergent in water; Omniclean), rinsed thoroughly with tap water, and then washed with methanol, and thoroughly rinsed with tap water and finally with demineralized water. Prior to each experiment, all tubes and the flow chamber were filled with adhesion buffer solution, taking care to remove all air bubbles from the system. Once the system was filled, a bacterial suspension of $3 \times 10^8$ per ml in buffer was allowed to flow through the system. Bacterial adhesion to the bottom glass plate of the flow chamber was determined with a phase-contrast microscope (Olympus BH-2) coupled to a CCD-MXR camera (High Technology, Eindhoven, the Netherlands) equipped with a ×40 ultra-long-working-distance lens (Olympus ULWD-CD plan 40 PL). The camera was coupled to an image analyzer (TEA; Difa, Breda, the Netherlands). The bottom glass plate was coated with saliva by immerging overnight (16 h) at room temperature and was used directly for further experiments.

The bacterial flow rate was adjusted to 1.4 ml $min^{-1}$ under the influence of a hydrostatic pressure yielding a shear rate of 15 $s^{-1}$. Live images were taken every 1 to 2 min during the first 30 min and thereafter at 10 to 30 min intervals up to 4 h, where after flow was stopped. Each image (512 × 512 pixels, with 8-bit resolution) was obtained after summation of 15 consecutive images (time interval 1 s) in order to enhance the signal-to-noise ratio, and to eliminate moving bacteria from the analysis. The surface area covered by an image was 0.017 $mm^2$. Adhesion experiments were performed five times with separate bacterial cultures. In order to verify whether the salivary coatings did not desorb during flow, X-ray Photoelectron Spectroscopy was

done on clean glass, and glass prior to and after exposure to flow (no bacteria). The N/Si surface concentratio ratio, indicative of the adsorbed protein film thickness, was 0.0 on clean glass due to the absence of the proteins, and amounted 2.6 and 3.2 on saliva coated glass prior to and after flow, respectively, which demonstrates that there is no protein desorption during flow.

The number of adhering bacteria per unit area $n(t)$ was recorded as a function of time by image sequence analysis during 4 h and the affinity of an organism for the saliva- coated glass surface was expressed as the initial deposition rate $j_0$, representing the initial increase of $n(t)$ with time. Note that since the initial deposition rate is derived only from the initially adhering bacteria, it represents the affinity of the organisms for the adsorbed film of salivary proteins without intervening influences of interactions between adhering bacteria, as occurs in the number of adhering bacteria after 4 h (Busscher and Van der Mei, 2006). After a stationary end-point had been reached, an air bubble was passed through the flow chamber in order to obtain an indication of the adhesion force of attached bacteria, i.e., their retention capacity.

***Statistical analysis***

Data were analyzed with the Statistical Package for the Social Sciences (Version 11.0, SPSS, Chicago, Illinois, USA). Descriptive statistics, including mean, median, mode and range of the repulsive force at contact ($F_0$) and its Statistical Analysis decay length ($\Lambda$) upon approach, as well as the adhesion force ($F_{adh}$) upon retract, are presented for each bacterial strain. The Wilcoxon signed rank test for the median was used for statistical analyses of the AFM force data. A Student's t-test was used to determine significant differences in initial deposition rate and adhesion number after 4 h. The level of significance was set at $p < 0.05$.

## Results

The repulsive force at contact ($F_0$), and its decay length ($\Lambda$) upon approach, as well as the adhesion force ($F_{adh}$) upon retraction for *S. mutans* LT11 and IB03987 at pH 6.8 and pH 5.8 are given in Figures 1-3, respectively. As these distributions are clearly

non-parametric, medians, modes and ranges of these distributions are summarized in Table 1. The median of the repulsive forces to be overcome in order to allow for contact between the streptococcal cell surfaces and the salivary protein films are similar for LT11 and IB03987. For both strains, repulsion is significantly smaller at pH 6.8 (median 3.0 and 3.1 nN, respectively) than at pH 5.8 (median 4.6 and 4.7 nN, respectively). There were also no significant differences in decay lengths of the repulsive forces for both strains, varying between 19 to 37 nm. Upon retraction at pH 6.8, adhesion forces were significantly stronger for the parent strain LT11 (median -0.4 nN) than for the mutant IB03987 (median 0.0 nN), whereas at pH 5.8 the median of the adhesion forces measured was 0.0 nN for both strains.

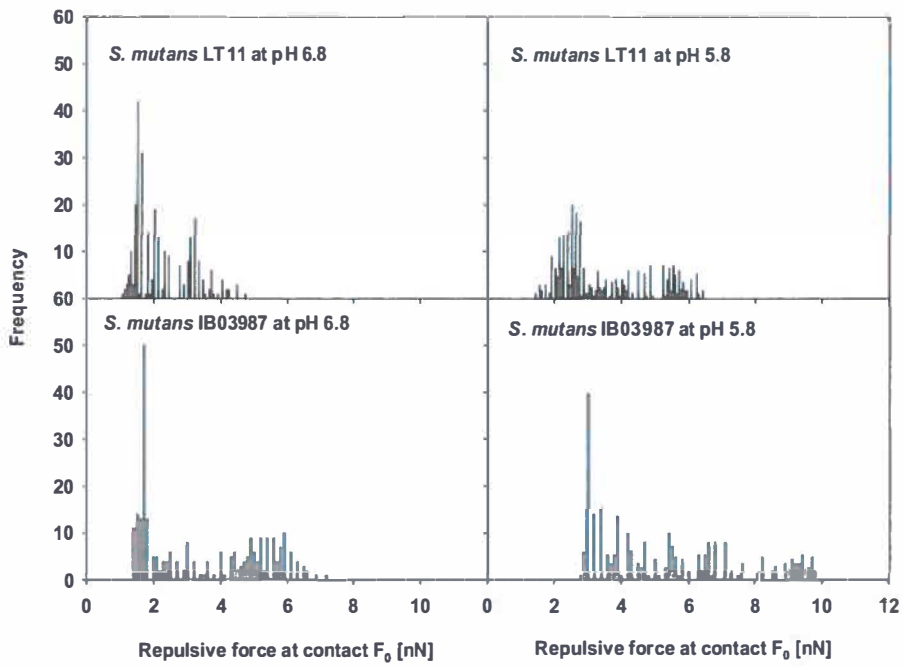


**Figure 1.** Distribution of the repulsive force at contact ($F_0$) for *S. mutans* LT11 and IB03987 in the approaching mode of a saliva-coated AFM tip and the bacterial cell surfaces. Each histogram involves 200-300 force-distance curves, equally divided over five different bacteria.

**Table 1.** Median, mode and range of the distributions measured[1]) for $F_0$, $\Lambda$ and $F_{adh}$ for the interaction between *S. mutans* LT11 and an isogenic mutant without antigen I/II, IB03987 and saliva-coated AFM tips in adhesion buffer at pH 6.8 and 5.8. All experiments were done in five-fold with separately prepared saliva-coated AFM tips and different bacterial cultures, yielding the indicated number of N force-distance curves.

| pH | parameter | Repulsive force range $\Lambda$ (nm) | | Repulsive force at contact $F_0$ (nN) | | Adhesion force $F_{adh}$ (nN) | |
|---|---|---|---|---|---|---|---|
| | | IB03987 | LT11 | LT11 | IB03987 | LT11 | IB03987 |
| 6.8 | Median | 3.0 | 3.1 | 21 | 19 | -0.4 | 0.0 |
| | Mode | 1.7 | 2.4 | 19 | 11 | -0.3 | 0.0 |
| | Range | 7.2 | 5.8 | 52 | 56 | -2.9 | -0.4 |
| | N | 270 | 274 | 274 | 270 | 274 | 270 |
| 5.8 | Median | 4.7 | 4.6 | 23 | 37 | 0.0 | 0.0 |
| | Mode | 3.0 | 4.2 | 11 | 46 | 0.0 | 0.0 |
| | Range | 7.0 | 8.2 | 67 | 66 | -1.2 | -0.1 |
| | N | 260 | 283 | 283 | 260 | 283 | 260 |

[1]) distribution functions were made taking class widths of 0.05 nN, 0.5 nm and 0.05 nN for $F_0$, $\Lambda$ and $F_{adh}$, respectively.

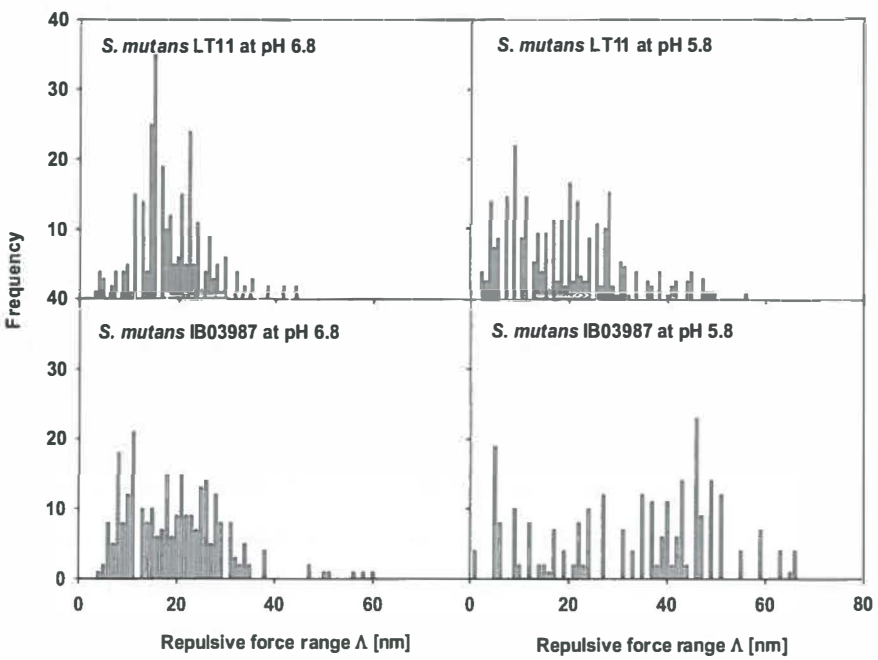


**Figure 2.** Distribution of the decay length of repulsive force ($\Lambda$) for *S. mutans* LT11 and IB03987 in the approaching mode of a saliva-coated AFM tip and the bacterial cell surfaces. Each histogram involves 200-300 force-distance curves, equally divided over five different bacteria.

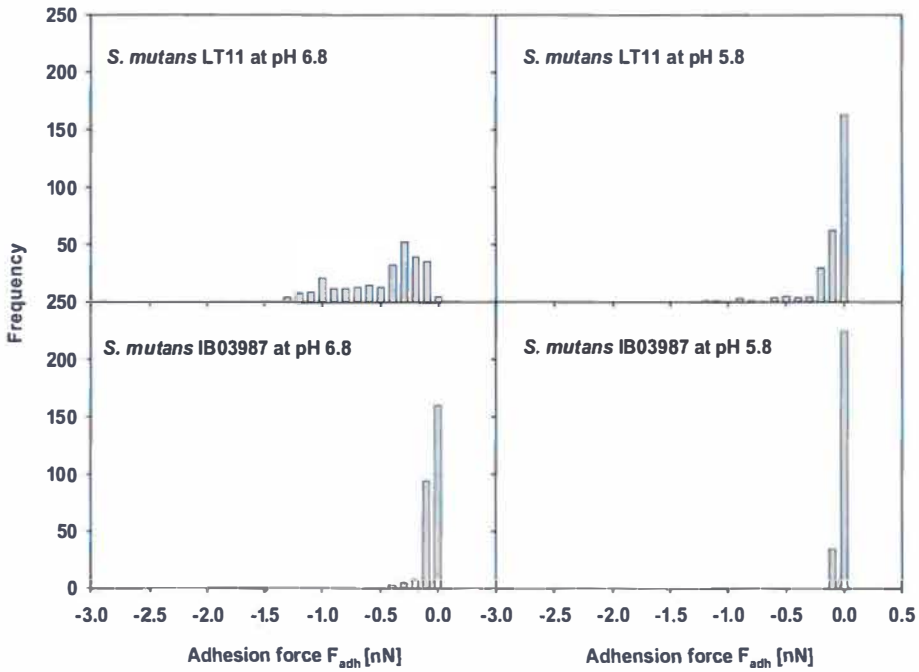


**Figure 3.** Distribution of the adhesion force ($F_{adh}$) for *S. mutans* LT11 and IB03987 in the retracting mode of a saliva-coated AFM tip and the bacterial cell surfaces. Each histogram involves 200-300 force-distance curves, equally divided over five different bacteria.

Fig. **4** shows representative examples of the adhesion kinetics of *S. mutans* LT11 and IB03987 to salivary coatings in a parallel plate flow chamber at pH 6.8 and pH 5.8. Adhesion kinetics of *S. mutans* LT11 at both pH 5.8 and 6.8 are more or less linear during the first 90 min and similar to the kinetics of *S. mutans* IB03987 at pH 5.8, while eventually leveling off toward stationary numbers due to blocking of high affinity sites. However, for *S. mutans* IB03987 at pH 6.8, linearity only extends for about 30 min. The quantitative features of the adhesion kinetics of both strains are summarized in Table 2. At pH 6.8, initial deposition rates of an antigen I/II deficient *S. mutans* IB03987 (1441 $cm^{-2}s^{-1}$) are slightly, but, according to the Student's t-test, significantly lower than those of LT11 (1679 $cm^{-2}s^{-1}$), whereas there were no significant differences found between the strains at pH 5.8. In a stationary phase, i.e. after 4 h and at pH 6.8, *S. mutans* IB03987 adhered in much lower numbers to salivary coatings under flow ($2.5 \times 10^6$ $cm^{-2}$) than the parent strain LT11 ($9.6 \times 10^6$ $cm^{-2}$),

whereas adhesion to bare glass (see footnote to Table 2), which is not mediated by antigen I/II, but by the overall physico-chemical properties of the interacting surfaces, is similar for both strains at pH 6.8. The difference in adhesion to salivary films between the strains, as existing at pH 6.8, disappeared at pH 5.8. Furthermore, at pH 6.8 a large fraction (45%) of the adhering LT11 bacteria is not removed from the salivary coating by a passing air bubble, which implies strong adhesion. For the IB03987 strain at pH 6.8 and both strains at pH 5.8, the strongly adhering fraction is only 25%.

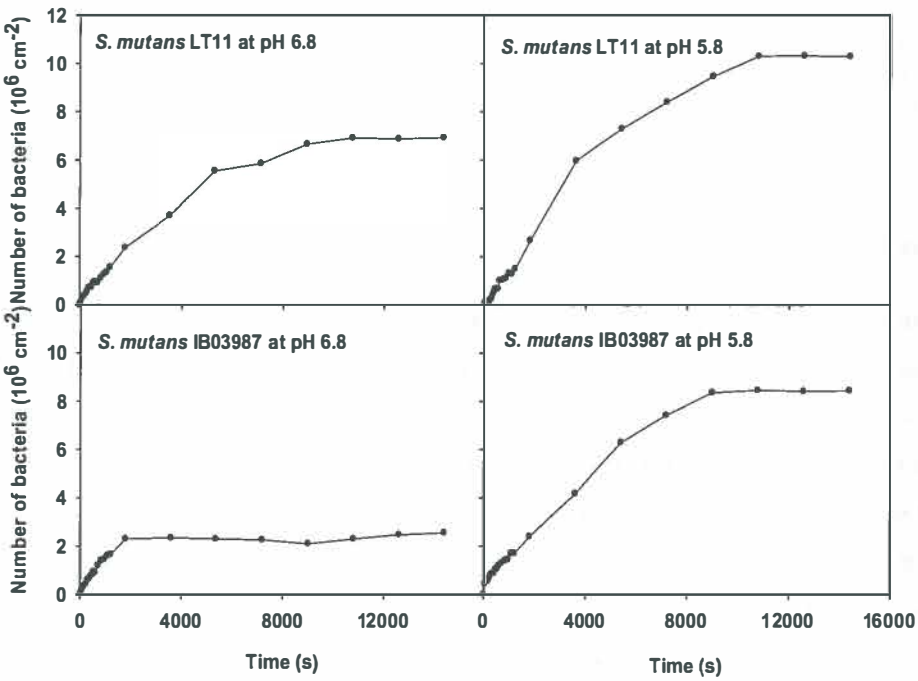


**Figure 4.** Representative examples of the adhesion kinetics of *S. mutans* LT11 and IB03987 to salivary films in a parallel plate flow chamber.

**Table 2.** Initial deposition rate ($j_0$), number of adhering bacteria per unit area after 4 h deposition ($n(t)$) and percentage of adhering bacteria detached by a passing air bubble for the interaction between *S. mutans* LT11 and an isogenic mutant without antigen I/II, IB03987 and salivary films[1)] in a parallel plate flow chamber from adhesion buffer at pH 5.8 and 6.8. All experiments were done in five fold with separately prepared saliva-coated glass slides and different bacterial cultures. ± represents SD over 5 separate experiments.

| Suspension pH | *S. mutans* | Initial deposition rate ($cm^{-2}s^{-1}$) | Number after 4 h ($10^6 cm^{-2}$) | Number of strong adhesion ($10^6 cm^{-2}$) | Detachment (%) |
|---|---|---|---|---|---|
| 6.8 | LT11 | 1679 ± 165 | 9.6 ± 2.3 | 4.3 ± 0.9 | 55 ± 9 |
| | IB03987 | 1441 ± 119 | 2.5 ± 0.7 | 0.6 ± 0.1 | 76 ± 2 |
| 5.8 | LT11 | 1315 ± 28 | 12.7 ± 1.1 | 3.4 ± 0.4 | 73 ± 3 |
| | IB03987 | 1258 ± 169 | 10.5 ± 2.1 | 2.5 ± 0.6 | 76 ± 5 |

[1)] control experiments to bare glass at pH 6.8 in the absence of a salivary film demonstrated that there was no significant difference between adhesion of both strains after 4 h (12.1 ± 2.0 × $10^6$ $cm^{-2}$ and 11.8 ± 1.1 × $10^6$ $cm^{-2}$ for LT11 and IB03987, respectively).

## Discussion

In this paper we quantify for the first time the interaction forces between *S. mutans* strains with and without surface antigen I/II and salivary protein films. At pH 6.8, the presence of antigen I/II was reflected by an elevated adhesion force upon retraction of a salivary protein-coated AFM tip away from immobilized bacteria. Concurrently at pH 6.8, the strain with antigen I/II adhered under flow in higher numbers to salivary protein films than the strain without antigen I/II, whereas in the absence of a salivary film, both strains adhered in similar numbers to glass. At pH 5.8, however, there were no significant differences between adhesion forces of both strains. Interestingly, AFM experiments demonstrated that the repulsive forces to be overcome in order to allow contact between the bacterial cells and salivary films do not significantly differ between LT11 and IB03987. However, the repulsive forces are higher at pH 5.8 than at pH 6.8. This is in line with slightly higher initial deposition rates at pH 6.8 compared to pH 5.8.

At both pHs, the bacteria are negatively charged. For LT11 the zeta potential at pH 5.8 is more negative than at pH 6.8, while for IB03987 the zeta potential at pH 5.8

is less negative than at pH 6.8 (Petersen *et al.*, 2002). The salivary protein layer is negatively charged as well at both pH 5.8 and 6.8 (Göcke *et al.*, 2002). According to the Derjaguin-Landau-Verwey-Overbeek (DLVO) theory, the repulsive force scales with the product of the zeta potentials of the bacterial cell and the saliva-coated surface. Hence, for IB03987 the repulsive force should be stronger at pH 6.8, whereas for LTl1 the repulsion is stronger at pH 5.8. However, the experimental data reveal that, also in the case of IB03987, the repulsive force is stronger at pH 5.8. Furthermore, in a medium of 150 mM potassium chloride, as is the case for the adhesion buffer in our experiments, the decay length for electrostatic interaction is about 1.4 nm, which is much shorter than the decay length of the experimentally observed repulsive force. Therefore, the repulsive force is probably not dominated by electrostatic interactions (Norde, 2003), but may also involve a steric component.

Bacterial adhesion has been described as an interplay between specific and non-specific interaction forces. At pH 6.8, the adhesion experiments carried out measured by AFM clearly demonstrate the absence of specific interactions between IB03987 and salivary films with a median of the adhesion force of 0.0 nN, which is smaller than the combined non-specific and specific interactions between LTl1 and salivary films (median adhesion force -0.4 nN). It is of interest that similar differences in adhesion forces between specifically and non-specifically interacting organisms also occur when comparing with those of (non-)aggregating *E. faecalis*, and (non-)co-aggregating oral bacterial strains, as mentioned already in the introduction of this paper.

At pH 6.8, the initial deposition rate and, more so, the number of bacteria adhering after 4 h, as well as the percentage of strongly adhering bacteria in the parallel plate flow chamber experiments showed good correlation with the adhesion force upon retraction measured with AFM. Adhesion of LTl1 after 4 h to salivary coatings at pH 6.8 is much higher and stronger (less detachment by a passing air bubble) than that of IB03987, which is in line with the stronger adhesion forces measured for LTl1 upon the forced disruption of a saliva-coated tip from the bacterial cell surfaces at pH 6.8. Therewith the presence of antigen I/II adds a specific contribution to the streptococcal interaction with the salivary protein film that allows it

to remain adhering to salivary coatings under environmental conditions of fluctuating detachment forces.

The approach between two surfaces is always the first step in adhesion and occurs in the parallel plate flow chamber through convective-diffusion of bacteria. Once close to a surface and within the range of the attractive interaction forces, adhesion occurs. In other systems where specific interactions were absent and involving bacterial adhesion to inert substrata (Vadillo-Rodriguez *et al.*, 2004), initial deposition rates were generally found to increase with decreasing repulsive forces $F_0$. Here too, the stronger repulsive forces at pH 5.8 compared to those found at pH 6.8, tend to be reflected in lower initial deposition rates, although this difference is not significant for IB03987.

Usually, increased fluid flow results in faster adhesion of microorganisms due to increased mass transport, despite the presence of higher fluid shear stimulating their detachment. However, when fluid flow exceeds a critical limit, the increased wall shear stress prevents further adhesion or even detaches already adhering bacteria. The flow rate in our study was adjusted by hydrostatic pressure to 1.4 ml $min^{-1}$ yielding a shear rate of 15 $s^{-1}$ which, for a bacterial cell of 1 μm diameter implies a shear force of about $2.5 \times 10^{-5}$ nN. This indicates that the organisms should minimally be capable to interact with a force of $2.5 \times 10^{-5}$ nN in order to adhere, but stronger interaction forces may not be ruled out. Indeed, the adhesion forces derived from AFM are much stronger, although it should be emphasized that shear forces operate tangentially with respect to the surface, whereas the adhesive forces probed by AFM act perpendicularly to a substratum surface. Lift forces due to fluid flow do act perpendicularly to a surface as well, but they are generally considered too weak to cause microbial detachment (Busscher and Van der Mei, 2006; Sharma *et al.*, 1992).

The strong adhesion force measured for the adhesion of LT11 to a salivary protein coating at pH 6.8 is in accordance with the highly negative enthalpy measured at this pH for the adsorption of salivary proteins on LT11 cells. At pH 6.8, the enthalpy of adsorption of salivary proteins to the IB03987 is much smaller and similar to the enthalpy for adsorption at pH 5.8 to the cells of both strains (Xu *et al.*, 2007). This, together with the pH-dependency of the data in the present study indicate that the

non-specific contribution is essentially of non-electrostatic nature, whereas the specific contribution is mediated by electrostatic charge.

In conclusion, based on AFM and parallel plate flow measurements, we demonstrated the role of antigen I/II at the surface of *S. mutans* LT11 in specifically binding different salivary proteins and therewith promoting adhesion of this bacterial strain to saliva-coated surfaces. This specific contribution is short-ranged and mediated by electrostatic interactions, as it is effective at pH 6.8, but absent at pH 5.8 pointing to pairing of oppositely charged ions.

## Acknowledgment

The authors would like to thank Joop de Vries for his help with the X-ray photoelectron spectroscopy and AFM experiments, Eefje Engels and Minie Rustema-Abbing for their guidance with the flow chamber experiments and Hans Kaper for his help with the image analysis.

## References

**Binnig G, Quate CF, Gerber C (1986).** Atomic force microscope. *Phys. Rev. Lett.* 56: 930–933.

**Bowen WR, Fenton AS, Lovitt RW, Wright CJ (2002).** The measurement of *Bacillus mycoides* spore adhesion using atomic force microscopy, simple counting methods, and a spinning disk technique. *Biotechnol. Bioeng.* 79:170–179.

**Busscher HJ, Van der Mei HC (2006).** Microbial adhesion in flow displacement systems. *Clin. Microbiol. Rev.* 19:127–141.

**Cleveland JP, Manne S, Bocek D, Hansma PK (1993).** A nondestructive method for determining the spring constant of cantilevers for scanning force microscopy. *Rev. Sci. Instrum.* 64:403–405.

**Dufrêne YF (2003).** Recent progress in the application of atomic force microscopy imaging and force spectroscopy to microbiology. *Curr. Opin. Microbiol.* 6:317–323.

**Göcke R, Gerath F, Von Schwanewede H (2002).** Quantitative determination of salivary components in the pellicle on PMMA denture base material. *Clin. Oral Investigations.* 6:227–235.

**Hajishengallis G, Koga T, Russell MW (1994).** Affinity and specificity of the interactions between *Streptococcus mutans* antigen I/II and salivary components. *J. Dent. Res.* 73:1493–1502.

**Jenkinson HF, Demuth DR (1997).** Structure, function and immunogenicity of streptococcal antigen I/II polypeptides. *Mol. Microbiol.* 23:183–190.

**Kasas S, Ikai A (1995).** A method for anchoring round shaped cells for atomic force microscope imaging. *J. Biophys.* 68:1678–1680.

**Norde W (2003).** Water. pp 47–61. In: Colloid and Interfaces in Life Sciences. Editor by W. Norde. Marcel Dekker Inc, New York, US.

**Petersen FC, Assev S, Van der Mei HC, Busscher HJ, Scheie AA (2002).** Functional variation of the antigen I/II surface protein in *Streptococcus mutans* and *Streptococcus intermedius*. *Infect. Immun.* 70:249–256.

**Petersen FC, Pasco S, Ogier J, Klein JP, Assev S, Scheie AA (2001).** Expression and functional properties of the *Streptococcus intermedius* surface protein antigen I/II. *Infect. Immun.* 69:4647–4653.

**Postollec F, Norde W, De Vries J, Busscher HJ, Van der Mei HC (2006).** Interactive forces between co-aggregating and non-co-aggregating oral bacterial pairs. *J. Dent. Res.* 85:231–234.

**Sciotti MA, Yamodo I, Klein JP, Ogier J (1997).** The N-terminal half part of the oral streptococcal antigen I/IIf contains two distinct binding domains. *FEMS Microbiol. Lett.* 153:439–445.

**Sharma MM, Chamoun H, Sita Rama Sarma DSH, Schechter RS (1992).** Factors controlling the hydrodynamic detachment of particles from surfaces. *J. Colloid Interface Sci.* 149:121–134.

**Soell M, Holveck F, Schöller M, Wachsmann RD, Klein JP (1994).** Binding of *Streptococcus mutans* SR protein to human monocytes: production of tumor necrosis factor, interleukin 1, and interleukin 6. *Infect. Immun.* 62:1805–1812.

**Troffer-Charlier N, Ogier J, Moras D, Cavarelli J (2002).** Crystal structure of the V-region of *Streptococcus mutans* antigen I/II at 2.4 Å resolution suggests a sugar preformed binding site. *J. Mol. Biol.* 318:179–188.

**Vadillo-Rodriguez V, Busscher HJ, Norde W, De Vries J, Van der Mei HC (2004).** Relations between macroscopic and microscopic adhesion of *Streptococcus mitis* strains to surfaces. *Microbiol.* 150:1015–1022.

**Van der Mei HC, Busscher HJ, Bos R, De Vries J, Boonaert CJP, Dufrêne YF (2000).** Direct probing by atomic force microscopy of the cell surface softness of a fibrillated and nonfibrillated oral streptococcal strain. *Biophys. J.* 78:2668–2674.

**Vernier A, Diab M, Soell M, Haan-Archipoff G, Beretz A, Wachsmann D, Klein JP (1996).** Cytokine production by human epithelial and endothelial cells following exposure to oral viridans streptococci involves lectin interactions between bacteria and cell surface receptors. *Infect. Immun.* 64:3016–3022.

**Waar K, Van der Mei HC, Harmsen HJM, De Vries J, Atema-Smit J, Degener JE, Busscher HJ (2005).** Atomic force microscopy study on specificity and non-specificity of interaction forces between *Enterococcus faecalis* cells with and without aggregation substance. *Microbiol.* 151:2459–2464.

**Xu CP, Van de Belt-Gritter B, Busscher HJ, Van der Mei HC, Norde W (2007).** Calorimetric comparison of the interactions between salivary proteins and *Streptococcus mutans* with and without antigen I/II. *Colloids Surf. B.* 54:193–199.

## Schematic Picture

'Interaction forces between salivary proteins and *Streptococcus mutans* with and without antigen I/II' by Xu *et al.*

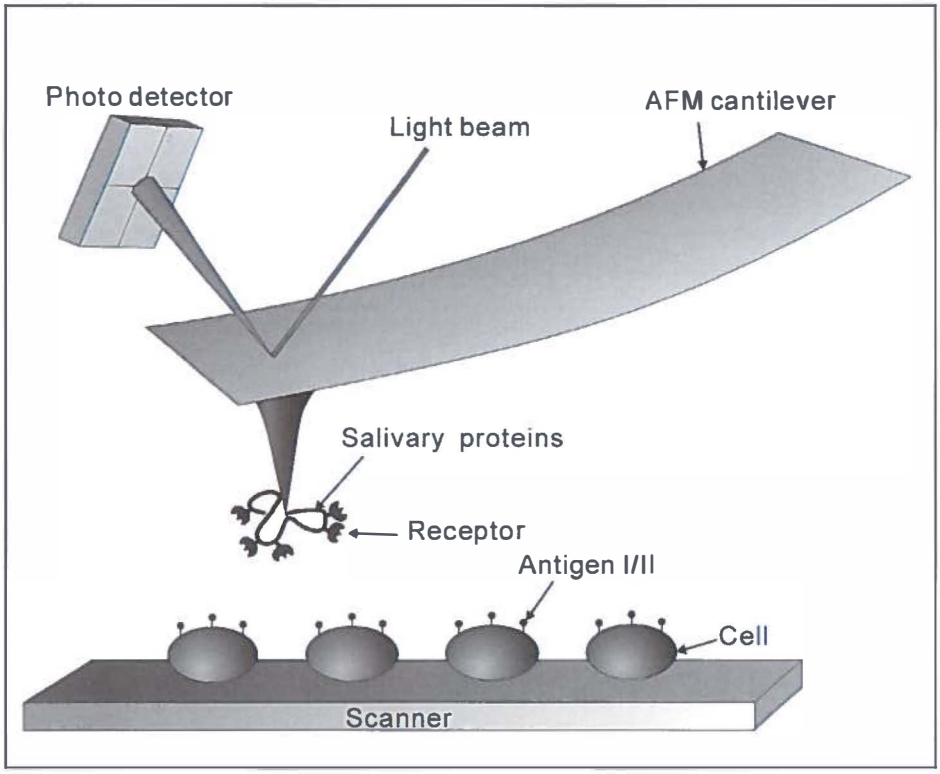

# 5

# Interaction enthalpies and adhesion forces between fibronectin and *S. aureus* with and without FnBP

Chun-Ping Xu, Joop de Vries, Henny C. van der Mei, Henk J. Busscher, Willem Norde

*Applied and Environmental Microbiology* (submitted)

## Introduction

*Staphylococcus aureus* can adhere to epithelial cells, endothelial cells, fibroblasts (Hess *et al.*, 2006) and plasma exposed biomaterials implant surfaces, causing potentially persistent infections. The best described mechanism of *S. aureus* adhesion to eukaryotic cells and other fibronectin coated surfaces involves the fibronectin (Fn) binding proteins FnBP A and FnBP B on the surface of *S. aureus* (Fowler *et al.*, 2000; Greene *et al.*, 1995). Peacock *et al.* (1999) demonstrated the significant role played by the FnBP's by comparing adhesion of different isogenic *S. aureus* strains to human endothelial cells. Moreover, in vitro adhesion of *S. aureus* strain Wood 46 to Fn-coated surfaces was demonstrated to be inhibited in a dose-dependent manner by anti-Fn antibodies (Vaudaux *et al.*, 1984a; Vaudaux *et al.*, 1984b).

At constant temperature and pressure, which is usually the case in biological systems, all physico-chemical interactions, including adsorption, adhesion, coaggregation and co-adhesion, are determined by changes in the Gibbs energy ($G$) of a system. These interactions can either be evaluated at a macroscopic level, in terms of Lifshitz-Van der Waals, electrostatic and hydrophobic forces originating from proteins, bacteria or substrata as a whole, or at a more microscopic or even nanoscopic level, where they involve highly specific interactions between stereo-chemical surface components, such as fibronectin and FnBP's. For a spontaneous process, the change in Gibbs energy ($\Delta G$) is negative. $\Delta G$ is composed of a change in enthalpy (H) and in entropy (S), according to

$$\Delta G = \Delta H - T\Delta S \qquad (1)$$

where T is the temperature in Kelvin. The enthalpy tends to reach a minimum value, whereas the entropy strives for a maximum. The enthalpy of a system is directly related to its heat content. At constant pressure, and if no work other than that related to volume change is involved, changes in the enthalpy can be determined as the heat exchange between a system and its environment. Direct determination of the entropy, however, is practically impossible as it would require counting all conformational and

configurational possibilities before and after a process. Many biological processes are characterized by strong enthalpy-entropy compensation (Haynes and Norde, 1995), that is, they occur spontaneously by virtue of an entropy increase that compensates for an unfavorable enthalpy effect, or vice versa.

The enthalpy of interaction between bacterial cell surfaces and proteins can be determined using isothermal titration calorimetry (ITC). ITC measures the enthalpy change of formation of a complex at constant temperature. Xu *et al.* (2007) determined the adsorption enthalpies of salivary proteins to *Streptococcus mutans* using ITC and found that *S. mutans* LT11 with antigen I/II, a cell surface binding protein involved in bacterial adhesion to extracellular matrix proteins, yielded a much higher, exothermic adsorption enthalpy when mixed at pH 6.8 with saliva than did *S. mutans* IB03987, lacking surface antigen I/II. It was thus assessed that antigen I/II at the surface of *S. mutans* LT11 specifically binds different proteins with different affinities from the large pool of proteins present in whole saliva. Furthermore, Busscher *et al.* (2007) used ITC to evaluate the adsorption of a single protein, laminin to these streptococcal cell surfaces and found that enthalpy is released upon adsorption of laminin to the surface of the parent strain LT11, but not upon adsorption to IB03987.

Whereas ITC operates at a macroscopic level, atomic force microscopy (AFM) operates at the nanometer level and allows to sense the force between a very sharp probe attached to a flexible cantilever and a sample surface and can thus distinguish between different functional surface proteins (Binnig *et al.*, 1985). Using AFM, differences in interaction forces between protein-coated AFM probes and streptococcal strains with and without antigen I/II have been measured. Generally upon retraction of streptococci from saliva- or laminin-coated probes, stronger forces were observed when the streptococcal strain possessed antigen I/II than when they did not.

The aim of this study is to analyze the role of FnBP's on staphylococcal (*S. aureus*) cell surfaces in their interaction with Fn using ITC and AFM, in particular with respect to the role of FnBP's in staphylococcal adhesion to Fn-coated surfaces under flow. To this end, we first determined adhesion of a *S. aureus* wild type strain 8325-4 and of FnBP's lacking isogenic mutant DU5883 deposited by convective-diffusion on Fn-coated glass slides in a parallel plate flow chamber. Subsequently, the

interactions forces between Fn-coated AFM tips and the cell surfaces were compared, while furthermore the enthalpies of adsorption of Fn to the surfaces of the *S. aureus* strains were measured. In order to study whether the Fn-binding to the *S. aureus* is specific or not, additional experiments were performed after coating either the substrata or the staphylococcal cells with a layer of bovine serum albumin (BSA).

## Materials and Methods

### *Bacterial strains and culture conditions*

*S. aureus* strain 8325-4 and its isogenic mutant lacking FnBP's, DU5883 (kindly provided by Dr T.J. Foster, Moyne Institute of Preventive Medicine, Dublin, Ireland), were used in this study. The bacterial cells were maintained at -80°C in tryptone soya broth (TSB; OXOID, Basingstoke, UK) broth containing 7% dimethylsulfoxide (DMSO; MERCK, Germany). For culturing, both strains were plated onto TSB agar plates overnight at 37°C. Subsequently, bacterial colonies were precultured in 10 ml TSB batch culture overnight under constant rotation. This preculture was used to inoculate a main culture of 190 ml TSB. After approximately 2 h of growth to early stationary phase, corresponding with peak expression of FnBP's in *S. aureus* 8325-4 (Saravia-Otten *et al.*, 1997), bacteria were harvested by centrifugation at 6500*g* for 5 min at 10°C and washed twice with demineralized water. Bacterial chains and aggregates were broken by mild sonication on ice for 3 × 10 s at 30 W (Vibra Cell model 375, Sonics and Materials Inc., Danbury, Connecticut, USA). Then bacteria were resuspended in phosphate-buffered saline (PBS; 10 mM potassium phosphate and 0.15 M NaCl, pH 7), to a concentration of $3 \times 10^8$ or $5 \times 10^9$ per ml for adhesion experiments or ITC, respectively, as determined in a Bürker-Türk counting chamber. In order to block non-specific adhesion sites on the staphylococcal cell surfaces, staphylococci were also incubated for 60 min at 37 °C in PBS supplemented with 1% BSA.

### *Bacterial adhesion to a Fn-coating in a parallel plate flow chamber*

The flow chamber (internal dimensions: length × width × height, 175 × 17 × 0.75 mm) and image analysis system have been described in detail previously (Busscher and Van

der Mei, 2006). Briefly, glass slides (76 × 26 mm) were sonicated for 3 min in a surfactant solution (2% RBS 35 detergent in water; Omniclean), rinsed thoroughly with tap water, and then washed with methanol, thoroughly rinsed with tap water and finally with demineralized water. Prior to each experiment, all tubes and the flow chamber were filled with PBS, taking care to remove all air bubbles from the system. Once the system was filled, a bacterial suspension of $3 \times 10^8$ per ml in buffer was allowed to flow through the system. The bottom glass plate was drop-coated with 0.05 ml Fn (20 μg $ml^{-1}$, human Fn purchased from Sigma-Aldrich BV, Zwijndrecht, The Netherlands) for 2 h at room temperature to create a circular Fn-coated region with a diameter of 1 cm. In addition, glass plates were prepared on which non-specific adhesion sites were blocked by immersing the entire glass after Fn drop-coating for 1 min in PBS containing 1% BSA and rinsed with demineralized water.

Bacterial adhesion to the bottom glass plate of the flow chamber was determined with a phase-contrast microscope (Olympus BH-2) coupled to a Firewire CCD camera (High Technology) equipped with a ×40 ultra-long-working-distance lens (Olympus ULWD-CD plan 40 PL). Therewith, the surface area covered by an image was $3.7 \times 10^{-4}$ $cm^2$. The sample was switched back-and-forth from the Fn-coated region to the uncoated region. The camera was coupled to an image analyzer (TEA; Difa).

The flow rate during the experiments was adjusted to 1.4 ml $min^{-1}$ under the influence of a hydrostatic pressure yielding a shear rate of 15 $s^{-1}$. Live images were taken every 1 to 2 min during the first 30 min and thereafter at 10 to 30 min intervals up to 4 h, where after flow was stopped. Each image (1392 × 1040 pixels, with 8-bit resolution) was obtained after summation of 15 consecutive images (time interval 0.25 s) in order to enhance the signal-to-noise ratio, and to eliminate moving bacteria from the analysis. Adhesion experiments were performed five times with separate bacterial cultures.

The number of adhering bacteria per unit area $n(t)$ was recorded as a function of time during 4 h and the affinity of an organism for the Fn coated glass surface was expressed as the initial deposition rate $j_0$, representing the initial increase of $n(t)$ with time. Note that since the initial deposition rate is derived only from the first adhering

bacteria, it represents the affinity of the organisms for the adsorbed Fn-coatings without intervening influences of interactions between adhering bacteria, as occurs due to crowding at the surface, such as after 4 h (Busscher *et al.*, 2007).

***Atomic force microscopy***

For AFM, the negatively charged bacteria were attached through electrostatic interactions to a glass slide, made positively charged by pre-adsorption of poly-L-lysine, as described before (Camesano *et al.*, 2000). To block non-specific binding sites on the bacterial cell surfaces, the glass slides with attached bacteria were immersed for 1 min into PBS containing 1% BSA and rinsed with demineralized water. AFM tips (DNP from Veeco, Woodbury, USA) were coated with a Fn film by immersion for 30 min in Fn (25 $\mu g\ ml^{-1}$ in PBS, pH 7) with the aid of a micromanipulator. All glass slides with immobilized bacteria and the Fn-coated AFM tips were immediately used after preparation.

AFM measurements were done at room temperature in PBS using a Dimension 3100 system (Nanoscope IV Digital Instrument, Woodbury, USA). An array of 32 × 32 force-distances curves with z-displacements of 100-200 nm at z-scan rates ≅10 Hz were collected on top of a bacterium over an area of approximately 300 × 300 $nm^2$. The slopes of the retract force curves, in the region where probe and sample are in contact, were used to translate the voltage into cantilever deflection. All AFM cantilevers were calibrated to convert deflection into force using resonant frequency measurements (Dufrêne, 2003; Cleveland *et al.*, 1993).

Force-distance curves were analyzed in order to yield adhesion maps from the retracting curves by taking the strongest adhesion force detected during retract at each position as the value for adhesion and by plotting that value against x-y position of each force-distance curve. This resulted in an adhesion distribution histogram from which median, mode and range values for the adhesion force upon retract were derived. A total of three different bacterial cells from separate cultures were examined for each particular case.

***Isothermal titration calorimetry***

The adsorption enthalpy of Fn to the bacterial cell surfaces was measured in a twin-type, isothermal microcalorimeter TAM 2277 (Thermometric, Sweden). The calorimeter was positioned in a temperature-controlled environment (20 ± 0.1 °C), allowing a baseline stability of ± 0.1 μW over 24 h (Nordmark *et al.*, 1984). The instrument had an electrical calibration with a precision better than 1% and proper calibration was regularly checked by measuring the dilution enthalpy of concentrated sucrose solutions (Wu *et al.*, 1996). Experiments were performed isothermally at 25°C in stainless steel ampoules of 4 ml. Four ampoules, connected with separate titration systems, were used inside the microcalorimeter. The use of a twin-type microcalorimeter allows the measurement of the heat (Q) flowing from the reaction ampoule as compared with a reference ampoule. The output signal was collected as power, $P$, versus time, $t$, and was integrated to evaluate the isobaric heat exchange (i.e. the enthalpy change) during adsorption, using the dedicated Digitam 4.1 software (Thermometric, Sweden). Notably, the measured heat effect should be corrected by the heat of dilution of the proteins to obtain the net adsorption enthalpy (Briggner and Wadsö, 1991).

Typically, all four reaction ampoules including the reference ampoule, were filled with 1.5 ml of bacterial suspension ($5 \times 10^9$ cells per ml) in PBS under constant stirring (90 rpm) with a specially designed two-blades stirrer. The ampoules were lowered gradually into the microcalorimeter and left in the measuring position to reach thermal equilibrium before data collection started. After equilibration, a stable baseline was obtained and the Fn was titrated into the reaction ampoules. Titration was done at a controlled rate of 2 μl $s^{-1}$ via a stainless steel cannula connected to a syringe. In order to study possible saturation of adsorption sites, Fn (25 μg $ml^{-1}$) was added in four consecutive injections of 60 μl into the ampoule with intervals of 40 min. All calorimetric experiments were done in fourfold.

### *Statistical analysis*

Data were analyzed with the Statistical Package for the Social Sciences (Version 11.0, SPSS, Chicago, Illinois, USA). Descriptive statistics, including median, mode and range of the adhesion force ($F_{adh}$) upon retract, are presented for each bacterial strain. The Wilcoxon signed rank test for the median was used for statistical analyses of the AFM force data. A Student's t-test was used to determine significant differences in initial deposition rates, adhesion numbers after 4 h and interaction enthalpies. The level of significance was set at $p < 0.05$.

## Results

### *S. aureus adhesion to Fn films*

Fig. 1 shows representative examples of the adhesion kinetics of *S. aureus* 8325-4 and DU5883 to Fn-coatings in a parallel plate flow chamber in PBS at pH 7. The adhesion kinetics of both *S. aureus* strains are linear during approximately 4000-5000 s prior to leveling off toward stationary numbers. The linear trajectories of the curves are taken to calculate the initial deposition rates, as summarized in Table 1.

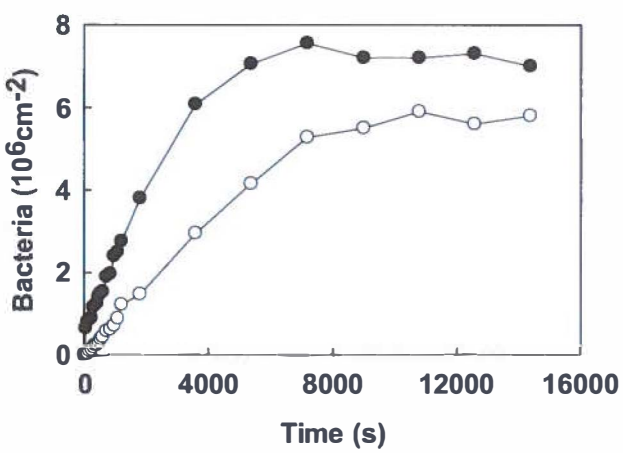


**Figure 1**. Representative examples of the adhesion kinetics of *S. aureus* 8325-4 (●) and DU5883 (○) to Fn-films in PBS.

Adhesion to bare glass, which is not mediated by FnBP's, but by the overall physico-chemical properties of the interacting surfaces, is similar for both strains. Initial deposition rate of a FnBP deficient *S. aureus* DU5883 to Fn-coated glass is significantly (Student t-test, $p < 0.05$) lower than that of 8325-4, which indicates the high affinity of strain 8325-4 for Fn-coatings. Also after 4 h of adhesion, strain 8325-4 adheres in higher numbers than FnBP's deficient DU5883, but the difference is not two-fold anymore as in the initial deposition rates. After exposure of either the Fn-coating or the staphylococci to BSA, initial deposition rates and the numbers of bacteria adhering after 4 h decreased significantly for both strains. The values of initial deposition rates of the FnBP's deficient *S. aureus* DU5883 remained lower than those of 8325-4 to Fn-coatings exposed to BSA or after the staphylococci were exposed to BSA prior to the flow experiments, but these differences are not statistically significant.

**Table 1.** Initial deposition rates ($j_0$), and numbers of adhering staphylococci per unit area after 4 h for *S. aureus* 8325-4 and isogenic mutant DU5883 without FnBP's in a parallel plate flow chamber from PBS at pH 7 to Fn-coatings. In addition, experiments were performed after exposure of the substrata or the staphylococci to a 1% BSA solution. All experiments were done in five fold with separately prepared Fn-coated glass slides and different bacterial cultures. Average standard deviations over 5 separate experiments amount ± 110 $cm^{-2}$ $s^{-1}$ and 0.5 × $10^6$ $cm^{-2}$ over the initial deposition rates and numbers of bacteria adhering after 4 h, respectively.

| Experiments | Initial deposition rate ($cm^{-2}s^{-1}$) | | Number after 4 h ($10^6cm^{-2}$) | |
|---|---|---|---|---|
| | 8325-4 | DU5883 | 8325-4 | DU5883 |
| **Fn-coated glass** | 2438 | 1290 | 7.0 | 5.2 |
| **Glass** | 1485 | 1407 | 8.4 | 8.0 |
| **Fn-coated glass + BSA** | 815 | 678 | 5.2 | 4.4 |
| **Glass + BSA** | 614 | 597 | 5.1 | 4.9 |
| **Fn-coated glass*** | 704 | 527 | 3.9 | 3.5 |
| **Glass*** | 718 | 598 | 3.4 | 3.1 |

* These experiments were carried out with staphylococci exposed to 1% BSA prior to the experiments.

***Interaction forces between Fn-coatings and the S. aureus cell surface***

The distributions for the adhesion force ($F_{adh}$) upon retraction for *S. aureus* 8325-4 and DU5883 from Fn-coated AFM tips in PBS are given in Fig. 2. As these distributions are clearly non-parametric, medians, modes and ranges of these distributions are summarized in Table 2. Upon retraction, median adhesion forces were significantly stronger for the parent strain 8325-4 than for the mutant DU5883. Also upon exposure of the staphylococci to 1% BSA, median adhesive forces remained stronger for the parent strain 8325-4 than for mutant DU5883 without FnBP's.

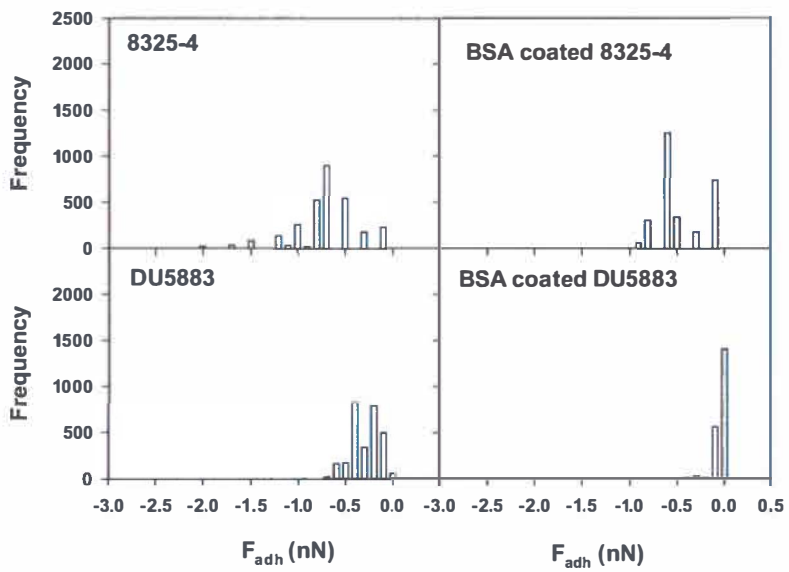


**Figure 2.** Distribution of the adhesion force ($F_{adh}$) for *S. aureus* 8325-4 (top panel) and DU5883 (bottom panel) for a Fn-coated AFM tip and the staphylococcal cell surfaces in PBS. Each histogram involves 2000-3000 force-distance curves, equally divided over three different bacteria. Right panel data refer to staphylococci first exposed to 1% BSA.

**Table 2.** Median, mode and range of the distribution[1)] of $F_{adh}$ for the interaction between Fn-coated AFM tips and *S. aureus* 8325-4 and an isogenic mutant without FnBP's, DU5883 prior to and after bacterial exposure to 1% BSA in PBS. All experiments were done in three-fold with separately prepared Fn-coated AFM tips and different bacterial cultures, yielding the indicated number of N force-distance curves.

| | Parameter | Adhesion force Fadh (nN) | |
|---|---|---|---|
| | | 8325-4 | DU5883 |
| No BSA | Median | -0.7 | -0.3 |
| | Mode | -0.7 | -0.4 |
| | Range | -2.4 | -0.7 |
| | N | 3008 | 2863 |
| 1% BSA | Median | -0.6 | 0 |
| | Mode | -0.6 | 0 |
| | Range | -0.8 | -0.4 |
| | N | 2879 | 2011 |

[1)] distribution functions were made taking a class width of 0.1 nN.

### *Enthalpies of adsorption of Fn to S. aureus cell surface*

The measurement of adsorption enthalpies of Fn to the *S. aureus* cell surfaces requires correction for the heat of diluting the proteins in PBS. For four consecutive injections of 60 µl of a 25 µg $ml^{-1}$ Fn-solution into 1.5 ml of PBS yielded heat effects of, respectively, -55, -56, -37 and -37 µJ. Fig. 3 summarizes the adsorption enthalpies upon consecutive injections of Fn to the staphylococcal suspensions, after correction for protein dilution. Clearly, adsorption enthalpies decrease with the number of injections done especially for the parent strain 8325-4 with FnBP's, but no saturation of adsorption sites seems to be reached within four injections. The cumulative adsorption enthalpies after the four injections are shown in Table 3, as expressed per bacterium and per $m^2$ bacterial cell surface. Fn adsorption to the bacterial cell surfaces is an exothermic process in all cases, i.e. enthalpy is released upon adsorption. Adsorption of Fn to *S. aureus* 8325-4 with FnBP's is enthalpically significantly more favorable than to *S. aureus* DU5883. After exposure to BSA of *S. aureus* 8325-4, the adsorption enthalpy decreases significantly, but remains larger than those for *S. aureus* DU5883. No significant effect is seen for exposure to BSA on the adsorption enthalpy of *S. aureus* DU5883, lacking FnBP's.

**Table 3.** Cumulative adsorption enthalpies per bacterium ($10^{-9}$μJ) and per $m^2$ bacterial cell surface (mJ $m^{-2}$) after four consecutive injections of 60 μl Fn solution (25 μg $ml^{-1}$) into 1.5 ml bacterial suspensions in PBS. Average standard deviations over 4 separate experiments amount ± 25 × $10^{-9}$ μJ per bacterium and 8 mJ $m^{-2}$, respectively.

| Experiments | Cumulative adsorption enthalpies per bacterium ($10^{-9}$μJ) | | Cumulative adsorption enthalpies per $m^2$ (mJ) | |
|---|---|---|---|---|
| | 8325-4 | DU5883 | 8325-4 | DU5883 |
| No BSA | -140 | -43 | -44 | -14 |
| 1% BSA | -102 | -54 | -32 | -17 |

* for calculation of the adsorption enthalpies per $m^2$, it was assumed that the bacterial cell radius was 0.5 μm.

## Discussion

In this paper, we compare the interactions mediating adhesion to Fn-coated surfaces of two strains of *S. aureus*, one containing FnBPs and the other one being FnBP-deficient by three entirely different techniques. Adhesion of the two strains is determined in a parallel plate flow chamber under convective-diffusion. In addition, the adhesion forces to Fn-coated AFM tips were measured as well as the adsorption enthalpies of Fn to the staphylococcal cell surfaces. In general, adhesion of the strain with FnBP's to Fn-coated substrata is higher than of the strains deficient of FnBP's and, in line, adhesion forces and adsorption enthalpies are higher. Surprisingly, however, adsorption of BSA to either the Fn-coated substrata or the staphylococcal cell surfaces with the purpose of blocking non-specific adhesion/adsorption sites, also obstructs the accessibility of the FnBP's on strain 8325-4 during convective-diffusional mass transport, as, in this case, adhesion approaches the one of the FnBP-deficient strain DU5883.

AFM demonstrates involvement of relatively strong specific contributions in the interaction between the FnBP's-containing *S. aureus* 8325-4 strain and a Fn-coated tip as compared with the FnBP's deficient strain DU5883. It is remarkable that, unlike for the initial deposition rate in the parallel plate flow chamber, bacterial exposure to BSA hardly affects the adhesion force measured by AFM. This could be due to the

forced nature of the contact between the bacterial cell surface and the adsorbed fibronectin. Possibly, even in the presence of adsorbed BSA, forced contact between the Fn-coated AFM tip and the FnBP's containing bacterial cell surface, as is established prior to retracting the AFM tip, allows penetration of the tip into the adsorbed protein mass yielding specific FnBP-Fn interactions. Interestingly, the median adhesion force between the Fn-coated AFM tip and the *S. aureus* 8325-4 cell surface of about -0.6 to -0.7 nN corresponds extremely well with identically measured (Yongsunthon *et al.*, 2007) adhesion forces for 15 different tissue-invasive *S. aureus* isolates (0.57 ± 0.05 nN) and is about two-fold higher than for 15 non-invasive control isolates (0.29 ± 0.05 nN).

The enthalpy changes associated with the interaction between Fn and the *S. aureus* cells are all exothermic, but they differ markedly between the two strains, as shown in Fig. 3 and Table 3. For the FnBP-deficient DU5883 strain the enthalpy change is essentially the same for each injection step, as is to be expected for non-specific adsorption in the sub-saturation range. Assuming that the staphylococcal cell diameter equals 1 μm, it can be calculated that in the ITC ampoule there is $23.6 \times 10^{-3}$ $m^2$ of bacterial surface area available for adsorption. Since each fibronectin injection adds $1.5 \times 10^{-3}$ mg Fn, the maximal cell surface coverage by fibronectin after 4 consecutive injections amounts 0.25 mg Fn per $m^2$ bacterial cell surface, which is far below the saturation limit by non-specifically adsorbed Fn, which would amount to at least a few mg $m^{-2}$ (Sousa *et al.*, 2007). Assuming that all Fn added is adsorbed, the cumulative enthalpy effect measured of -14 mJ $m^{-2}$ corresponds to $-2.3 \times 10^{-17}$ J per Fn molecule, as calculated using a molar mass of 250 kDa. Taking into account the large molar mass of Fn, this value is quite reasonable when compared with enthalpy effects reported for non-specific adsorption of various proteins to different surfaces (Haynes and Norde, 1994). The enthalpy effects measured for the FnBP's containing 8325-4 strain are more exothermic than for the FnBP-deficient DU5883 strain. This indicates involvement of enthalpically favorable specific Fn-binding sites. The downward trend of the interaction enthalpy with consecutive injection steps, displayed in Fig. 3 (left panel), suggests that not all specific binding sites are equally favorable, or, alternatively, that they become gradually saturated, so that for each subsequent

addition a smaller fraction of Fn binds to FnBP's on the cell surface. Assuming that all Fn added during the first injection binds to FnBP, the measured -250 μJ corresponds to $-41.7 \times 10^3$ kJ per mol Fn. This value seems extraordinary high, and is about 300× higher than the enthalpy of the biotin-streptavidin interaction (Moy *et al.*, 1994). However, it should be realized that the much larger Fn molecule may interact through more binding sites than the number of sites involved in e.g. a single biotin-streptavidin interaction.

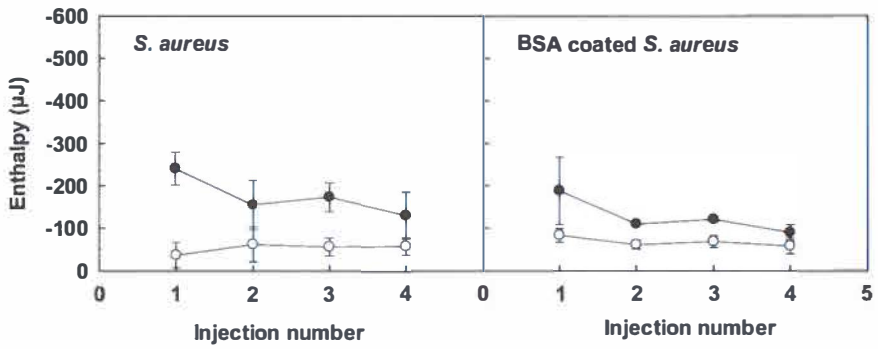


**Figure 3.** Adsorption enthalpies (μJ), after correction for dilution effects, of Fn to *S. aureus* cell surfaces upon consecutive injections of 60 μl Fn solution (25 μg $ml^{-1}$) into 1.5 ml bacterial suspension of *S. aureus* 8325-4 (●) and *S. aureus* DU5883 (○) in PBS. Right panel data refer to staphylococci first exposed to 1% BSA.
Error bars indicate standard deviation based on four independent measurements.

Exposure of the bacteria to a BSA solution hardly influences the enthalpy of interaction between Fn and the FnBP-deficient DU5883 strain. In contrast, BSA exposure of the FnBP-containing 8325-4 strain significantly suppresses the enthalpy of interaction with Fn, but not even nearly to the level of non-specific interaction. However, the downward trend in enthalpy for the BSA-coated 8325-4 strain (Fig. 3, right panel) seems to indicate that for the later Fn injections a smaller fraction of added Fn finds FnBP's, as compared to the non-BSA-coated cells. This is completely in line with the lack of effects on adhesion forces observed using AFM and attests to the forceful contact established during AFM or stirring in the microcalorimeter as

compared with the spontaneous and relatively mild nature of the interaction during convective-diffusion in the parallel plate flow chamber.

## Conclusions

The combined use of a parallel plate flow chamber, AFM and ITC has yielded new insights in the mechanisms of interaction between *S. aureus* strains with and without FnBP's and adsorbed fibronectin films. Most interestingly, exposure of either Fn-coatings or staphylococcal cell surfaces to BSA, reduces staphylococcal adhesion under convective-diffusion, but not their enthalpy of fibronectin adsorption nor the adhesion force upon retracting a Fn-coated tip from the staphylococcal cell surface. This demonstrates that convective-diffusional mass transport in a parallel plate flow chamber represents a milder form of establishing contact than during AFM or stirring in a microcalorimeter.

## Acknowledgements

We like to thank ZON-MW for grant 91105005 enabling the purchase of the Nanoscope IV Digital Instrument.

## References

**Binnig G, Quate CF, Gerber C (1986).** Atomic Force Microscope. *Phys. Rev. Lett.* 56:930–933.

**Briggner LE, Wadsö I (1991).** Test and calibration processes for microcalorimeters, with special reference to heat conduction instruments used with aqueous systems. *J. Biochem. Biophys. Methods* 22:101–118.

**Busscher HJ, Van de Belt-Gritter B, Dijkstra RJB, Norde W, Petersen FC, Scheie AA, Van der Mei HC (2007).** Intermolecular Forces and Enthalpies in the Adhesion of *Streptococcus Mutans* and Antigen I/II Deficient Mutant to Laminin Films. *J. Bacteriol.* 189:2988–2995.

**Busscher HJ, Van der Mei HC (2006).** Microbial adhesion in flow displacement systems. *Clin. Microbiol. Rev.* 19:127–141.

**Camesano TA, Natan MJ, Logan BE (2000).** Observation of changes in bacterial cell morphology using tapping mode atomic force microscopy. *Langmuir* 16:4563–4572.

**Cleveland JP, Manne S, Bocek D, Hansma PK (1993).** A nondestructive method for determining the spring constant of cantilevers for scanning force microscopy. *Rev. Sci. Instrum.* 64:403–305.

**Dufrêne YF (2003).** Recent progress in the application of atomic force microscopy imaging and force spectroscopy to microbiology. *Curr. Opin. Microbiol.* 6:317–323.

**Fowler T, Wann ER, Joh D, Johansson S, Foster TJ, Hook M (2000).** Cellular invasion by *Staphylococcus aureus* involves a fibronectin bridge between the bacterial fibronectin-binding MSCRAMMS and host cell β1 integrins. *Eur. J. Cell Biol.* 79:672–679.

**Greene C, McDevitt D, Francois P, Vaudaux PE, Lew DP, Foster TJ (1995).** Adhesion properties of mutants of *Staphylococcus aureus* defective in fibronectin-binding proteins and studies on the expression of fnb genes. *Mol. Microbiol.* 17:1143–1152.

**Haynes CA, Norde W (1994).** Globular proteins at solid/liquid interfaces. *Colloid. Surf. B* 2:517–566.

**Haynes CA, Norde W (1995).** Protein Adhesion Force Dynamics and Single Adhesion Events. *J. Colloid Interface Sci.* 169:313–328.

**Hess DJ, Henry-Stanley MJ, Erlandsen SL, Wells CL (2006).** Heparan sulfate proteoglycans mediate *Staphylococcus aureus* interactions with intestinal epithelium. *Med. Microbiol. Immunol.* 195:133–141.

**Moy VT, Florin EL, Gaub HE (1994).** Intermolecular forces and energies between ligand and receptors. *Science* 266:257–259.

**Nordmark MG, Laynez J, Schön A, Suurkuusk J, Wadsö I (1984).** Design and testing of a new microcalorimetric vessel for use with living cellular systems and in titration experiments. *J. Biochem. Biophys. Methods* 10:187–202.

**Peacock SJ, Foster TJ, Cameron BJ, Berendt AR (1999).** Bacterial fibronectin-binding proteins and endothelial cell surface fibronectin mediate adherence of *Staphylococcus aureus* to resting human endothelial cells. *Microbiol.* 145:3477–3486.

**Saravia-Otten P, Muller HP, Arvidson S (1997).** Transcription of *Staphylococcus aureus* fibronectin binding protein genes is negatively regulated by agr and an agr-independent mechanism. *J. Bacteriol.* 179:5259–5263.

**Sousa SR, Manuela Brás M, Moradas-Ferreira P, Barbosa MA (2007).** Dynamics of fibronectin adsorption on $TiO_2$ surfaces. *Langmuir* 23:7046–7054.

**Vaudaux P, Suzuki R, Waldvogel FA, Morgenthaler JJ, Nydegger UE (1984a).** Foreign body infection: role of fibronectin as a ligand for the adherence of *Staphylococcus aureus*. *J. Infect. Dis.* 150:546–553.

**Vaudaux PE, Waldvogel FA, Morgenthaler JJ, Nydegger UE (1984b).** Adsorption of fibronectin onto polymethyl-methacylate and promotion of *Staphylococcus aureus* adherence. *Infect. Immunol.* 45:768–774.

**Wu CF, Chen WY, Lee JF (1996).** Microcalorimetric Studies of the interactions of imidazole with immobilized Cu(II): Effects of pH value and salt concentration. *J. Colloid Interface Sci.* 183:236–242.

**Xu CP, Van de Belt-Gritter B, Busscher HJ, Van der Mei HC, Norde W (2007).** Calorimetric comparison of the interactions between salivary proteins and *Streptococcus mutans* with and without antigen I/II. *Colloids Surf. B* 54, 193–199.

**Yongsunthon R, Fowler VGJ, Lower BH, Vellano FP, Alexander E, Reller LB, Corey GR, Lower SK (2007).** Correlation between fundamental binding forces and clinical prognosis of *Staphylococcus aureus* infections of medical implants. *Langmuir* 23: 2289–2292.

# 6

# Bond ageing in the adhesion of *Staphylococcus aureus* strains with and without fibronectin-binding proteins to fibronectin films

Chun-Ping Xu, Joop de Vries, Hans J. Kaper, Henny C. van der Mei, Willem Norde, Henk J. Busscher

*Applied and Environmental Microbiology* (submitted)

## Introduction

*Staphylococcus aureus* is an extremely versatile pathogen, which can adhere to epithelial cells, endothelial cells, fibroblasts as well as to biomaterials surfaces in the human body (Lowy, 1998). *S. aureus* is thought to adhere to eukaryotic cells and biomaterials surfaces by interaction with adsorbed host plasma and matrix proteins such as fibronectin (Fn), a high molecular weight glycoprotein (approximately 250 kDa)(Vaudaux *et al.*, 1984). Adhesion to Fn-films involves the fibronectin binding proteins (FnBP) A and B on the staphylococcal cell (Fowler *et al.*, 2000; Greene *et al.*, 1995) and in vitro adhesion of *S. aureus* strain Wood 46 to Fn-coated surfaces was demonstrated to be inhibited in a dose-dependent manner by anti-Fn antibodies (Cleveland *et al.*,1993; Dabros and Van de Ven, 1982).

Initial microbial adhesion is reversible, but over time the bond strength may increase and adhesion becomes gradually less reversible. The kinetics of microbial adhesion and desorption can be investigated simultaneously in a parallel plate flow chamber with *in situ* observation and real-time image analysis. Moreover, by registering the time of arrival and detachment of an adhering microorganism from a surface, desorption can be measured as a function of the residence time of an adhering organism (Dabros and Van de Ven, 1982; Sjollema *et al.*,1990; Van de Ven, 1989). Dabros and Van de Ven (1982) proposed that the desorption rate coefficient of a particle adsorbed at time $\tau$ and desorbing at time $t$, i.e. after residing on the surface for a time $(t-\tau)$, changes exponentially from an initial value $\beta_0$ to a final value $\beta_\infty$ during ageing of the bond with a relaxation time $1/\delta$ according to

$$\beta(t-\tau) = \beta_\infty - (\beta_\infty - \beta_0)e^{-\delta(t-\tau)} \qquad (1)$$

Meinders *et al.* (1994) applied this equation to analyze the residence time-dependent desorption of *Streptococcus thermophilus* B during non-specific adhesion from glass, and found that the desorption rate coefficient decreased according to Eq.(1) from an initially high value $\beta_0$ ($2.5 \times 10^{-3}$ $s^{-1}$) to an almost negligibly low value $\beta_\infty$ ($0.1 \times 10^{-4}$ $s^{-1}$) over a time scale of approximately 50 s. Many years later, atomic force

microscopy (AFM) was applied to directly measure the strengthening of the adhesion force between *S. thermophilus* B and the silicon nitride ($Si_3Ni_4$) AFM tip and bond strengthening was found to occur by a factor of 2 to 3 to occur over a similar time scale as the residence-time dependent desorption (Vadillo-Rodríguez, *et al.*, 2004).

*S. thermophilus* B adheres to glass utilizing non-specific adhesion mechanisms, which are very different from the specific mechanisms applied by *S. aureus* strains in their adhesion to Fn-films. Specific and non-specific mechanisms have been compared in different studies with respect to adhesion, adhesion forces and interaction enthalpies (Abu-Lail and Camesano, 2006; Busscher *et al*, 2007; Xu *et al.*, 2007), but never with respect to an influence on residence-time dependent desorption and bond strengthening. Therefore, the aim of this study is to determine the residence-time dependent desorption of two *S. aureus* strains with and without FnBp's from Fn-films. In addition, residence-time dependent desorption will be compared with AFM analysis of bond strengthening between Fn-coated tips and immobilized *S. aureus* cells.

## Materials and Methods

### *Bacterial strains and culture conditions*

*S. aureus* strain 8325-4 and its isogenic mutant lacking FnBP's, DU5883 (kindly provided by Dr T.J. Foster, Moyne Institute of Preventive Medicine, Dublin, Ireland), were used in this study. The bacterial cells were maintained at -80 °C in tryptone soya broth (TSB; OXOID, Basingstoke, UK) containing 7% dimethylsulfoxide (MERCK, Germany). For culturing, both strains were plated onto TSB agar plates overnight at 37°C. Subsequently, bacterial colonies were precultured in 10 ml TSB batch culture overnight on a rotary shaker incubator (150 rpm). This preculture was used to inoculate a main culture of 190 ml TSB. After approximately 2 h of growth to early stationary phase, corresponding with peak expression of FnBP's on the surface of strain 8325-4 (Saravia-Otten *et al.*, 1997), bacteria were harvested by centrifugation at 6500*g* for 5 min at 10°C and washed twice with demineralized water. Bacterial aggregates were broken by mild sonication on ice for 3 × 10 s at 30 W (Vibra Cell model 375, Sonics and Materials Inc., Danbury, Connecticut, USA). Then, bacteria

were resuspended in phosphate-buffered saline (PBS, 10 mM potassium phosphate and 0.15 M NaCl; pH 7) to a concentration of $3 \times 10^8$ per ml for adhesion experiments, as determined in a Bürker-Türk counting chamber. In order to block non-specific adhesion sites on the staphylococcal cell surfaces, staphylococci were also incubated for 60 min at 37°C in PBS supplemented with 1% bovine serum albumin (BSA).

***Bacterial deposition to a Fn-film in a parallel plate flow chamber***

The deposition experiments were carried out in a parallel plate flow chamber (internal dimensions: length × width × height, 175 × 17 × 0.75 mm) equipped with image analysis options, as described in detail previously (Busscher and Van der Mei, 2006). The bottom glass plate of the flow chamber was drop-coated with 0.05 ml Fn (20 μg $ml^{-1}$, Sigma-Aldrich BV, Zwijndrecht, The Netherlands) for 2 h at room temperature to create a circular Fn-coated region with a diameter of approximately 1 cm on which staphylococcal adhesion was monitored. In addition, glass plates were prepared on which non-specific adhesion sites were blocked by immersing the entire glass, including the Fn-coated region for 1 min in PBS containing 1% BSA. Glass plates were rinsed after protein coating with demineralized water. Bacterial adhesion was monitored with a phase-contrast microscope (Olympus BH-2) coupled to a Firewire CCD camera (High Technology) equipped with a ×40 ultra-long-working-distance lens (Olympus ULWD-CD plan 40 PL). Therewith, the surface area covered by an image was $2.8 \times 10^{-4}$ $cm^2$.

The flow rate during the experiments was adjusted to 1.4 ml $min^{-1}$ under the influence of a hydrostatic pressure yielding a shear rate of 15 $s^{-1}$. During flow experiments, 15 frames (size 1392 × 1040 pixels) were grabbed every 1 s in order to distinguish between adhered and in focus moving bacteria. These frames were averaged on a pixel by pixel basis and computer-stored for subsequent offline analysis using proprietary software based on the Matlab Image Processing Toolkit (The Mathworks, MA, USA). Further analysis consisted of locating the staphylococci on the substratum surface and comparison of their positions in a current image with their positions in previous images to determine the total number of adhering bacteria $n(t)$ as

a function of time and their desorption rate coefficient $\beta(t-\tau)$ as a function of residence-time$(t-\tau)$ (Meinders *et al.*, 1994), according to

$$\beta(t-\tau) = \sum_{j=1}^{N-1} \frac{1}{N-j-1} \sum_{i=j+1}^{N} \frac{\Delta n_{des}(t_i)}{\Delta n_{ads}(\tau_{i-j})(t_i - t_{i-1})} \qquad (2)$$

where $N$ is the number of images taken, $\Delta n_{des}(t_i)$ is the number of bacterial desorbing between time $t_{i-1}$ and ti and adsorbing between time $\tau_{i-j-1}$ and $\tau_{i-j}$, and $\Delta n_{ads}(t_{i-j})$ is the total number of adsorbed bacteria between time $\tau_{i-j-1}$ and $\tau_{i-j}$.

Subsequently, residence-time dependent desorption rates were fitted to Eq.(1) to yield the initial and final desorption rate coefficients ($\beta_0$ and $\beta_\infty$, respectively) and their relaxation time $1/\delta$. Residence-time dependent desorption rate coefficients were determined in three-fold with separate bacterial cultures.

***Atomic force microscopy***

For AFM, the negatively charged bacteria were attached through electrostatic interactions to a glass slide, made positively charged through pre-adsorption of poly-L-lysine, as described before (Camesano *et al.*, 2000). AFM tips (DNP from Veeco, Woodbury, USA) were coated with a Fn-film by immersion for 30 min in a Fn-solution (25 μg $ml^{-1}$ in PBS, pH 7) with the aid of a micromanipulator. All glass slides with immobilized bacteria and Fn-coated AFM tips were immediately used after preparation. To block non-specific binding sites on the bacterial cell surfaces, the glass slides with attached bacteria were also immersed for 1 min into PBS containing 1% BSA and rinsed with demineralized water.

AFM measurements were done at room temperature in PBS using a Dimension 3100 system (Nanoscope IV Digital Instrument, Woodbury, USA). Nanoscope imaging software (version 6.13r1, Veeco) was used to analyze the resulting images. All AFM cantilevers were calibrated using resonant frequency measurements (Cleveland *et al.*, 1993; Saravia-Otten *et al.*, 1997) and the conversion of deflection to force was carried out as has been previously described by others (Dufrêne, 2000). The

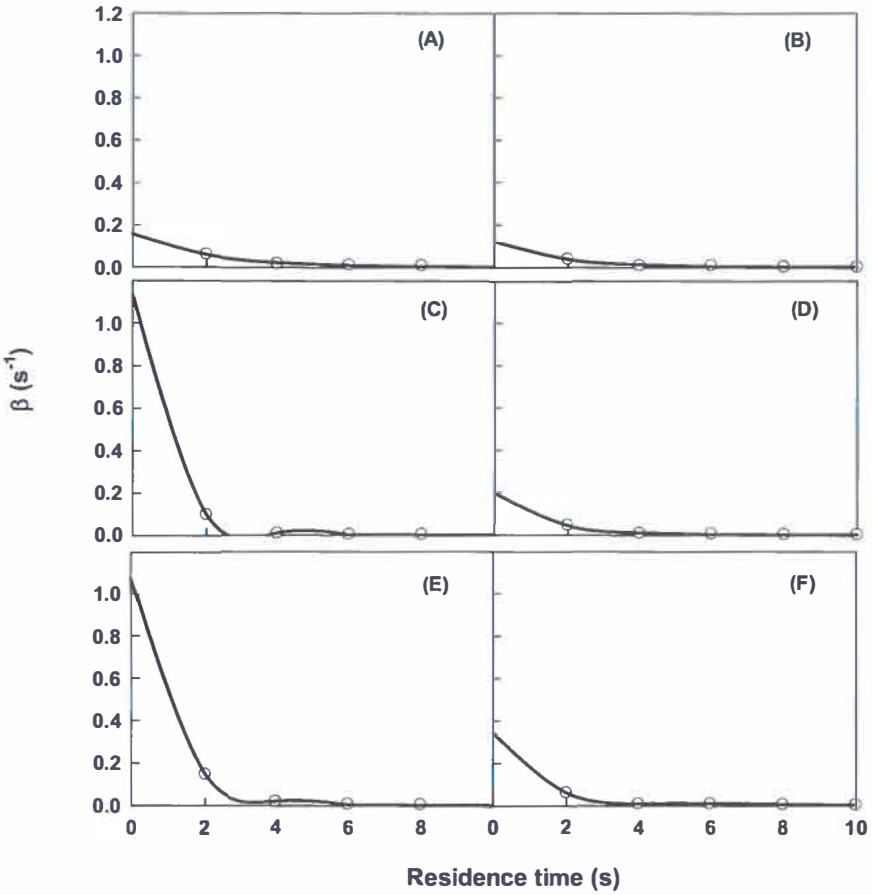


**Figure 1.** Representative examples of the desorption rate coefficient $\beta(t-\tau)$ as a function of residence time $(t-\tau)$ for
(A) *S. aureus* 8325-4 from Fn-film
(B) *S. aureus* DU5883 from Fn-film
(C) *S. aureus* 8325-4 from BSA coated Fn-film
(D) *S. aureus* DU5883 from BSA coated Fn-film
(E) BSA coated *S. aureus* 8325-4 from Fn-film
(F) BSA coated *S. aureus* DU5883 from Fn-film
in PBS in a parallel plate flow chamber.

repulsive force at contact after approach and the adhesion force $F_0$ upon retract were registered. Retracting of the tip from the bacterial surface was carried out after 0 and 2 s contact time between the AFM tip and staphylococcal cell surface. Retract curves were integrated to yield the bond strength energy for the two surface delay times

evaluated. A total of three different bacterial cells were examined for each particular case, yielding 30 force-distance curves.

### *Statistical analysis*

Data were analyzed with the Statistical Package for the Social Sciences (Version 11.0, SPSS, Chicago, Illinois, USA). Median values of the repulsive force at contact ($F_0$) upon approach, the adhesion force ($F_{adh}$) upon retract, as well as of the bond strength energy, are presented for each bacterial strain. The Wilcoxon signed rank test for the median was used for statistical analyses of the AFM data. A Student's t-test was used to determine significant differences in the initial and final desorption rate coefficients, and their relaxation time. The level of significance was set at $p < 0.05$.

**Table 1.** Mean values for the initial ($\beta_0$) and final desorption rate coefficients ($\beta_\infty$) together with the relaxation time for bond ageing ($1/\delta$) for *S. aureus* 8325-4 with FnBp's and isogenic mutant DU5883 without FnBP's from Fn-coatings. Experiments were performed prior to and after exposure of the substrata or the staphylococci to a 1% BSA solution. All experiments were done in three fold with separately prepared Fn-films and different bacterial cultures.

| Substratum | Initial desorption rate $\beta_0$ ($10^{-3}$ $s^{-1}$) | | Final desorption Rate $\beta_\infty$ ($10^{-3}$ $s^{-1}$) | | Relaxation time for bond ageing $1/\delta$ (s) | |
|---|---|---|---|---|---|---|
| | 8325-4 | DU5883 | 8325-4 | DU5883 | 8325-4 | DU5883 |
| **Fn-coated glass** | 192 ± 52 | 116 ± 48 | 0.5 ± 0.2 | 0.5 ± 0.4 | 1.8 ± 0.4 | 1.7 ± 0.3 |
| **Fn and BSA-coated glass** | 1268± 291 | 160 ± 42 | 0.5 ± 0.1 | 0.4 ± 0.1 | 1.1 ± 0.6 | 1.7 ± 0.5 |
| **Fn-coated glass*** | 946 ±112 | 352 ±1 | 0.4 ± 0.1 | 0.4 ± 0.0 | 1.1 ± 0.1 | 1.5 ± 0.1 |

* These experiments were carried out with staphylococci exposed to 1% BSA prior to the experiments.

## Results

### *Residence time dependent desorption of S. aureus from Fn-films*

Fig. 1 shows representative examples of the residence-time dependent desorption of *S. aureus* 8325-4 and DU5883 from Fn-coatings. Table 1 summarizes the quantitative features of these graphs. Desorption rates decrease with increasing residence-times for both strains, regardless of the absence or presence of a BSA-coating on the surfaces. Initial desorption rate coefficients ($\beta_0$) from Fn-films are similar for *S. aureus* 8325-4 with FnBp's as for *S. aureus* DU5883 without FnBp's, but blocking non-specific binding sites, either on the bacterial cell surface or on the Fn-film, results in higher initial desorption rate coefficients; the increase is much stronger for the strain with FnBp's than for the strain without FnBp's (Student t-test, $p < 0.05$). Final desorption rate coefficients ($\beta_\infty$) are similar for both strains without significant influences of additional BSA-coatings and bond ageing occurs over a time-scale of 1 to 2 s.

### *Bond strengthening between Fn-coatings and S. aureus cell surfaces*

Fig. 2 and 3 show examples of force-distance curves measured with AFM for both strains and an Fn-coated AFM tip, in the absence and presence of additional BSA-coatings, respectively, while their quantitative features are presented in Table 2. The repulsive force at contact $F_0$, is significantly ($p < 0.05$) stronger for *S. aureus* 8325-4 with FnBp's than for *S. aureus* DU5883, both for a 0 s as well as for a 2 s surface delay. Blocking of non-specific binding sites on the staphylococcal cell surfaces has little (*S. aureus* DU5883) or no (*S. aureus* 8325-4) influence on the repulsive force upon approach. However, upon retract, median adhesion forces were significantly stronger after a 2 s surface delay than when measured immediately, i.e. with a 0 s surface delay. There is no significant difference in adhesion forces between the two strains. Interestingly, the range over which the adhesion forces are operative differs considerably between the different conditions applied, which translates in significant differences in bond strength energies. Initial bond strength energies of *S. aureus* 8325-4 with FnBp's are significantly ($p < 0.05$) higher than for *S. aureus* DU5883 without FnBp's, regardless of exposure of the staphylococci to a 1% BSA solution. Both

strains show a significant increase in bond strength energy when the surface delay time is increased from 0 to 2 s by a factor 2 to 3 for *S. aureus* 8325-4 and even more (factor 4 to 5) for *S. aureus* DU5883. Furthermore, after a surface delay time, effects of BSA exposure of the staphylococci on bond strength disappear.

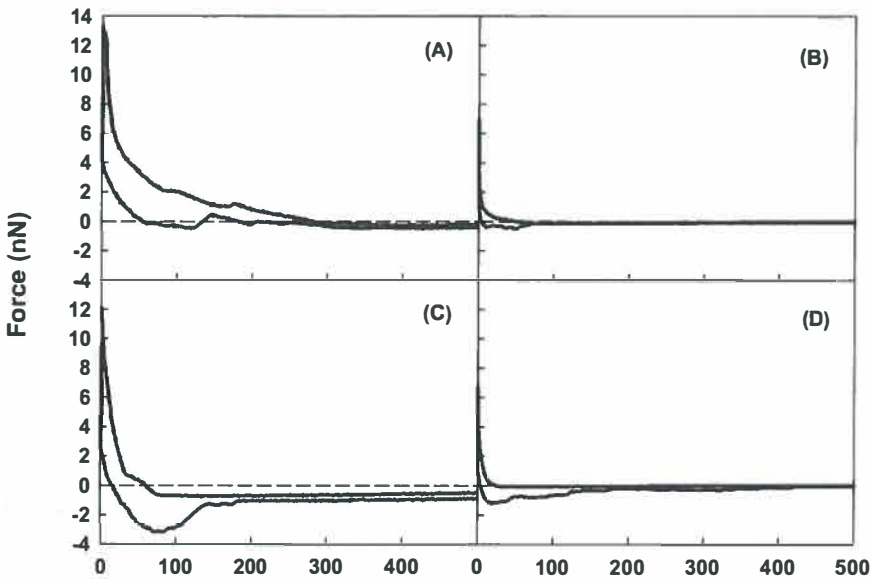


**Figure 2.** Representative examples of force-distance curve between an Fn-coated AFM tip and staphylococcal cell surfaces.
(A) *S. aureus* 8325-4 after 0 s surface delay
(B) *S. aureus* DU5883 after 0 s surface delay
(C) *S. aureus* 8325-4 after 2 s surface delay
(D) *S. aureus* DU5883 after 2 s surface delay

**Table 2.** Median values for the repulsive forces at contact $F_0$ upon approach, adhesion force Fadh upon retract and associated bond strength energies for the interaction between Fn-coated AFM tips and *S. aureus* 8325-4 and an isogenic mutant without FnBP's, DU5883 prior to and after bacterial exposure to 1% BSA. All experiments were done in three-fold with separately prepared Fn-coated AFM tips, yielding thirty N force-distance curves.

| Delay time (s) | Treatment | Repulsive force at contact $F_0$ (nN) | | Adhesion force $F_{adh}$ (nN) | | Bond strength energy ($10^{-16}$J) | |
|---|---|---|---|---|---|---|---|
| | | 8325-4 | DU5883 | 8325-4 | DU5883 | 8325-4 | DU5883 |
| 0 | No BSA | 9.3 | 6.0 | 0.7 | 0.6 | 98 | 32 |
| | 1% BSA | 9.4 | 3.6 | 0.6 | 0.5 | 64 | 21 |
| 2 | No BSA | 8.9 | 6.0 | 1.5 | 1.7 | 187 | 181 |
| | 1% BSA | 8.7 | 4.2 | 1.1 | 1.1 | 176 | 149 |

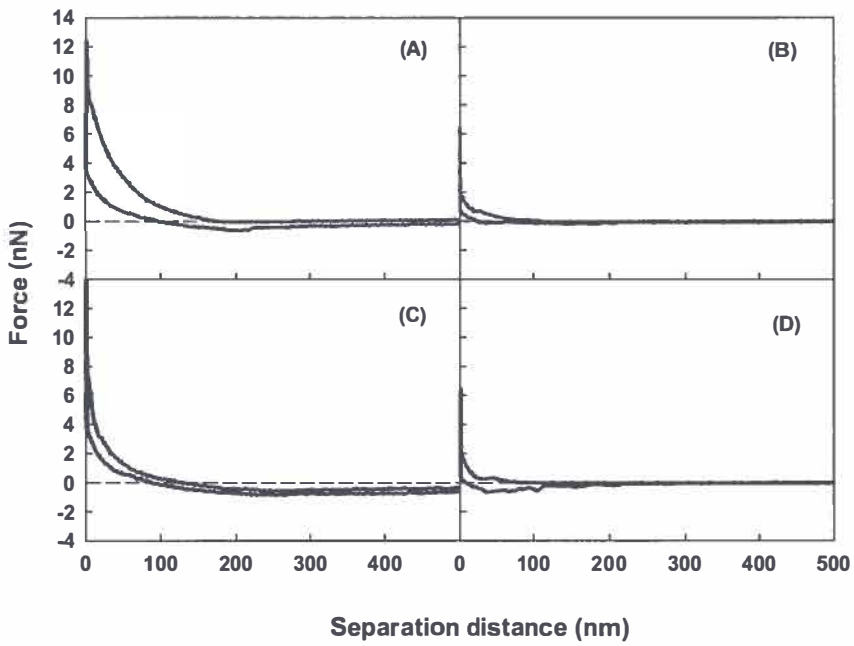


**Figure 3.** Representative examples of force-distance curve between an Fn-coated AFM tip and staphylococcal cell surfaces after exposure of the staphylococci to a 1% BSA solution.
(A) *S. aureus* 8325-4 after 0 s surface delay
(B) *S. aureus* DU5883 after 0 s surface delay
(C) *S. aureus* 8325-4 after 2 s surface delay
(D) *S. aureus* DU5883 after 2 s surface delay

## Discussion

This paper compares bond ageing in the adhesion of two *S. aureus* strains with and without FnBp's to an Fn-coated surface. Strengthening of the bond is evident from the chamber as well as from a comparison of the adhesion forces and adhesive bond strength energies measured after 0 and 2 s surface delays in AFM.

First of all, it is interesting to note that desorption of *S. thermophilus* from glass surfaces (Meinders *et al.*, 1994) follows completely different kinetics than the two staphylococcal strains studied here. Adhesion of *S. thermophilus* to glass proceeds in the full absence of specific contributions to the adhesion process, while adhesion to Fn-films of at least *S. aureus* 8325-4 is expected to be dominated by specific contributions (Xu *et al.*, in preparation; Yongsunthon *et al.*, 2007). Desorption rate coefficients decrease by a factor of 250 in non-specific *S. thermophilus* adhesion, but by a factor of 1500 in specific *S. aureus* adhesion. More strikingly, the larger decrease in desorption observed for *S. aureus* occurs extremely fast within 2 s, while *S. thermophilus* desorption decreases over a time scale of 50 s. Both for *S. thermophilus* as well as for *S. aureus*, these time constants could be confirmed by independent AFM measurements. This suggests that in case of non-specific adhesion, bond ageing may involve relatively slow removal of water between the bacterium and the hydrophilic glass surface, whereas specific adhesion is a fast "click-on" process of stereo-chemical components on the interacting surfaces.

AFM adhesion forces to Fn-coated surfaces are similar for both *S. aureus* strains. This is unexpected considering their different abilities to bind Fn (Saravia-Otten *et al.*, 1997). Adsorption of Fn is a process occurring at the outermost cell surface. However, the Fn-coated AFM tip penetrates into the outermost cell surface. Upon penetration, it is clear that both *S. aureus* strains FnBP's or other adhesins are encountered for, also for strain DU5883 generally considered to be devoid of FnBP's (Saravia-Otten *et al.*, 1997). However, the spatial distribution of FnBP's in strain 8325-4 must be completely different than in strain DU5883, as its adhesion forces reach out much further and consequently strain 8325-4 has a higher Fn-bond strength energy than strain DU5883. The suggestion that the penetrating tip reveals hidden

FnBP's is also corroborated by the observation that BSA-coating of the staphylococci significantly increases their initial desorption with little effect on the AFM probed adhesion forces. Under the conditions of convective-diffusion prevailing in the parallel plate flow chamber, it can be envisaged that bacteria land mildly at the substratum surface, therewith invoking interaction with only the outermost region of the cell wall. Contrarily, the penetrating AFM tip senses similar bond strength energies with no influence of an adsorbed BSA-film over the cell surface. Mendez-Vilas *et al.* (2006; 2007) has suggested that a penetrating AFM tip may cause irreversible damage to the inner cell surface, as concluded from saw-tooth patterns in the force-distance curves at close approach. As we observed no such patterns in our force-distance curves (see Figs. 2 and 3), it is considered unlikely that the AFM tip has caused such cell surface damage. Moreover, we also regularly checked whether interaction of our Fn-coated tips with clean glass yielded the same force values, and this was always the case within one series of experiments. In this respect it is important to note that our initial *S. aureus* adhesion forces, as determined with a Fn-coated tip, are essentially identical to those measured in exactly the same way by Yongsunthon *et al.* (2007), who reported values of 0.57 ± 0.05 nN for 15 different tissue-invasive *S. aureus* isolates. Fifteen non-invasive control isolates had lower adhesion forces of 0.29 ± 0.05 nN, suggesting both our strains to be tissue-invasive (Brouillette *et al.*, 2003).

Provided that for a given bacterial strain/surface combination all bacteria adhere with the same bond strength, a staphylococcal bond strength energy can also be calculated from the desorption rate coefficients measured in the parallel plate flow chamber, by applying

$$\beta_{esc} = \frac{j_0}{c\Delta h} e^{\varphi_m / kT} \qquad (3)$$

where $\beta_{esc}$ is the desorption rate coefficient, $j_0$ the initial deposition rate, c the bacterial cell concentration at the entrance of the flow chamber, Δh the width of the energy minimum, φm depth of the energy minimum and $kT$ the energy of thermal motion (Meinders *et al.*, 1994; Xia *et al.*, 1994). The initial bond strength energies of our

staphylococcal strains to a Fn-film in the absence of a BSA-coating can be calculated from the initial desorption rate coefficients and ranges between 3.6 to 3.7 $kT$. After bond ageing, the use of the final desorption rate coefficients yields bond strength energies between 9.1 and 9.7 $kT$. These bond strength energies are comparable to those calculated for *S. thermophilus*. Yet, these bond strength energies are orders of magnitude smaller than derived from AFM, and conversion of the bond strength energies from Table 2 to a thermal energy scale yields values of around $10^6$ $kT$. This huge number attest to the fact that the penetrating, Fn-coated AFM tip must have encountered numerous receptor sites in the cell surface.

## Conclusions

In conclusion, this paper demonstrates that bond strengthening in the specific adhesion of *S. aureus* strains to Fn-films occurs on a much faster time scale than in non-specific adhesion. Times scales of bond ageing as derived from residence-time dependent desorption measurements in a parallel plate flow chamber were confirmed by independent AFM measurements. Bond strength energies calculated from the retract force-distance curves in AFM were orders of magnitude larger than calculated from desorption rate coefficients, suggesting that the penetrating Fn-coated AFM tip probes multiple receptor sites in the outermost layer of the cell surface, even for *S. aureus* DU5883, generally considered devoid of FnBP's. Mild landing of an organism on a Fn-coated substratum as during convective-diffusion in the parallel plate flow chamber clearly does not invoke specific interaction with deeper located receptors.

## References

**Abu-Lail NI and Camesano TA (2006).** Specific and nonspecific interaction forces between Escherichia coli and silicon nitride, determined by Poisson statistical analysis. *Langmuir* 22:7296–7301.

**Brouillette E, Grondin G, Shkreta L, Lacasse P, Talbot BG (2003).** In vivo and in vitro demonstration that *Staphylococcus aureus* is an intracellular pathogen in the presence or absence of fibronectin-binding proteins. *Microb. Pathog.* 35:159–68.

**Busscher HJ and Van der Mei HC (2006).** Microbial adhesion in flow displacement systems. Clin. Microbiol. Rev. 19:127–141.

**Busscher HJ, Van de Belt-Gritter B, Dijkstra RJB, Norde W, Petersen FC, Scheie AA, Van der Mei HC (2007).** Intermolecular forces and enthalpies in the adhesion of *Streptococcus mutans* and antigen I/II deficient mutant to laminin films. *J. Bacteriol.* 189:2988–2995.

**Camesano TA, Natan MJ, Logan BE (2000).** Observation of changes in bacterial cell morphology using tapping mode atomic force microscopy. *Langmuir* 16:4563–4572.

**Cleveland JP, Manne S, Bocek D, Hansma PK (1993).** A nondestructive method for determining the spring constant of cantilevers for scanning force microscopy. *Rev. Sci. Instrum.* 64:403–305.

**Dabros T and Van de Ven TGM (1982).** Kinetics of coating by colloidal particles. *J. Colloid Interface Sci.* 89:232–244.

**Dufrêne YF (2000).** Direct characterization of the physicochemical properties of fungal spores using functionalized AFM probes. *Biophys. J.* 78:3286–3291.

**Fowler T, Wann ER, Joh D, Johansson S, Foster TJ, Hook M (2000).** Cellular invasion by *Staphylococcus aureus* involves a fibronectin bridge between the bacterial fibronectin-binding MSCRAMMS and host cell β1 integrins. *Eur. J. Cell Biol.* 79:672–679.

**Greene C, McDevitt D, Francois P, Vaudaux PE, Lew DP, Foster TJ (1995).** Adhesion properties of mutants of *Staphylococcus aureus* defective in fibronectin-binding proteins and studies on the expression of fnb genes. *Mol. Microbiol* 17:1143–1152.

**Lowy FD (1998).** *Staphylococcus aureus* infections. *N. Engl. J. Med.* 339:520–532.

**Meinders JM, Van der Mei HC, Busscher HJ (1994).** Physicochemical aspects of deposition of *Streptococcus thermophilus* B to hydrophobic and hydrophilic substrata in a parallel plate flow chamber. *J. Colloid Interface Sci.* 164:355–363.

**Mendez-Vilas A, Gallardo-Moreno AM, González-Martín ML (2006).** Nano-mechanical exploration of the surface and sub-surface of hydrated cells of *Staphylococcus epidermidids*. *Antonie van Leeuwenhoek.* 89:373–386.

**Mendez-Vilas A, Gallardo-Moreno AM, Calzado-Montero R, Gonzalez-Martin ML (2007).** AFM probing in aqueous environment of *Staphylococcus epidermidis* cells naturally immobilized on glass: Physico-chemistry behind successful immobilization. *Col. Surf. B: Biointerfaces* doi:10.1016/j.colsurfb. 2007.11.011.

**Saravia-Otten P, Muller HP, Arvidson S (1997).** Transcription of *Staphylococcus aureus* fibronectin binding protein genes is negatively regulated by agr and an agr-independent mechanism. *J. Bacteriol.* 179:5259–5263.

**Sjollema J, Van der Mei HC, Uyen HM, Busscher HJ (1990).** Direct observations of cooperative effects in oral streptococcal adhesion to glass by analysis of the spatial arrangement of adhering bacteria. *FEMS Microbiol. Lett.* 69:263–269.

**Vadillo-Rodríguez V, Busscher HJ, Norde W, De Vries J, Van der Mei HC (2004).** Atomic force microscopic corroboration of bond ageing for adhesion of *Streptococcus thermophilus* to solid substrata. *J. Colloid. Interface Sci.* 278:251–254.

**Vaudaux P, Suzuki R, Waldvogel FA, Morgenthaler JJ, Nydegger UE (1984).** Foreign body infection: role of fibronectin as a ligand for the adherence of *Staphylococcus aureus*. *J. Infect. Dis.* 150:546–553.

**Van de Ven TGM (1989).** Effects of electrolytes, polymers and polyelectrolytes on particle deposition and detachment. *Colloids Surf.* 39:107–126.

**Xia Z, Goldsmith HL, Van de Ven TG (1994).** Flow-induced detachment of red blood cells adhering to surfaces by specific antigen-antibody bonds. *Biophys. J.* 66:1222–1230.

**Xu CP, Van de Belt-Gritter B, Busscher HJ, Van der Mei HC, Norde W (2007).** Calorimetric comparison of the interactions between salivary proteins and *Streptococcus mutans* with and without antigen I/II. *Colloids Surf. B* 54:193–199.

**Xu CP, De Vries J, Norde W, Van der Mei HC, Busscher HJ (2008).** Interaction enthalpies and adhesion forces between fibronectin and *S. aureus* with and without FnBP (in preparation).

**Yongsunthon R, Fowler VGJ, Lower BH, Vellano FP, Alexander E, Reller LB, Corey GR, Lower SK (2007).** Correlation between fundamental binding forces and clinical prognosis of *Staphylococcus aureus* infections of medical implants. *Langmuir* 23: 2289–2292.

# 7

# General discussion

Bacterial adhesion plays an essential role in not only the establishment of many natural microbial communities, but also in such diverse phenomena as the salubrious or pathogenic colonization associated with maintenance of health or disease, phagocytic host defense and industrial fouling (Chan *et al.*, 1985). Therefore, bacterial adhesion is of major importance to areas of environmental, medical and industrial interest (Costerton *et al.*, 1995).

Recent research has provided insight into the mechanisms of some bacteria-protein interactions, revealing complexity and diversity, as described in chapter 1. Results of the current research, aimed at elucidating protein adsorption to bacterial surfaces, are usually explained by the molecular heterogeneity and structural complexity of the bacterial surfaces (Buscher *et al.*, 2006; Corrigan *et al.*, 2007; Raibaud, *et al.* 2005). As a consequence, most of the theoretical models trying to deal with macroscopic as well as molecular aspects of bacterial adhesion present a microscopic approach of the observed phenomena up to a molecular level (Castonguay *et al.*, 2006; Chambless and Stewart, 2007; George *et al.*, 2007; Girard and Mourez, 2006; Grare *et al.*, 2007).

The challenge of this thesis was to present a multiple approach to study bacteria-protein interactions, based on the use of a parallel plate flow chamber (PPFC), isothermal titration calorimetry (ITC) and atomic force microscope (AFM), to characterize interactions operative in initial bacterial adhesion which accounts for non-specific macroscopic as well as specific molecular interactions.

## Techniques Used to Study Bacteria-Protein Interactions

Interactions involving bacteria and protein(s) are extremely complex and need to be assessed by multiple techniques. Three techniques were used to evaluate the interaction of bacteria with proteins. PPFC, AFM and ITC were employed to measure the probability, the force and the enthalpy of adhesion, respectively. Comparison between different techniques applied in this study is not always possible as the preparation for the experiments in the PPFC, ITC and AFM differ and also the area detected by the various techniques differs in magnitude. Nevertheless, the application

of complementary approaches is necessary in order to gain better insight on bacterial interactions. It should be emphasized that PPFC and ITC measurements derive average behavior from an ensemble of cells (bacterial suspensions of $3 \times 10^8$ cells per ml in the PPFC and of $5 \times 10^9$, $5 \times 10^8$, or $5 \times 10^7$ cells per ml in ITC) and the whole system is complex and dynamic, whereas AFM measurements derive the properties of only one immobilized cell per time. On the other hand, the contact surface between one bacterium and protein(s) in the flow chamber ($< 0.8 \times 10^{-12}$ $m^2$) and AFM ($< 1.3 \times 10^{-15}$ $m^2$) is far smaller than the whole bacterial surface ($3.1 \times 10^{-12}$ $m^2$) contacted with protein(s) in the ITC. Hence, it is inevitable that the results obtained from measurements that are based on different principles and different techniques are not always consistent. Combination of the three techniques described above is considered to be innovative and seems most appropriate to investigate the complicated mechanism underlying bacteria-protein interaction.

## Single and Multiple Protein(s)-Bacterium Interactions

Bacteria-protein interactions are controlled by a complex array of specific and non-specific interactions. Specific interactions between bacteria and proteins are mediated by antigens on the bacterial surface called adhesins as e.g. lectins. To investigate these specific interactions, single protein and a mixture of proteins have been used to interact with both a wild type and a mutant strain, respectively, in our research. Two species of organisms were used in our study, i.e., streptococci (*Streptococcus mutans* with and without antigen I/II), and staphylococci (*Staphylococcus aureus* with and without fibronectin-binding proteins). The mutant has less ability to adhere to a protein film than the wild type cells in the PPFC at certain conditions, and this ability was influenced by factors, such as electric charge (chapter 3 and 4), and the presence of proteins (chapter 5 and 6).

By comparing the interaction of a mixture of proteins (whole saliva) and a single protein (fibronectin) with the bacterial cell surface, a better understanding of the operating interaction mechanisms can be obtained. For a single specific binding protein as fibronectin, the process is relatively simple as it avoids the influence of

other proteins present in the system. However, if multiple proteins are involved as in saliva, cooperativity between various proteins may be an important aspect of specific binding to surfaces (Ubbink and Schär-Zammaretti, 2007). Adsorption of proteins onto bacterial cell surfaces is time-dependent, which can be monitored with ITC during the interaction of saliva with the bacteria. According to the "Vroman-effect", the adsorption patterns have to be regarded as a result of sequences of adsorption of proteins present in high concentrations in the mixture with low affinity and their displacement by proteins with higher affinity but present in lower concentration (Göppert and Müller, 2005). This is in agreement with the change in enthalpy per unit adsorbed salivary proteins, shown in Fig. 4 of Chapter 3: the enthalpy effects for the first and second injection are similar, but the adsorbed amount of salivary proteins in the second injection is much lower than in the first injection.

### Recommendation for future research

For future research in bacteria-protein interactions in bacterial adhesion by different techniques, e.g. PPFC, ITC and AFM, it is recommended to focus on the interactions between purified proteinaceous structures (adhesins) from bacterial cell surfaces and single or multiple protein(s). Moreover, the adsorption capacity of different single proteins to the bacterial surface might be compared with their adsorption from complex mixtures of proteins and the possible displacement of one protein with low affinity by another protein with higher affinity should be investigated. This would be highly relevant as most biological fluids contain mixtures of different proteins, which is reflected in the (transient) composition of adsorbed protein films to which bacteria adhere.

## References

**Buscher AZ, Grass S, Heuser J, Roth R, St Geme JW III (2006).** Surface anchoring of a bacterial adhesin secreted by the two-partner secretion pathway. *Mol. Microbiol.* 61:470–483.

**Castonguay MH, Van der Schaaf S, Koester W, Krooneman J, Van der Meer W, Harmsen H, Landini P (2006).** Biofilm formation by *Escherichia coli* is stimulated by synergistic interactions and co-adhesion mechanisms with adherence-proficient bacteria. *Res. Microbiol.* 157:471–478.

**Chambless JD and Stewart PS (2007).** A three-dimensional computer model analysis of three hypothetical biofilm detachment mechanisms. *Biotechnol Bioeng.* 97:1573–1584.

**Chan RCY, Irvin RT, Bruce AW, Costerton JW (1985).** Competitive exclusion of uropathogens from human uroepithelial cells by lactobacillus whole cells and cell wall fragments. *Infect. Immun.* 47:84–89.

**Corrigan RM, Rigby D, Handley P, Foster TJ (2007).** The role of *Staphylococcus aureus* surface protein SasG in adherence and biofilm formation. *Microbiol.* 153:2435–2446.

**Costerton JW, Lewandowski Z, Caldwell DE, Korber DR, Lappin-Scott HM (1995).** Microbial biofilms. *Annu. Rev. Microbiol.* 49:711–745.

**George NP, Konstantopoulos K, Ross JM (2007).** Differential kinetics and molecular recognition mechanisms involved in early versus late growth phase *Staphylococcus aureus* cell binding to platelet layers under physiological shear conditions. *J. Infect. Dis.* 639–646.

**Girard V and Mourez M (2006).** Adhesion mediated by autotransporters of Gram-negative bacteria: structural and functional features. *Res. Microbiol.* 157:407–416.

**Göppert TM, Müller RH (2005).** Adsorption kinetics of plasma proteins on solid lipid nanoparticles for drug targeting. *Int. J. Pharm.* 302:172–186.

**Grare M, Dague E, Mourer M, Regnouf-de-Vains JB, Finance C, Duval JF, Duval RE, Gaboriaud F (2007).** Microelectrophoresis and atomic force microscopy: new tools to explore mechanism of action of antibacterial compounds. *Pathol. Biol.* 55:465–471.

**Raibaud S, Schwarz-Linek U, Kim JH, Jenkins HT, Baines ER, Gurusiddappa S, Höök M, Potts JR (2005).** *Borrelia burgdorferi* binds fibronectin through a tandem beta-zipper, a common mechanism of fibronectin binding in staphylococci, streptococci, and spirochetes. *J. Biol. Chem.* 280:18803–18809.

**Ubbink J, Schär-Zammaretti P (2007).** Colloidal properties and specific interactions of bacterial surfaces. *Curr. Opin. Colloid Interface Sci.* 12:263–270.

# Summary

Bacterial adhesion, is of importance in a large number of different fields, from medical microbiology and pathology to food technology, and from environmental engineering to biomaterials science. An understanding of bacterial adhesion to various substratum surfaces according to theoretical models (see **chapter 1**) may help in the development of new preventive measures to reduce bacterial adhesion. Because in natural environments bacteria adhere to protein-covered surfaces rather than to pristine surfaces, detailed knowledge of the physical-chemical mechanism of bacterial adhesion to protein films is required, which is the aim of this thesis.

In **chapter 2**, the main techniques, including the parallel plate flow chamber, isothermal titration calorimetry (ITC) and atomic force microscopy (AFM), used in this thesis to evaluate the interaction of bacteria with protein-coated substrata, are described in detail. These respective techniques are aimed at measuring the probability of adhesion, the enthalpy of adhesion, and the force of adhesion at the level of a single bacterial cell.

Antigen I/II can be found on streptococcal cell surfaces and is involved in their interaction with salivary proteins. In **chapter 3**, we determine the adsorption enthalpies of salivary proteins to *Streptococcus mutans* LT11 and *S. mutans* IB03987 with and without antigen I/II, respectively using isothermal titration calorimetry. In addition, protein adsorption to the cell surfaces was determined spectrophotometrically. *S. mutans* LT11 with antigen I/II, yielded a much higher, exothermic adsorption enthalpy at pH 6.8 (ranging from $-2073 \times 10^{-9}$ to $-31707 \times 10^{-9}$ μJ per bacterium) when mixed with saliva than did *S. mutans* IB03987 ($-165 \times 10^{-9}$ to $-1107 \times 10^{-9}$ μJ per bacterium) at all bacterial concentrations studied ($5 \times 10^{9}$, $5 \times 10^{8}$, and $5 \times 10^{7}$ per ml). The largest enthalpy effects per bacterium were observed for the lowest concentration. However, the enthalpy of salivary protein adsorption to *S. mutans* LT11 became smaller at pH 5.8. Adsorption isotherms for the *S. mutans* LT11 showed considerable protein adsorption at pH 6.8 (1.2 to 2.1 mg $m^{-2}$), that decreased only slightly at pH 5.8 (1.1 to 1.6 mg $m^{-2}$), with the largest amount adsorbed at the lowest bacterial concentration. This suggests that the protein(s) in the saliva with the strongest affinity for antigen I/II is (are) readily depleted from saliva. In conclusion, antigen I/II surface proteins on *S. mutans* play a determinant role in adsorption of salivary proteins,

especially at pH 6.8 (compared to pH 5.8) through the creation of enthalpically favorable adsorption sites.

In **chapter 4**, the interaction forces between salivary proteins and *S. mutans* with (LT11) and without (IB03987) antigen I/II were investigated using AFM and related with the adhesion of the strains to saliva-coated glass in a parallel plate flow chamber. Upon approach of a saliva-coated AFM tip toward bacteria, both strains experienced a similar repulsive force, that was significantly smaller at pH 6.8 (median 3.0 and 3.1 nN for LT11 and IB03987, respectively) than at pH 5.8 (median 4.6 and 4.7 nN). The decay length of these repulsive forces was between 19 to 37 nm. Upon retraction at pH 6.8, combined specific and non-specific adhesion forces were significantly stronger for the parent strain LT11 (median -0.4 nN) than for the mutant IB03987 (median 0.0 nN), whereas at pH 5.8 the median of the adhesion forces measured was 0.0 nN for both strains. Moreover at pH 6.8, the parent strain LT11 adhered in significantly higher numbers ($9.6 \times 10^6$ $cm^{-2}$) to a salivary coating than the mutant strain IB03987 ($2.5 \times 10^6$ $cm^{-2}$). Similar to the difference in adhesion forces between both strains at pH 5.8, also the difference in adhesion between both strains disappeared at pH 5.8, which suggests the involvement of attractive electrostatic forces in the interaction between antigen I/II and salivary coatings at pH 6.8. In summary, this study shows that antigen I/II at the surface of *S. mutans* LT11 is responsible for its increased adhesion to salivary coatings under flow through an additional attractive electrostatic force.

To obtain a deep understanding of the mechanism of bacteria-protein interaction, experiments were also carried out with a single protein rather than with a pool of different proteins as in saliva. Fibronectin binding proteins (FnBP's) on staphylococcal cell surfaces mediate adhesion of *Staphylococcus aureus* to fibronectin(Fn)-coated surfaces, such as encountered on implants or tissue cells. In **chapter 5**, we compare adhesion of two *S. aureus* strains with (8325-4) and without (DU5883) FnBP's to Fn-coated surfaces in a parallel plate flow chamber. ITC was employed to determine the adsorption enthalpies of Fn to the staphylococcal cell surfaces, while AFM was used to measure the adhesion forces between the staphylococci and Fn-coated surfaces. The staphylococcal strain with FnBP's adhered

significantly faster (2438 $cm^{-2}s^{-1}$) to a Fn-coating than the mutant strain without FnBP's (1290 $cm^{-2}s^{-1}$). In line, staphylococcal adhesion forces to Fn-coated glass were stronger for the parent strain with FnBP's (median -0.7 nN) than for the mutant without FnBP's (median -0.3 nN). In addition, the adsorption enthalpies of Fn to the cell surfaces were exothermic and higher (-140 × $10^{-9}$ μJ per bacterium) when the strain possessed FnBP's than when the strain lacked FnBP's (-43 × $10^{-9}$ μJ per bacterium). After exposure of either Fn-coatings or staphylococcal cell surfaces to bovine serum albumin (BSA), the parent and mutant strain behaved similarly with respect to their adhesion to Fn-coated glass, suggesting that BSA blocked specific interactions both through adsorption to the Fn-coating or to the staphylococcal cell surface. However, adhesion forces and adsorption enthalpies were largely unaffected by BSA adsorption. This implies that under the mild contact conditions of convective-diffusion in the parallel plate flow chamber, adsorbed BSA inhibits specific interactions to occur, but the forced contact during AFM or stirring in the microcalorimeter allows interaction between FnBP's and fibronectin, despite an adsorbed BSA film.

In **chapter 6**, we compare the residence-time dependent desorption of two *S. aureus* strains with (8325-4) and without (DU5883) FnBP's from Fn-coated surfaces in a parallel plate flow chamber. Bond strengthening in the specific adhesion of the *S. aureus* strains to Fn-films occurred on a much faster time scale (2 s) than in non-specific adhesion, the latter taking several tens of seconds. Time scales of staphylococcal bond ageing as derived from residence-time dependent desorption measurements in the parallel plate flow chamber were confirmed by independent AFM measurements. Bond strength energies calculated from the retract force-distance curves in AFM were orders of magnitude larger than calculated from desorption rate coefficients, suggesting that the penetrating Fn-coated AFM tip probes multiple receptor sites in the outermost cell surface, even for *S. aureus* DU5883, generally considered devoid of FnBP's. Mild landing of an organism on a Fn-coated substratum as during convective-diffusion in the parallel plate flow chamber clearly does not reach deeper located receptors.

As summarized in the **general discussion**, use of a parallel plate flow chamber, AFM and ITC, provide us with a deeper understanding of the mechanisms of bacterial adhesion to adsorbed protein films, which appears to be a complex interplay of physical-chemical mechanisms, involving non-specific contributions and specific, molecular recognition phenomena.

# Samenvatting

Aanhechting van bacteriën speelt op veel verschillende gebieden een rol, variërend van medische microbiologie tot voedingswetenschap en van milieutechnologie tot biomaterialen. Als het bekend zou zijn volgens welke theoretische modellen (zie **hoofdstuk 1**) bacteriën hechten aan bepaalde materialen kunnen er nieuwe mogelijkheden ontwikkeld worden om dit tegen te gaan. Omdat in een natuurlijke omgeving bacteriën voornamelijk hechten aan met eiwit bedekte oppervlakken in plaats van aan kale oppervlakken is vooral kennis van het fysich-chemisch mechanisme van bacteriële hechting aan eiwitten van belang. Dit is dan ook het doel van dit proefschrift.

In **hoofdstuk 2** worden de belangrijkste technieken, waaronder de parallelle plaat stroomkamer, isotherme titratie calorimetrie (ITC) en atomaire kracht-microscopie (AFM), welke in dit proefschrift gebruikt worden om de interactie tussen bacteriën en met eiwit bedekte oppervlakken te bestuderen, uitgebreid beschreven. Deze technieken worden respectievelijk gebruikt om de waarschijnlijkheid van aanhechting, de enthalpie van aanhechting en de sterkte van de aanhechting te meten op het niveau van één enkele bacterie.

Sommige streptococcen hebben het eiwit antigeen I/II op hun oppervlak, wat een belangrijke rol speelt bij de interactie met speekseleiwitten. In **hoofdstuk 3** worden de adsorptie-enthalpiën bepaald van de interactie van *Streptococcus mutans* LT11 (met antigeen I/II) en *S. mutans* IB03987 (zonder antigeen I/II), met speekseleiwitten, met behulp van isotherme caloriemetrie. Ook is de adsorptie aan bacterieoppervlakken spectrofotometrisch bepaald. De reactie van *S. mutans* LT11, met antigeen I/II, met speekseleiwit geeft een veel hogere exotherme adsorptie-enthalpie bij pH 6,8 ( varierend van $-2073 \times 10^{-9}$ tot $-31707 \times 10^{-9}$ μJ per bacterie) dan *S. mutans* IB03987 ($-165 \times 10^{-9}$ tot $-1107 \times 10^{-9}$ per bacterie), bij alle gemeten bacterieconcentraties ( $5 \times 10^{9}$, $5 \times 10^{8}$ en $5 \times 10^{7}$ per ml). De hoogste enthalpie per bacterie werd gemeten bij de laagste bacterieconcentratie. Bij pH 5,8 werd het enthalpie-effect van de adsorptie van speekseleiwit aan *S. mutans* LT11 kleiner. Adsorptie-isothermen van *S. mutans* LT11 laten een behoorlijke eiwitadsorptie zien bij pH 6,8 (1,2 tot 2,1 mg $m^{-2}$) die slechts een beetje afneemt bij pH 5,8 (1,1 tot 1,6 mg $m^{-2}$), waarbij de meeste adsorptie bij de laagste bacterieconcentratie wordt waargenomen.

Dit suggereert dat het speeksel vrij snel uitgeput raakt van de eiwit(ten) met een hoge affiniteit voor antigeen I/II. Concluderend kan gezegd worden dat de antigeen I/II oppervlakeiwitten op *S. mutans* een belangrijke rol spelen bij de adsorptie van speekseleiwitten, vooral bij pH 6,8 (in vergelijking met pH 5,8), door het creëren van enthalpisch gunstige adsorptieplaatsen.

In **hoofdstuk 4** worden de interactiekrachten tussen speeksel eiwitten en *S. mutans* met (LT11) en zonder (IB03987) antigen I/II onderzocht met behulp van AFM en in verband gebracht met de hechting aan met speeksel bedekt glas in de parallelle plaat stroomkamer. Tijdens het naderen van de met speeksel bedekte AFM- tip naar de bacteriën treedt er, voor beide stammen, een vergelijkbare afstotende kracht op. Deze is voor pH 6,8 (mediaan 3,0 en 3,1 nN voor LT11 en IB03987, respectievelijk) significant kleiner dan voor pH 5,8 (mediaan 4,6 en 4,7 nN voor LT11 en IB03987, respectievelijk). Het vervaltraject van deze afstotende kracht ligt tussen 19 en 37 nm. De specifieke en niet-specifieke hechtingskrachten waren significant groter voor de LT11 stam (mediaan -0,4 nN) dan voor de IB03987 stam (mediaan 0,0 nN) bij pH 6,8, daarentegen was de mediaan van de hechtingskracht gemeten bij pH 5,8 voor beide stammen 0,0 nN. In de parallelle plaat stroomkamer waren bij pH 6,8 significant meer bacteriën gehecht van de LT11 stam ($9,6 \times 10^6$ $cm^{-2}$) dan van de IB 03987 stam ($2,5 \times 10^6$ $cm^{-2}$) aan het met speeksel bedekte oppervlak. Vergelijkbaar met het verschil in hechtingskracht gemeten met AFM tussen beide stammen bij pH 5,8, verdwijnt ook het verschil in de hechting aan de speeksellaag in de stroomkamer bij pH 5,8, hetgeen suggereert dat er een invloed is van aantrekkende elektrostatische krachten bij de interacties tussen antigen I/II en het speeksel bij pH 6,8. Samengevat laat deze studie zien dat antigen I/II op het oppervlak van *S. mutans* LT11 verantwoordelijk is voor de verhoogde hechting aan speeksel-coatings door middel van vergrote aantrekkende elektrostatische krachten.

Om het mechanisme van de bacterie-eiwit interactie beter te begrijpen, zijn er ook experimenten uitgevoerd met één eiwit in plaats van met meerdere eiwitten zoals dat in speeksel voorkomt. Fibronectine bindende eiwitten (FnBP's) op het oppervlak van een bacterie zijn de verbindingsschakel tussen cellen van *Staphylococcus aureus* en het oppervlak van bijvoorbeeld implantaten of een weefsel waarop fibronectine (Fn)

voorkomt. In **hoofdstuk 5** vergelijken we de hechting van twee *S. aureus* stammen met (8325-4) en zonder (DU5883) FnBP's aan met Fn bedekt glas in de parallelle plaat stroomkamer. De ITC is gebruikt om de adsorptie-enthalpie van Fn aan staphylokokken te meten, terwijl de AFM is gebruikt om de hechtingskrachten tussen de staphylokokken en de Fn-bedekte oppervlakken te meten. De bacterie met FnBP's hechten significant sneller (2438 $cm^{-2}s^{-1}$) aan het met Fn bedekte oppervlak dan de bacterie zonder FnBP's (1290 $cm^{-2}s^{-1}$). In overeenstemming hiermee is de gemeten hechtings-kracht tussen de bacterie met FnBP's groter (mediaan -0,7 nN) dan de mutant zonder FnBP's (mediaan -0,3 nN). Ook is gevonden dat de adsorptie-enthalpie van Fn aan het celoppervlak exotherm en hoger is voor de stam met FnBP's ($140 \times 10^{-9}$ µJ per bacterie) dan voor de stam zonder FnBP's ($-43 \times 10^{-9}$ µJ per bacterie). Nadat de Fn-coatingen behandeld zijn met albumine (BSA) hebben zowel de originele als de mutant dezelfde adhesie-parameters, waaruit we concluderen dat BSA de specifieke interacties tussen het Fn-bedekte glas en/of het bacterieoppervlak blokkeert. Echter de hechtings-krachten en de adsorptie-enthalpiën veranderden nauwelijks na toevoeging van BSA. Dit betekent dat onder milde contact omstandigheden, die optreden bij convectieve diffusie in de parallelle stroomkamer, het geadsorbeerde BSA specifieke interacties tegengaat, maar dat bij het geforceerde contact tijdens de AFM experimenten en het roeren in de caloriemeter er, ondanks de BSA coating, nog steeds interacties optreden tussen Fn en FnBP's.

In **hoofdstuk 6** wordt de contacttijd-afhankelijke desorptie van twee *S. aureus* stammen, met (8325-4) en zonder (DU5883) FnBP's, van Fn-bedekte oppervlakken in een parallelle plaat stroomkamer vergeleken. De specifieke bindingskrachten werden veel sneller (2 s) sterker dan de niet-specifieke bindingskrachten die 10 s of meer in beslag namen. De tijdschalen voor deze bindingskrachten zijn met onafhankelijke AFM metingen bevestigd. Bindingssterkte berekend uit de curve waarbij de AFM-tip van het oppervlak wordt getrokken zijn vele malen groter dan die berekend zijn uit de hechtings-experimenten in de stroomkamer. Hieruit kan geconcludeerd worden dat de Fn-gecoate tips bij AFM interacties heeft met meerdere receptorplaatsen in de buitenste laag van het celoppervlak, zelfs voor de mutant *S. aureus* DU5883, waarvan aangenomen wordt dat deze geen receptorplaatsen op het oppervlak heeft. Bij het

milde contact dat plaats vindt in de stroomkamer worden deze dieper gelegen receptoren niet bereikt.

Zoals samengevat is in de **general discussion** geeft het gebruik van de parallelle plaat stroomkamer, AFM en ITC ons een betere kijk op het mechanisme van bacteriële adhesie aan geadsorbeerde eiwitlagen. Gebleken is dat dit een complex samenspel is van fysisch-chemische mechanismen bestaande uit niet-specifieke en specifieke, moleculaire herkennings fenomenen.

*Translated by Betsy van de Belt-Gritter, René J. B. Dijkstra, and Joop de Vries*

Acknowledgments

*"When you drink the water, think of those who dug the well."*

----------*An Old Chinese Saying*

First of all, I would like to express my deepest appreciation to my supervisor, Prof. dr. Henk J. Busscher, for his guidance throughout the course of this research. I learned a lot from him, including scientific research methods, theoretical knowledge and communication skills.

My sincere gratitude also goes to my co-supervisor Prof. dr. H.C. van der Mei for her professional support, scientific discussion and reinforcement in all aspects of this research.

I would also like to thank Prof. dr. Willem Norde. I really appreciate the opportunity to work with him and always found him understanding and encouraging. He is always ready to share his knowledge and give constructive comments towards the project.

I would like to acknowledge Dr. Y.J. Gu and Prof. dr. Andrew Sandham for the many encouragements they have given me, both in my academic pursuit as well as my personal life during the study in Groningen.

I would like to thank Betsy van de Belt-Gritter for her help with my research experiments, Joop de Vries for his help with the X-ray photoelectron spectroscopy and AFM experiments, René J. B. Dijkstra for his help with AFM experiments, Dr. Bastiaan Krom and Dr. Prashant Sharma for the many discussions of my research work, Eefje Engels and Minie Rustema-Abbing for their guidance with the flow chamber experiments and Hans Kaper for his help with the image analysis.

I am grateful to Professors L. Dijkhuizen, J.M. van Dijl and P.G. Rouxhet, for their role as my reading committee members and their careful examination of my thesis.

My sincere appreciation also goes to W.T.J. Kloppenburg, Ellen van Drooge and Ina Heidema–Kol for your endless help in the administration and organization of my Ph.D. defence.

Thanks are also due to Prof. Jong Won Yun, Prof. Linsong Wang, and Prof. Yuguo Zheng, who have given me constant support and warm-hearted help which has meant a lot to me.

I would like to extend my thanks to both my senior colleagues, Dr. Q. Qiu and Dr. Mervyn YH Chin for helping me when I was in troubles and made my stay at Groningen a pleasant one. I would also like to thank Ed de Jong, Marco Verkaik, Niels Boks, Ward van der Houwen, Marten Koetsier, Marieke Otten, Katya Paramonova, Jan Svêc, Guruprakash Subbiahdoss, Reza Nejadnik Anton Engelsman, and T. Das for helping me throughout my laboratory work. I would like to acknowledge Kevin Buijssen and Margareta Rinastiti for their help during my early days in the laboratory and all Chinese friends in Groningen, especially Lei Ke, Honglian Dai, Yanghua Lin, Bian Wu, Lebin Tan, Lijun Tan, Hongtao Tan, Hongwei Wang, Cheng Qian, Lu Zhou, Ying Wang, Hao Zhang, Li Duan, Hongyou Yu, Liqiang Qi, Qingsong Ye, Xia Yi, Xiangyi Li, Zhida Xu, Li Mei, Yan Zhao and many more.

Last but not least, I wish to express my heartfelt appreciation to my parents, my sister and brother-in-law for their continuous patience, sacrifice and encouragement which have kept me going all these years. I have owed their too much and only hope that I can pay them back in the rest of my life.

# Curriculum Vitae

**Chun-Ping Xu** (許春平, ｷｮｼｭﾝﾍﾟｲ, 허춘평) was born in 1977 in China. He started his scientific research in Zhejiang University of Technology, China from 2000 and subsequently obtained his master degree in 2003 funded by Foreign Research Fellowship from the Department of Biotechnology, Daegu University, Korea. After his graduation, he worked as a researcher in Department of Biological Functions and Engineering, Kyushu Institute of Technology, Japan. In 2005, University of Groningen, Faculty of Medicine, The Netherlands awarded him a Ubbo Emmius PhD research fellowship to continue his studies in the Department of Biomedical Engineering. His scientific career comprises Biochemical Engineering (enzyme technology, mammalian and fungal cell cultures, fermentation process, purification and biosensor development) and Biomedical Engineering (bacterial adhesion and biofilm formation).